Institut für Nutzpflanzenwissenschaften und Ressourcenschutz

Mechanistic details into NADPH oxidase mediated resistance against *Heterodera schachtii* in *Arabidopsis thaliana*

Inaugural-Dissertation

zur

Erlangung des Grades

Doktorin der Agrarwissenschaften

(Dr.agr.)

der

Landwirtschaftlichen Fakultät

der

Rheinischen Friedrich-Wilhelms-Universität Bonn

von

Christiane Michaela Matera

aus

Wuppertal

Bonn 2017

Referent:	Prof. Dr. F.M.W. Grundler
Koreferent:	Prof. Dr. H.W. Scherer
Tag der mündlichen Prüfung:	02.06.2016

Angefertigt mit Genehmigung der Landwirtschaftlichen Fakultät der Rheinischen Friedrich.Wilhelms-Universität Bonn

Table of Content

Abstract

The oxidative burst, production of Reactive Oxygen Species (ROS) in response to pathogen attack, is an important component of plant defence mechanisms. It is now generally recognised that the major source of ROS during an "oxidative burst" in plants is plasma membrane-bound NADPH oxidase. Plant NADPH oxidases have been named as **r**espiratory **b**urst **o**xidase **h**omolog (Rboh) and possess six transmembrane-spanning domains corresponding to the domains that have been identified in the gp91^{phox} subunit in mammals. Genetic analysis of plants disrupted in Rboh functions suggested that they are required for the production of a full oxidative burst in response to a variety of pathogens. Yet, this lack of ROS production by NADPH oxidase has variable effects on plant responses to pathogens in terms of cell death and resistance. On one hand, it is positively correlated with plant resistance by strengthening of cell walls via cross linking, lipid peroxidation, membrane damage and activation of defence genes. On the other hand, it is an important susceptibility factor for successful infection of plants by various pathogens. Nevertheless, the mechanistic details on the pathosystem-specific role of Rboh-mediated ROS are not yet known.

Heterodera schachtii is a cyst nematode that establishes a long-term biotrophic relationship with the roots of sugar beets and brassicaceaous plants, including *Arabidopsis thaliana*. Infective stage juveniles of cyst nematodes (J2s) invade the roots and move towards the vascular cylinder where they establish a syncytial nurse cell system. The syncytium is the only source of nutrients for nematodes throughout their life-span of several weeks. This thesis focuses on the characterization of the role of Rboh-mediated ROS in plant-nematode interactions using the *Arabidopsis thaliana – H. schachtii* model system.

In Arabidopsis, Rboh is encoded by ten genes (RbohA-RbohJ). We used loss-of-function mutants for Rboh genes and found that the number of female nematodes, the size of female nematodes, and the size of female-associated syncytium decreased greatly in *rbohD* and *rbohD/F*, but not in *rbohA, rbohB, rbohC, rbohE, rbohF, rbohG*, *rbohH and rbohJ* plants compared with Col-0 plants. A detailed microscopic, molecular and biochemical analysis showed that Rboh-dependent ROS are not required for root invasion; however, the syncytial establishment and development is impaired in the absence of ROS. To understand the mechanism

underlying the Rboh-mediated reduced susceptibility to nematodes, we performed a genome-wide comparative transcriptome analysis between Col-0 and *rbohD/F* during early stages of infection. The gene that was most strongly downregulated encodes the vacuolar auxin transporter, Walls Are Thin 1 (WAT1). Genetic disruption of WAT1 led to similar changes in nematode susceptibility as in *rbohD/F*, thus suggesting that Rboh-mediated reduction in susceptibility to nematode is dependent on WAT1. Interestingly, both *rbohD/F* and *wat1* are impaired in expression of key metabolic genes for indole metabolism including auxin biosynthesis upon nematode infection. In summary, our work provides for the first time a link between Rboh-mediated phenotypes and auxin metabolism. These data are the basis for a mechanistic understanding on the role of ROS as signals to promote nematode and other pathogen infections.

Kurzfassung

Die Produktion von reaktiven Sauerstoffspezien (englisch *reactive oxygen species*, ROS), auch „oxidativer Burst“ genannt, ist ein wichtiger Mechanismus bei der pflanzlichen Abwehr von Pathogenen. Produziert werden diese ROS hauptsächlich von einer Plasmamembran gebundenen NADPH Oxidase. Pflanzliche NADPH Oxidasen werden von RBOH (englisch *respiratory burst oxidase homolog*) Genen kodiert und bestehen aus einem N-terminalem Segment, einem zytosolischen C-terminalem Ende und sechs transmembranen Strukturen, ähnlich der gp91^{phox} Untereinheit in Säugetieren. Genetische Analysen mit Pflanzen, deren RBOH Gene eine Dysfunktion aufweisen, haben gezeigt, dass diese NADPH Oxidasen essentiell für einen vollständigen oxidativen Burst bei Angriffen durch verschiedene Pathogene sind. Die dadurch ausbleibende Produktion von ROS hat diverse Effekte hinsichtlich Zelltod und Resistenz. Auf der einen Seite, gibt es einen positiven Effekt auf die pflanzliche Abwehr, da die Zellwände gestärkt, Membranen zerstört und Abwehrgene aktiviert werden. Andererseits führt die Produktion von ROS aber auch zu einer erhöhten Anfälligkeit gegenüber verschiedenen Pathogenen. Die Mechanismen hinter dieser Pathogen-spezifischen Rolle von Rboh abhängigen ROS sind bisher noch unklar.

Der Zystennematode *Heterodera schachtii* ist ein obligat biotropher Pathogen und befällt Zuckerüben, wie auch andere *Brassicaceaen* einschließlich *Arabidopsis thaliana*. Die wurmförmigen Larven (J_2) schlüpfen aus Zysten, die als schützende Hülle im Boden überdauern, dringen in die Wurzel ein und induzieren die Bildung von spezifischen Nährzellen (Synzytien), welche ihnen während aller sedentären Entwicklungsstadien als permanente Nahrungsquelle zur Verfügung stehen. Die vorliegende Arbeit konzentriert sich darauf, die Rolle von Rboh vermittelten ROS durch die Nutzung des Modell-Systems *H.schachtii – A.thaliana* näher beschreiben.

In *Arabidopsis* existieren zehn Gene die für Rboh kodieren (RbohA-RbohJ). Durch die Nutzung genetisch veränderter Pflanzen (Loss-of-function Rboh) konnten wir zeigen, dass die Anzahl weiblicher Nematoden, sowie deren Größe und die dazugehörigen Synzytien in *rbohD* und *rbohD/F* signifikant verringert war. Im Gegensatz dazu hatten *rbohA, rbohB, rbohC, rbohE, rbohF, rbohG*, *rbohH* und *rbohJ* keinen Einfluss auf diese Parameter. Unsere detaillierten mikroskopischen, molekularen und biochemischen Analysen haben ergeben, das Rboh abhängige

ROS keinen Einfluss auf die Invasionsrate des Nematoden haben, wir konnten jedoch nachweisen, dass die Etablierung und Entwicklung des Synzytiums unter ROS Ausschluss erheblich gestört ist. Um die Mechanismen dieser durch Rboh vermittelten reduzierten Anfälligkeit zu verstehen, führten wir eine vergleichende Transkriptom-Analyse zwischen Col-0 und *rbohD/F* während der frühen Infektionsphase des Nematoden durch. Diese ergab, dass ein Gen, welches für den vaskulären Auxintransport verantwortlich ist (WAT1, Walls Are Thin1), erheblich abreguliert war. Pflanzen mit einer genetischen Veränderung an WAT1 zeigen einen ähnlichen Einfluss auf die Nematoden und Synzytien Entwicklung wie in *rbohD/F*. Daher vermuten wir, dass die Rboh reduzierte Anfälligkeit abhängig von WAT1 ist. Interessanterweise zeigen *rbohD/F* und *wat1* Pflanzen nach der Nematodeninfektion eine gestörte Genexpression im Indolemetabolismus einschließlich der Auxinbiosynthese. Zusammenfassend, stellt unsere Arbeit das erste Mal eine Vernetzung von Rboh reduzierter Anfälligkeit und Auxinmetabolismus dar. Diese Daten bilden somit die Basis, um Einblicke in die Rolle von ROS als Pathogeninfektion förderndes Signalmolekül zu bekommen.

Chapter 1

Introduction

Nematodes in general

Nematodes, or roundworms, belong to the phylum Nematoda and constitute one of the most diverse groups of animals. The existence of more than one million species is expected, although only 28.000 have been described so far (Lewis et al., 2004; Decraemer and Hunt, 2006). Nematodes are widely distributed and live under different environmental conditions; they all share certain common features. They are structurally simple organisms, and possess a vermiform, unsegmented body. Their body is bilaterally symmetrical, more or less translucent and round in cross section. Their muscles are attached longitudinally to the hypodermis, which only permits movement in the dorsal ventral direction (Decraemer and Hunt, 2006). Depending on their habitat, nematodes vary greatly in size. The smallest nematodes are not visible without a microscope, and they include plant-parasitic nematodes such as *Heterodera schachtii* and *Meloidogyne incognita*. In contrast, the largest nematode, *Placentonema gigantissima,* has been found in the placenta of a sperm whale with a size of 8.4 m and cross section of 4 cm (Gubanov, 1951).

Nematodes occupy nearly every global niche including salt and fresh water (50%), soil (25%), animals (15%) and plants (10%) (Jörgensen et al., 2004). Because of their wide distribution, nematodes are integrated into almost every ecological system and play important roles in energy flow, mineralization, nutrient cycling and detritus formation (Bardgett et al., 1999). Ecologically, nematodes can be differentiated as parasitic or free-living forms. The feeding habits of free-living nematodes are relatively specific; therefore they are grouped into bacterivores, fungivores, omnivores and predators (Fig.1). Parasitic nematodes establish a narrow relationship with their hosts because they feed on the host throughout their lifecycle. These parasitic nematodes are capable of infecting plants, animals and humans and are responsible for a number of diseases such as trichinosis, which is a roundworm infection, caused by *Trichinella spiralis*.

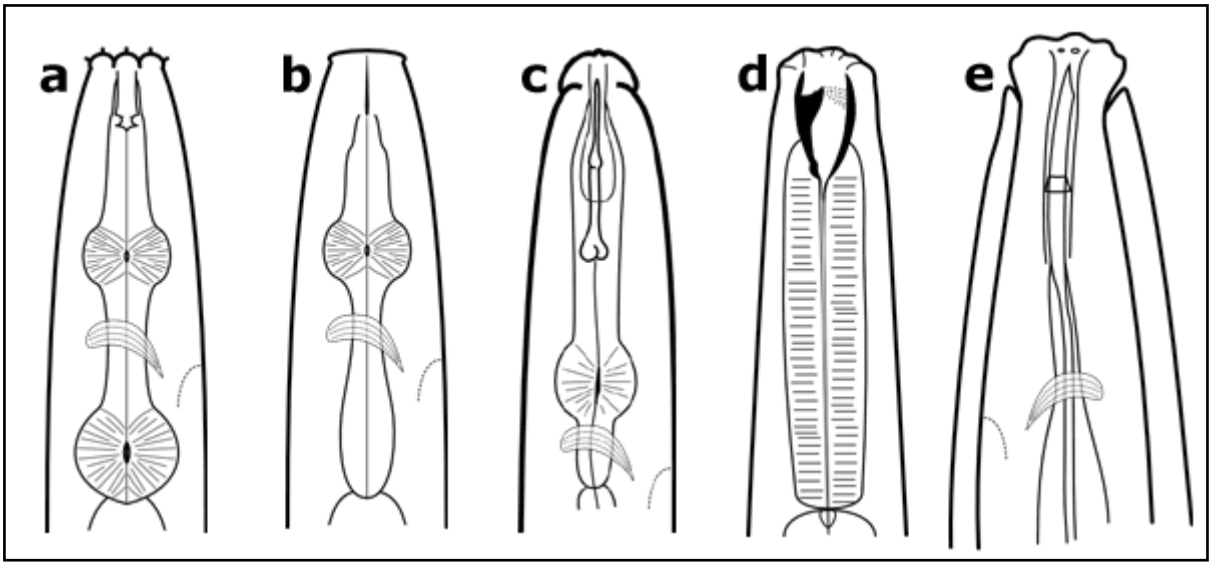

Figure 1. Classification of nematodes due to their feeding habit and structure of the mouthpart: (a) bacterivores have a tube like structure to suck up bacteria, (b) fungivores have a thin stylet to penetrate fungal cells, (c) herbivores also have a stylet to pierce cells and feed on them, (d) predators feed on other nematodes and small soil animals, (e) omnivores feed on different food sources (Ugarte et al., 2013)

Because of their advantageous features, including their small genome, simple morphology and easy handling, nematodes are often used as a research model for molecular genetics and cellular biology. The free-living nematode *Caenorhabditis elegans* was the first multicellular organism to have its entire genome sequenced (*C. elegans* Consortium, 1998). In addition, nematodes are effective biological control agents like the entomopathogenic nematodes *Steinernema* and *Heterorhabditis* from the order Rhabditida, which kill insects by releasing bacteria into the insect's body (Poinar et al., 1977, Poinar 1979).

Plant-parasitic nematodes

Of the 28,000 known nematode species, only 4,100 are plant-parasitic (Decreamer and Hunt, 2006). These nematodes are all obligate biotrophic pathogens and feed on almost all plant tissues, including flowers, leaves, stems and roots. A characteristic of this group is a specialized mouth spear, called a stylet that penetrates the plant cells and helps in feeding. Accordingly stylets can be used to identify their mode of feeding. Based on their feeding habit, plant-parasitic nematodes are grouped into endoparasites and ectoparasites.

Ectoparasites feed on a large number of hosts. Members of this group do not enter the plant with their entire body; instead, they feed from outside the plant tissue with their stylet, which remains at the plant surface. Depending on the length of the stylet, ectoparasites may feed on different plant tissues. Ectoparasites with short stylets, such as *Tylenchorhynchus* and *Helicotylenchus,* pierce cells in root hairs and epidermal cells, whereas those with long stylets, such as *Belonolaimus* and *Dolichodorus,* can access deeper tissues (Perry and Moens, 2006). After feeding for a period of time, these nematodes remove their stylet and search for a new feeding location. Because of this relatively primitive mode of parasitism, most ectoparasites cause limited tissue damage (Hussey, 1989).

Endoparasites have migratory or sedentary life styles. They all enter the root with their entire body and migrate through different tissue layers to find an optimal feeding location. Among migratory endoparasites, the genus *Pratylenchus* is most relevant because of its large number of host plants and worldwide distribution. Sedentary endoparasites such as root-knot (*Meloidogyne spp.)* and cyst (*Globodera and Heterodera ssp*.) nematodes are economically most important. For parasitism, they move through the roots until they find a suitable cell in the proximity of the vascular cylinder where they develop a specific feeding structure by injecting secretions with the help of their stylets (Hussey, 1989). This feeding structure provides nematodes with all of the nutrients throughout their life-span for several weeks.

The feeding behavior of plant parasitic nematodes damage plants in several ways. Penetration by the stylet creates wounds and openings that can be used by other pathogens to enter the plant. They also disrupt the vascular tissue during their movement through tissues and especially during the feeding period, which reduces the transport of water and minerals from the root system up to the leaves and stems of the plant. The global yield loss, which they cause, is around 12% (Ferraz and Brown, 2002). A small number of genera, including cyst nematodes (*Heterodera spp*. and *Globodera spp*.), root-knot nematodes (*Meloidygyne spp*.) and certain migratory nematodes (*Tylenchorhynchus spp.* and *Rotylenchulus spp*.) are responsible for most of this damage.

In Europe, one of the most important plant parasitic nematodes is the cyst nematode *H. schachtii*. This organism is capable of infecting more than 200 plants of 20 different families and constitutes a serious sugar beet pest, but is also a pathogen for

cabbage, broccoli, radish and *Arabidopsis thaliana* (Jones et al., 2011). For a number of years, the treatment with nematicides was the solution to reducing such infections by *H, schachtii*, but most of these chemical have been banned because of their toxicity. Other methods of controlling nematodes are based on fumigants, specific crop rotation cycles and development of resistant host varieties.

The natural resistance of host plants to nematodes is defined as reduced levels of parasitic reproduction (Trudgill, 1976), which indicates that nematodes can invade plants but are not able to complete their life cycle. Nematode resistance genes have been found and are an important component of crop breeding programs. Examples include $Hs1^{pro-1}$, which confers resistance to *H. schachtii,* and Mi-1 gene which confers resistance to root-knot nematodes and aphids (Vos et al., 1998). The use of resistant genes has been limited because of their narrow pathogen effectiveness. In addition, pathogens arise that can overcome the resistance (Kearney et al., 1988; Padgett and Beachy, 1993). Because of these limitations it is not only important to improve cultivars through traditional breeding, but a deeper mechanistic understanding of nematode pathogenicity mechanisms could also provide important contributions to increase the resistance of plants to nematodes.

Interactions between cyst nematodes and their hosts

The compatible interaction is best studied with the cyst nematode *H. schachtii* in Arabidopsis and other host plants. The cysts are oval-shaped with an approximate size of 0.8 mm * 0.5 mm and they contain eggs with infective second stage juveniles (J_2). Root exudates, which are released from young roots during the growth (Sikora and Bridge, 2005) stimulate the hatching of the larvae from egg, with the nematodes breaking through the eggshell and emerging from the cysts. Led by this attractant, the nematodes find and invade the plant. Like all other plant parasitic nematodes, *H. schachtii* has two specialized structures which are essential for certain aspects of parasitism: a hollow stylet to pierce cell walls and to release secretions that manipulate the host cell, and three oesophageal secretory glands that produce substances supportive of the nematodes invasion and feeding behavior (Hussey, 1989). Frequently, the nematode starts to penetrate the root in the elongation zone behind the root tip, and the stylet begins thrusting when stimulated by diffusates from

the host root (Grundler et al., 1991). After perforation of the rhizodermis with the stylet, the nematode uses its muscles to move through the root tissue. This intercellular movement is slowed by the cell walls. Penetration by the stylet is supported by cell wall degrading proteins and enzymes (CWDs), such as cellulases and pectinases, which are produced by two subventral pharyngeal gland cells (Smant et al., 1998; Vanholme et al., 2004) and secreted through the oesophageal lumen and stylet into the cell (Golinowski 1998). In fact nematodes were the first animals shown to produce CWDs. Aided by the stylet and CWDs, the juvenile advances from one cell to the next without feeding until it reaches the vascular cylinder where nutrients and water are transported. Here the nematode probes single cells one-by-one to find a suitable initial syncytial cell (ISC).The response of the pierced cell may produce a spontaneous collapse of cytoplasm, which forces the nematode to probe the next cell. These collapsed cells can be found in the pathway of the nematode. The selection of an ISC might require several hours, and the factors involved are generally not known.

Once the ISC is selected, the juvenile remains motionless for the next 6- to -8 hours with its stylet inside the ISC. With the beginning of this feeding-preparation period, the nematode changes its life-style and becomes sedentary (Wyss and Grundler, 1992). The developing nematode secretes several substances into the cell that result in remarkable reorganization of the plant's transcriptomic and metabolomics machinery (Hofmann et al. 2010; Hofmann *et al*. 2008; Siddique et al., 2009; Szakasits et al., 2009;). The central vacuole is fragmented into a number of smaller vacuoles, and the cytoplasm becomes highly active (Golinowski 1998, Sobczak 2011). Subsequently, the metabolism of this activated cell serves the nematode. Although certain nematode proteins have been identified that might be involved in the syncytium functioning (Jaubert et al., 2002; Vanholme et al., 2004; Gardner et al., 2015), little is known of the mechanisms by which nematodes induce the formation of the syncytium. Nevertheless, after 24 hours of ISC establishment, the surrounding cells are hypertrophied and fuse to a multinuclear cell complex by local dissolution of cell walls. This dissolution within developing syncytia is supported by plant genes encoding cell-wall degrading proteins and enzymes including expansins, cellulases, and pectin modifying and degrading enzymes. (Grundler et al.,1998; Wieczorek et al., 2006; Wieczorek et al., 2008; Wieczorek et al., 2014). Although the inner cell walls are partly degraded, certain parts of the outer cell walls of the growing syncytium are

thickened, which sustain the high osmotic pressure inside (Böckenhoff and Grundler, 1994). Additionally, cell wall ingrowths are formed at the interface with xylem vessels to facilitate the massive transport of water and nutrients. To perform these important structural changes and functions, the cell wall in syncytium are not only modified and digested but also concomitantly *de novo* synthesized (Siddique et al., 2012).

During the subsequent weeks, the nematode feeds in repeated cycles (Wyss and Grundler, 1992) and undergoes further moults (J3 and J4). A fully developed female-associated syncytium consists of approximately two hundred cells (Hussey and Grundler, 1998). In contrast to some root-knot nematodes, such as *M. incognita*,

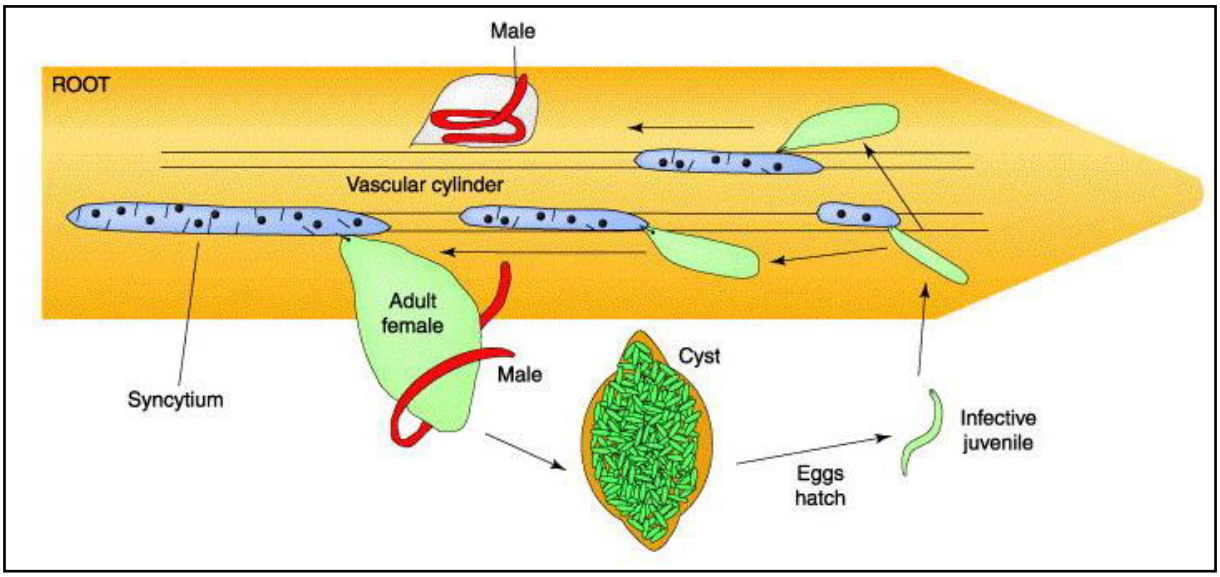

Figure 2. Life cycle of endoparasitic cyst nematode *H.schachtii* (Williamson and Gleason, 2003); In contrast to root-knot nematodes, which are first searching for the root tip of plants and migrate then up the root (Wyss, Grundler, Munch, 1992), the juveniles of cyst nematodes try to reach directly the vascular cylinder (Wyss and Zunke, 1986) to induce the feeding cell. Sex is not predetermined and depends on the environmental conditions and size of developed syncytium

which are not dependent on the presence of males to produce mature eggs, females of *H. schachtii* copulate with a male to generate fertile eggs. In general, males develop more quickly and are attracted to females by pheromones, causing them to leave the root in search of adult females. After copulation, the female dies and a brown cyst with eggs remains inside. The sex of a *H. schachtii* is not pre-determined, and mechanism involved in sex differentiation is not well understood. However, it is generally accepted that under favorable growth conditions, more female develop and poor nutrient conditions lead to an increase in males. Factors such as the number of eggs, development of the syncytium and penetration rate are influenced by the host

plant (Cai et al., 1997; Grundler et al., 1991; Hofmann et al., 2008; Lelivelt and Hoogendoorn, 1993; Siddique et al., 2009).

Reactive oxygen species

Reactive oxygen species (ROS) are oxygen-containing molecules that are highly reactive because of the presence of unpaired valence shell electrons. ROS are by-products formed inside plant cells during normal oxygen metabolism, such as the mitochondrial electron transport of aerobic respiration. The ROS of biological significance include superoxide (O_2^-), hydrogen peroxide (H_2O_2) and hydroxyl radicals (•OH) (Bedard and Krause, 2007), which are generated by electron transfer and proton acceptance. The production of ROS is enhanced under various stress conditions, such as salt, drought, high light, temperature, and pathogen infections. Superoxide and hydrogen peroxide are relatively unreactive molecules compared with hydroxyl radicals, which react with nearly every molecule. Nonetheless, a high concentration of any ROS can lead to oxidative destruction of cellular components, such as DNA, lipids and proteins, highlighting the importance of organized interactions between ROS -production, -perception and ROS –scavenging for the evolution of aerobic life.

ROS in plants

Although ROS have toxic characteristics, they also act as signalling molecules and play an important role in plants growth, development and interaction with environment. Recent work has demonstrated that ROS are key regulators of biological processes, including growth, development and stress responses (Kovtun et al., 2000; Foreman et al., 2003; Miller et al. 2009) where they act as signalling molecules that activate signaling cascades or gene expression (Hancock et al., 2001). This view is explained by the fact that most abiotic or biotic stresses disrupt the cellular metabolic processes, which results in enhanced ROS production, thereby a change in the redox state of the cell. These changes are sensed and transmitted by receptors, proteins and enzymes in the plant and can modulate pathways involved in

development, metabolism and stress (Georgiou, 2002). To manage and use different level of ROS, plants have developed sensitive production, -perception and –scavenging machinery for ROS, consisting of approximately 152 genes (Mittler et al., 2004).

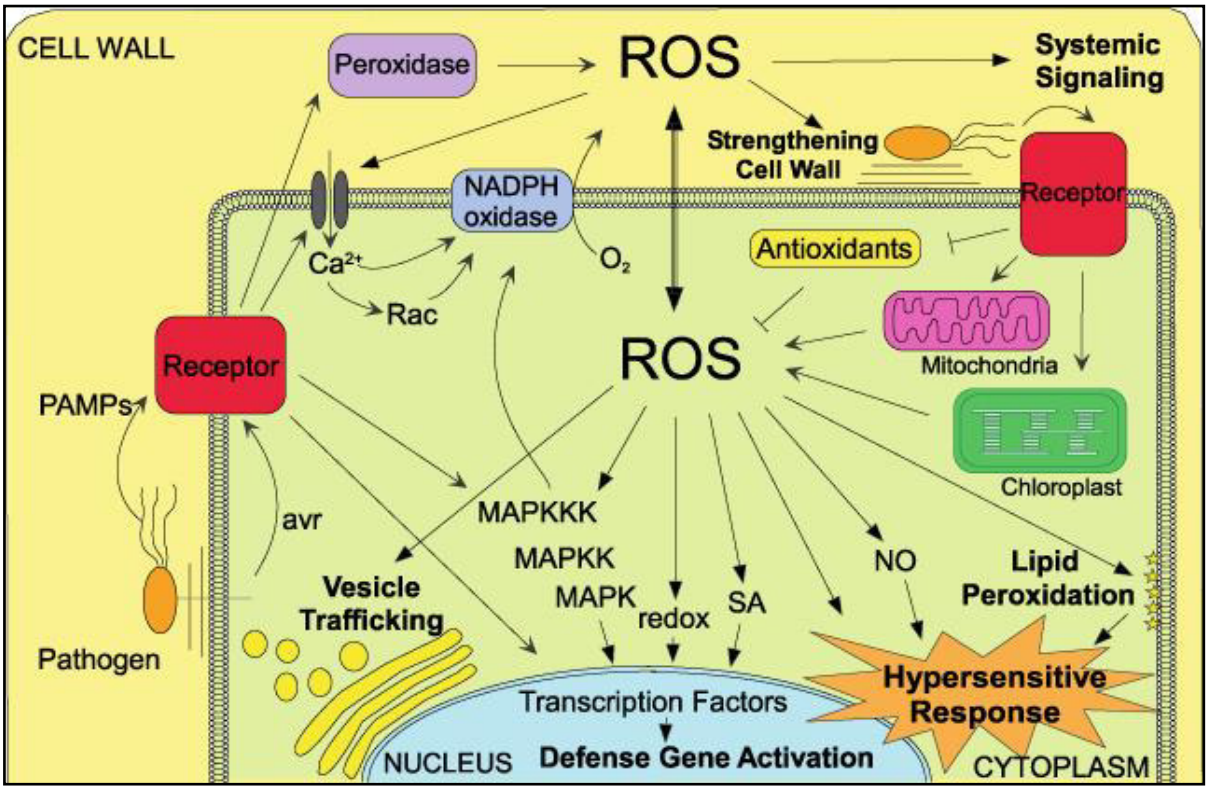

Figure 3. **Production and function of ROS in plant-pathogen interaction:** ROS are generated in the apoplast as well in the cytosol in response to pathogen detection. This oxidative burst leads not only to hypersensitive response (HR) to prevent spreading of the pathogen within the tissue, but ROS are also known to support the strengthening of the cell walls, to activate transcription factors, to enable defense genes, and to initiate various forms of systemic signaling (Graves 2012).

H_2O_2 is significant among ROS and it has been shown to act as a signalling molecule through the induction of phytoalexins, which have antimicrobial activity (Wojtaszek, 1997). Moreover, because of its relatively long life, ability to cross membranes and low reactivity, H_2O_2 may also be responsible for long distance signalling in plant-pathogen interactions. In fact, H_2O_2 has been shown to be involved in the establishment of local and systemic resistance in *A. thaliana* after infection with avirulent *Pseudomonas syringae* (Alvarez et al., 1998). The site of ROS production varies, depending on their function in the plant, but in general ROS are generated in organelles with a high metabolic activity or with an intense rate of electron flow, i.e.

mitochondria and chloroplasts or by enzymes like peroxidase and oxidase. Recent findings indicate that the origin of pathogenesis-related ROS is a plasma membrane-bound NADPH oxidase (Lamp, 1997).

NADPH oxidase is homologous to a plasma membrane bound enzyme in mammalian phagocytes that destroys microbes. This complex consists of a catalytic subunit gp91phox, which is responsible for the transfer of electrons to molecular oxygen to generate superoxide, and three cytosolic subunits which can be activated by cytosolic proteins on the catalytic site (Torres et al., 1998). The NADPH oxidase in plants can be divided into three domains. The first part is inside the membrane, and it consists of six transmembrane-spanning domains with two haem (Fe) groups. This is used for electron transport from inside to outside the cell and a subsequent reduction of O_2 to O_2^-, the source for ROS such as H_2O_2. The second part is a cytosolic 300-amino-acid N-terminal domain that contains calcium binding EF-hand motifs and acts as an activator of the oxidase complex. Interestingly, this domain is similar to certain NOX5 and DUOX oxidases that function in animal immunity (Torres and Dangl, 2005). The direct activation of this domain by calcium allows Ca^{2+} to assume a key role of in the rapid stimulation of oxidative bursts and highlights one of the most significant differences between the mammalian and the plant NADPH oxidase proteins: both are regulated by calcium, but mammalian NADPH oxidase requires additional cytosolic components (Torres and Dangl, 2005a). The third part of the NADPH oxidase protein is a 105 to 112 kD long carboxyl-terminal region containing NADPH- and FAD-binding domains that transfer electrons from the oxidation of NADPH to the transmembrane section (Apel, 2004; Torres, 1998). The structure of the NADPH oxidase in plants and mammals is well researched, and based on the homology to the mammalian oxidase, the encoding genes in plants are called *respiratory burst oxidase homologues* (RBOH).

Certain genes that encode for RBOH proteins in plants have been discovered in *Arabidopsis*, tomato, tobacco and potato. The *rice respiratory oxidase homolog* (OsrbohA gene) was the first plant NADPH oxidase identified, and ten genes of this family have been found in *A. thaliana* (AtRBOHA - AtRBOHJ) (Torres et al., 1998). The mechanism that controls the expression of different RBOH genes is not well understood; however, their spatio-temporal distribution hint that different RBOHs have different roles and are capable of complementing each other functions.

AtRBOHD and AtRBOHF are reportedly involved in most ROS produced in response to avirulent bacteria and oomycetes (Torres et al., 2002), whereas AtRBOHC is required for ROS production during root hair growth.

ROS production mediated by NADPH oxidase during plant-pathogen interaction

Apoplastic ROS production during pathogen attack is one of the earliest observed defense responses in plants, and two different mechanisms are known to be involved. In case of pattern-triggered immunity (PTI), the plant recognizes pathogen- or microbial-associated molecular patterns (PAMPS or MAMPS) using pattern recognition receptors (PRR) on the surface of the cell. Effector-triggered immunity (ETI) begins after the detection of effector proteins, which are released by pathogens and can be sensed by nucleotide-binding domain leucine-rich repeat proteins (NB-PRR) inside the plant. However, the amount and amplitude of ROS production vary depending on plant-pathogen interactions (Feng and Shan, 2014). In general, ETI is accompanied by a biphasic ROS accumulation with a low-amplitude, a transient first phase followed by a sustained high-intensity phase. In comparison, only a low-amplitude transient first -phase occurs during PTI (Torres et al., 2006).

The contribution of RBOH-mediated ROS has been shown to play diverse roles in plant-pathogen interactions during both PTI and ETI (see above Figure 3). On one hand, it is positively correlated with plant defense against pathogens by strengthening cell wall, killing pathogens, activating defense genes or by interaction with other signaling components such as phosphorylation cascades (Levine et al., 1994, Kovtun et al., 2000, Mou et al., 2003, Mur et al., 2008). On the other hand, they act as an important susceptibility factors and promote infection by suppressing cell death (Torres et al., 2002, 2005, 2005a). However, the mechanistic details for this dual role of RBOH-mediated ROS remain to be known.

The importance of ROS in the context of nematode-plant interaction has been shown in a few studies. First analyses to demonstrate the involvement of ROS-related metabolites were performed on tomato plants infested by *Meloidogyne incognita* (Zacheo et al.,1982).Using enzymatic activity assays, they investigated the activities

of peroxidase and superoxide dismutase (SOD) in resistant and susceptible tomato cultivars and found out that SOD activity increases in susceptible cultivars upon nematode infection. However, the activity of SOD was slightly decreased in resistant cultivars after inoculation with nematodes. In a following study, the same authors investigated the involvement of superoxide in the susceptible and resistant interaction of tomato plants to *Meloidogyne incognita* attack. They found out that the generation of superoxide, as identified by reduction of nitroblue tetrazolium, is enhanced during nematode infection in resistant tomato roots. The reduction of NBT is further increased by addition of NADPH in reaction medium hinting the involvement of NADPH oxidase in resistant response (Zacheo and Bleve-Zacheo, 1988). In line with these findings is a recent study which shows that the hypersensitive cell response (HR) in resistant tomato plants carrying *Mi* resistance gene prevented the establishment of an avirulent pathotype of *M. Incognita*. In contrast, the virulent pathotype overcame the *Mi* resistance and induced feeding sites without triggering a HR (Melillo et al. 2006). These data also showed that generation of ROS in the form of an oxidative burst occurs very early both during host and non-host interaction. Nevertheless, intensity and duration of oxidative burst is enhanced in cells undergoing HR (Melillo et al. 2006).

Waetzig et al. (1999) for the first time showed the localization of ROS in plant-nematode interactions. The authors found that the *Arabidopsis* roots shows symptoms of HR during an incompatible interaction with soybean cyst nematode *Heterodera glycines.* Although, the source of ROS in this study was not investigated, the plasma membrane localization of ROS led these authors to suggest that plasma membrane-based oxidases might be responsible for the ROS production (Grundler *et al.*,1997; Waetzig et al. 1999) In another study, it has been shown that wheat apoplastic peroxidase genes has different expression patterns in resistant and susceptible varieties and might be responsible for the different responses of plants to the cyst nematode *Heterodera avenae* (Simonetti et al., 2009).

Plant hormones

Plant hormones are signaling molecules that are produced and secreted by different cells and regulate a number of processes in plants at very low concentrations. Plant support diverse functions, such as the development of leaves, flowers, root, fruit ripening or seed growth, and it has been shown that a number of plant hormones are involved in regulation of these processes. In the last years, diverse plant hormones have been identified like brassinosteroids or polyamines, but best known are the classical five plant hormones: cytokinin, abscisic acid (ABA), gibberelline, ethylene and auxin (reviewed by Kende and Zeevaart, 1997). The cytokinins are mainly responsible for shoot formation, cell division, cytokinesis, differentiation and delayed tissue senescence, whereas ABA is often produced under stress situations and affects bud and fruit growth, seed dormancy and germination. Gibberellins tend to have functions similar to those of ABA but they also mobilize storage materials during seed germination, are responsible for the elongation of stems and can induce flowering under non-inductive conditions. Ethylene has a destructive character because it is mainly synthesized during the abscission of leaves, senescence of flowers and ripening of fruit. Based on the results of my current work, the plant hormone auxin will be described in more detail here.

Auxins are among most important growing substances in plants and belong to the class of hormones with morphogen-like characteristics. These molecules are specifically required for cell division and expansion, lateral root initiation, flowering and tropic responses (Davies, 2010). To establish these findings, a number of bioassays with Arabidopsis mutants have been conducted, including overexpression lines that present significantly increased number of lateral roots and hypocotyls as well as epinastic leaves and cotyledons (Boerjan *et al*., 1995; Delarue *et al*., 1998; Zhao *et al*., 2001). In contrast, mutants that lack auxin synthesis display a long primary root, but limited number of short lateral roots and hypocotyls. It has also been shown that plants produce four different auxins, namely, indole-3-acetic acid (IAA), 4-chloroindole-3-acetic Acid (4-Cl-IAA), indole-3-butyric Acid (IBA) and phenylacetic acid (PAA) (Simon, 2011). IAA is mainly responsible for the major effects during plant development and signaling. The structure of these auxins varies; however, they have an aromatic ring and a carboxylic acid group in common.

Auxin is regulated by two different pathways in Arabidopsis*:* tryptophan (Trp)-dependent and Trp -independent. The precursors of both pathways are synthesized in chloroplasts via the shikimate pathway and start with chorismate (Fig.4). In the Trp-independent pathway, indole-3-glycerol phosphate (IGP) and indole act as precursors; however, the subsequent biochemical pathway leading to IAA is not well understood (Zhang et al., 2008). The precursor of the Trp-dependent pathways is L-Trp, which is synthesized from indole by Trp-synthase and localized in the cytosol. Two different Trp-dependent pathways leading to IAA have been identified in Arabidopsis: the IAM pathway, in which tryptophan is converted to indole-3-aceramide by Trp-monooxygenase (iaamM) and the IPA pathway where Trp-aminotransferase (TAA1) synthesizes Indole-3-pyruvic acid (Mano and Nemoto, 2012).

Young shoots are the main source of auxin synthesis, which are transported to destination tissues (Morris et al., 1969). Recently, additional plant compartments have been recognized as capable of producing auxin in significant amounts (Ljung et al., 2001, Petersson et al., 2009) including roots, particularly the meristematic primary root tips (Ljung et al., 2005).

The transport of auxin involves two different modes. Long distance transport from source to sink is managed through vascular tissue (non-polar transport in phloem), whereas the cell-to-cell transport is regulated by specific membrane-bound polar auxin transport proteins. In Arabidopsis, four putative auxin influx carriers (AUX1, LAX1, LAX2, LAX3) and 2 groups of proteins which are involved in auxin export (PIN and MDR/PGP) have been identified (Parry et al., 2001, Petrásek et al., 2006; Mravec et al., 2008).

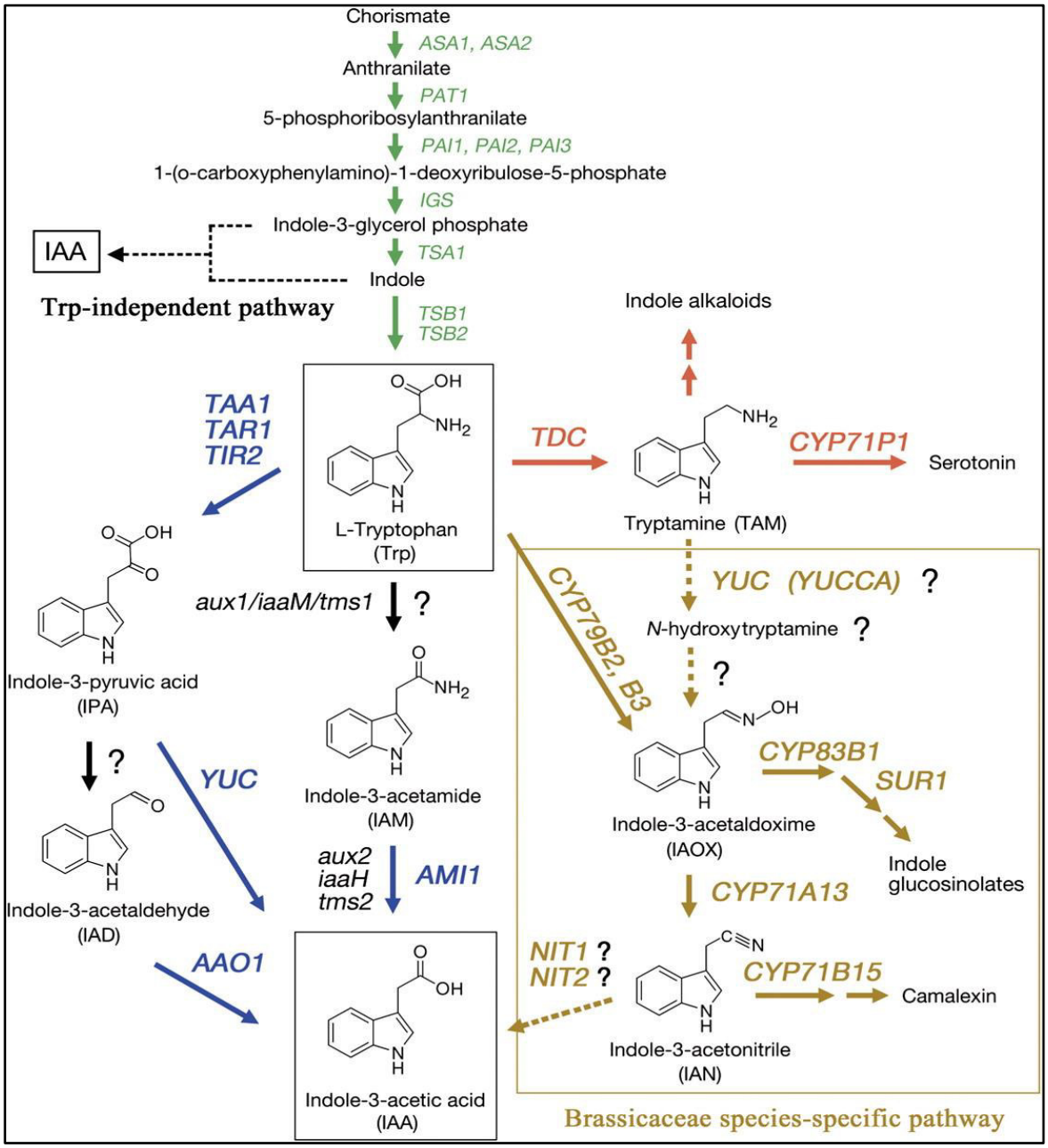

Figure 4. Presumptive pathways for IAA biosynthesis in plants. Green arrows indicate the tryptophan synthetic pathway in the chloroplast. A thin dashed black arrow denotes the tryptophan-independent IAA biosynthetic pathway. Blue arrows indicate steps for which the gene and enzymatic function are known in the tryptophan-dependent IAA biosynthetic pathway. Red arrows indicate the indole alkaloid and serotonin biosynthetic pathway. Mustard-coloured arrows indicate the Brassicaceae species-specific pathway. Black arrows indicate steps for which the gene(s) and enzymatic function(s) are unknown. Dashed mustard-coloured arrows indicate steps for which the gene and enzymatic function(s) remain poorly understood. Letters in italics show genes involved in the conversion process. Lower case letters in italics indicate bacterial genes (Mano and Nemoto, 2012).

Role of auxin during plant-nematode interaction

Plant hormones are not only responsible for the signaling network of developmental and environmental processes in plants, but they also play an important role during stress situations such as drought, cold and pathogen attack. “Defense hormones” such as jasmonic acid, ethylene and salicylic acid, have already been well described and established in the context of plant-pathogen interactions, however additional hormones are suggested to play an important role during defense responses. This assumption is supported by the fact that hormones often interact with each other via suppression, e.g. salicylic acid and auxin (Wang et al., 2007) or enhancement, e.g. auxin and ethylene (Swarup et al., 2002)

Pathogens such as nematodes establish a close relationship with their host and are capable of manipulating the host’s gene expression to facilitate their infection. Because of the importance of auxin during root growth, auxin was thought to require during the induction and development of syncytium. Moreover, lateral root formation and syncytium formation have certain common features, including initiation in the differentiated root zone, cell cycle reactivation, and a subsequent dedifferentiation processes. In addition, large-scale screens of promoter trap lines have shown that that lateral roots and feeding cells express a huge number of similar genes (Scheres et al., 1997).

By the early 1960s, indole compounds, which are the precursors of auxin, had been found in extracts of tomato roots after infection by *M. incognita* (Balasubramanian et al., 1962). In addition, the treatment of peach with NAA, a synthetic auxin, increases its susceptibility to *M. javanica* (Kochba, 1971). Similar observations were made when tomato plants were treated with IAA prior to nematode infection (Glazer et al., 1986). In contrast, studies with auxin-insensitive tomato mutants (*dgt*) demonstrated strongly decreased susceptibility to the potato cyst nematode *Globodera rostochiensis* (Goverse et al., 2000). The authors described that penetration and also migration in the *dgt* roots was normal, but the nematodes were not capable to develop into adult females. Moreover, the mutant tomato plants showed a range of phenotypes including reduced number of cysts per plant (71%), reduction in egg number per cyst, decrease in size of the cysts, and degradation of syncytial cytoplasm as compared to the control. These authors hypothesized that a local

increase of auxin occurs upon nematode infection, which is important for morphogenesis of syncytium. Moreover, a cross-talk between auxin and ethylene was suggested to be important for local activation of host cell wall degrading enzymes. The role of cell wall degradation for syncytium formation has already been discussed above (see: Interactions between cyst nematodes and their hosts).

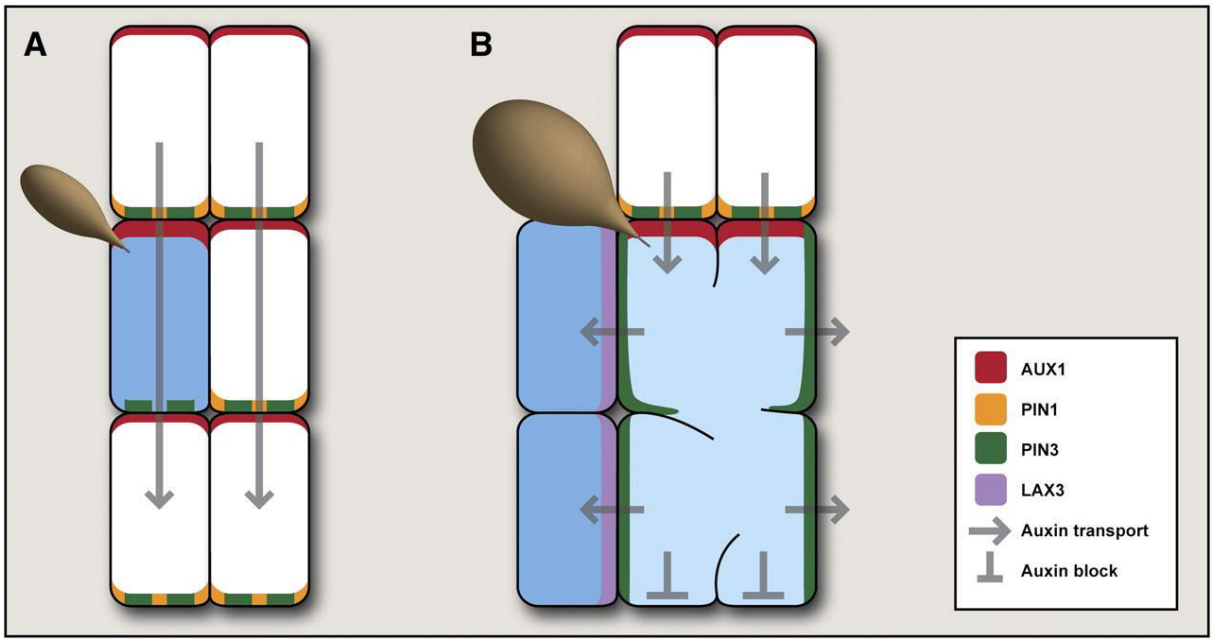

Figure 5. Grunewald et al. (2009) described how Cyst Nematodes manipulate the host auxin transport machinery during syncytium formation in *Arabidopsis thaliana*. In the early stage, auxin (blue colour) is accumulated in the ISC due to increased expression of influx carriers (AUX1) und decrease in efflux carrier (PIN1). To enlarge the syncytium, lateral auxin transport is enhanced by PIN3 and LAX3 supports auxin accumulation in neighboring cells.

Few years later, Grunewald et al. (2009) visualized auxin accumulation at a cellular level during nematode infection by using an auxin responsive reporter line (*DR5::GUS*). They found out that the GUS staining persists in the developing syncytium until two days post inoculation and becomes less specific to the syncytium during the later stages of development. To accumulate auxin at infection site, nematodes must manipulate the cell in such a way that either its influx is increased or efflux is inhibited. Therefore, the authors infected *PIN::GUS* transgenic plants and were capable to show that especially *PIN3* and *PIN4* were specifically and highly expressed during syncytium development. Interestingly, *PIN1* and *PIN7* activity was missing in the developing syncytium and only detectable in the vasculature of infected and uninfected tissue. These findings suggest that nematodes manipulate

not only upregulation of *PIN* expression but also downregulation to facilitate their infection. In Addition, Grunewald et al. (2009) performed infection assays with *pin* mutations resulting in 10-25% reduction in number of cysts, whereby *PIN3* and *PIN4* led only to smaller cysts, indicating their importance in later stages of infection. Other recent studies have shown that also AUX1-mediated auxin influx is enhanced during syncytium formation and early syncytium establishment (Fig.5). However, it remained largely unknown which signals are used by nematodes to manipulate host hormonal network in general and auxin in particular.

References

Alvarez M.E.**,** Pennell R., Meijer P-J., Ishikawa A., Dixon R.A., Lamb C. (1998): Reactive oxygen intermediates mediate a systemic signal network in the establishment of plant immunity. Cell 92: 773-784

Apel K., Hirt H. (2004): Reactive oxygen species: metabolism, oxidative stress, and signal transduction. Plant Biology 55: 373-99

Balasubramanian M., Rangaswami G. (1962): Presence of indole compounds in nematode galls. Nature 194: 774-775

Bardgett R.D., Cook R., Yeates, G.W., Denton C.S. (1999): The influence of nematodes on below-ground processes in grassland ecosystems. Plant and Soil 212: 23-33

Boerjan W., Cervera M. T., Delarue M., Beeckman T., Dewitte W., Bellini C., Inzé D. (1995): Superroot, a recessive mutation in Arabidopsis, confers auxin overproduction. The Plant Cell Online *7*(9): 1405-1419

Böckenhoff A. and Grundler F.M.W. (1994): Studies on the nutrient uptake by the beet cyst nematode *Heterodera schachtii* by in situ microinjection of fluorescent probes into the feeding structures in *Arabidopsis thaliana*. Parasitology 109: 249-254

Brenner S. (1974): The genetics of Caenorhabditis elegans. Genetics 77: 71–94

Bedard K., Krause K-H. (2007): The NOX family of ROS generating NADPH oxidase: Physiology and Pathophysiology. Physiological Reviews 87: 245-313

Cai D.G., Kleine M., Kifle S., Harloff HJ., Sandal N.N., Marcker K.A., KleinLankhorst R.M., Salentijn E.M.J., Lange W., Stiekema W.J., Wyss U., Grundler F.M.W, Jung C., (1997): Positional cloning of a gene for nematode resistance in sugar beet. Science 275: 832-834

Daub M., Heirichs Ch. (2011): Einsatz der Schwadbeprobung von Feldbesatzdichten mit *Heterodera schachtii* im Zuckerübenanbau - dreizehn Jahre Erfahrung aus der Praxis Rheinland. Journal für Kulturpflanzen 63: 9

Davies P.J. (2010): The Plant Hormones: Their nature, occurrence, and functions. Plant hormones. Springer Netherlands 1-15

Decraemer W. and Hunt D.J. (2006): Structure and classification. Plant Nematology. Perry, R.N. and Moens, M. eds., CABI North American Office, 3-32

Delarue M., Prinsen E., Va H., Caboche M., Bellini C. (1998): Sur2 mutations of *Arabidopsis thaliana* define a new locus involved in the control of auxin homeostasis. The Plant Journal 14(5): 603-611

Feng B., Shan L. (2014): ROS open roads to roundworm infection. Science signaling *7*(320): pe10

Ferraz L.C.C.B., Brown D.J.F. (2002): An introduction to Nematodes: Plant Nematology Pensoft: sofia, pp. 221

Foreman J., Demidchik V., Bothwell J.H., Mylona P., Miedema H., Torres M.A., Linstead P., Costa S., Brownlee C., Jones J.D. (2003): Reactive oxygen species produced by NADPH oxidase regulate plant cell growth. Nature 422: 442-446

Gardner M., Verma A., Mitchum M. G. (2015): Emerging roles of cyst nematode effectors exploiting plant cellular processes. Advances in Botanical Research 73: 259-291

Glazer I., Epstein E., Orion D., Apelbaum A. (1986): Interactions between auxin and ethylene in root-knot nematode (*Meloidogyne javanica*) infected tomato roots. Molecular Plant-Microbe Interaction 13: 1121-1129

Georgiou G. (2002): How to flip the (redox) swich. Cell 111(5): 607-610

Golinowski W. (1998): Formation of wall openings in root cells of *Arabidopsis thaliana* following infection by the plant parasitic nematode *Heterodera schachtii*. Plant Pathology 104: 545-551

Goverse A., Overmars H., Engelbertink J., Schots A., Bakker J. (2000): Both induction and morphogenesis of cyst nematode feeding cells are mediated by auxin. Molecular Plant-Microbe Interaction 13: 1121-1129

Graves D.B. (2012): The emerging role of reactive oxygen and nitrogen species in redox biology and some implications for plasma applications to medicine and biology. Journal of Physics 45: 26

Grundler F.M.W., Schnibbe L., Wyss, U. (1991): *In vitro* studies on the behavior of second-stage juveniles of *Heterodera schachtii* (Nematoda: Heteroderidae) in response to host plant root exudates. Parasitology 103: 149-155

Grundler F.M.W., Betka M., Wyss U. (1991): Influence of changes in the nurse cell system (syncytium) on sex determination and development of the cyst nematode *Heterodera schachtii* - Total amounts of proteins and amino-acids. Phytopathology 81: 70-74

Grundler F.M.W., Sobczak M., Lange S. (1997): Defense response of *Arabidopsis thaliana* during invasion and feeding site induction by the plant-parasitic nematode *Heterodera glycines*. Physiol Mol Plant P 50: 419-429

Grundler F.M.W., Sobczak M., Golinowski W. (1998): Formation of wall openings in root cells of *Arabidopsis thaliana* following infection by the plant–parasitic nematode *Heterodera schachtii.* Eur. J. Plant Pathol. 104: 545–551

Grunewald W., Cannoot B., Friml J., Gheysen G. (2009): Parasitic nematodes modulate PIN-mediated auxin transport to facilitate infection. PLoS Pathog 5(1): e1000266

Gubanov N.M. (1951): Giant nematoda from the placenta of celacea; Placentonema gigantissima nov. gen., nov. sp. Doklady Akademii Nauk SSSR 77(6): 1123-1125

Hancock J.T., R. Desikan, S.J. Neill; (2001): Role of reactive oxygen species in cell signaling pathways. Biochemical and Biomedical Aspects of Oxidative Modification, 29(2): 345-350

Hofmann J., El Ashry A., Anwar S., Erban A., Kopka J., Grundler F.M.W. (2010): Metabolic profiling reveals local and systemic responses of host plants to nematode parasitism. Plant Journal 62: 1058-1071

Hofmann J., Szakasits D., Blochl A., Sobczak M., Daxbock-Horvath S., Golinowski W., Bohlmann H., Grundler F.M.W. (2008): Starch serves as carbohydrate storage in nematode-induced syncytia. Plant Physiol 146(1): 228-235

Hussey R.S. (1989): Disease-inducing secretion of plant parasitic nematodes. Phytopathology 27: 123-41

Hussey R.S., Grundler F.M.W. (1998): Nematode parasitism of plants. In: The Physiology and Biochemistry of Free-living and Plantparasitic Nematodes (Perry, R.N. and Wright, D.J., eds), pp. 213-243. Wallingford, UK: CABI Publishing

Jaubert S., Ledger T.N., Laffaire J.B., Piotte C., Abad P., Rosso M.N. (2002): Direct identification of stylet secreted proteins from root-knot nematodes by a proteomic approach. Molecular and Biochemical Parasitology 121(2): 205-11

Jörgensen R.G., Potthoff M., Sauke H. (2004): Zoologie der Wirbellosen. Skript Universität Kassel, S.15ff

Jones J., Gheyson G., Fenoll C. (2011): Genomics and molecular genetics of plant nematode interactions. Chapter 1, 4, 8

Kende H., Zeevaart J. (1997): The five "classical" plant hormones. The plant cell 9(7): 1197

Kearney B., Ronald P.C., Dahlbeck D., Staskawicz B.J. (1988): Molecular basis for evasion of plant host defence in bacterial spot disease of pepper. Nature 332: 541-543

Kochba J., Samish R.M. (1971): Effect of kinetin and 1-naphthylacetic acid on root-knot nematodes and tomato. Exp Parasitol 15: 242-248

Kovtun Y., Chiu W-L., Tena G. (2000): Functional analysis of oxidativ stress-activated mitogen-activated protein kinase cascade in plants. Proc Natl Ascad Sci USA 97: 2940-2945

Lamp C., Dixon R.A. (1997): The oxidative burst in plant disease resistance. Plant Physiology 48: 251-75

Lewis S.A., David J., Chitwood D.J. and McGawley E.C. (2004): Nematode biology, morphology, and physiology. Dekker Encyclopedia of Plant and Crop Science 781-783

Levine A., Tenhaken R., Dixon R., Lamb C.J. (1994): H_2O_2 from the oxidative burst orchestrates the plant hypersensitive disease resistance response. Cell 79: 583–593

Ljung K., Bhalerao R.P., Sandberg G. (2001): Sites and homeostatic control of auxin biosenthesis in *Arabidopsis* during vegetative growth. Plant Journal 28: 465-474

Ljung K., Hull A.K., Celenza J., Yamada M., Estelle M., Normanly J., Sandberg G. (2005): Sites and regulation of auxin biosynthesis in Arabidopsis roots. Plant Cell 17: 1090-1104

Lelivelt C.L.C., Hoogendoorn J. (1993): The development of juveniles of *Heterodera schachtii* in roots of resistant and susceptible genotypes of S*inapis alba, Brassica napus, Raphanus-sativus* and Hybrids. Netherlands Journal Plant Pathology 99: 13-22

Mano Y., Nemoto K. (2012): The pathway of auxin biosynthesis in plants. J.Exp.Bot 63: 2853-2872

Miller G., Schlauch K., Tam R., Cortes D., Torres M., Shulaev V., Dangle J.L., Mittler R. (2009): The plant NADPH oxidase RBOHD mediates rapid systematic signaling in response to diverse stimuli. Science Signal 2(84): ra45-ra45

Mittler R., Vanderauwera S., Gollery M., Van Breusegem F. (2004): Reactive oxygen gene network in plants. Trends Plant Science 9: 490-498

Mou Z., Fan W., Dong X. (*2003*): Inducers of plant systemic acquired resistance regulate NPR1 function through redox changes. Cell 113*:* 935–944

Mravec J., Kubeš M., Bielach A., Gaykova V., Petrášek J., Skůpa P., Friml J. (2008): Interaction of PIN and PGP transport mechanisms in auxin distribution-dependent development. Development, 135(20): 3345-3354

Mur L.A.J., Kenton P., Lloyd A.J., Ougham H., Prats E. (*2008*): The hypersensitive response; the centenary is upon us but how much do we know? J Exp Bot 59*:* 501–520

Parry R.N., Moens M., (2006): Plant Nematology. CABI S. 155ff.

Petersson S.V., Johansson A.I., Kowalczyk M., Makoveychuk A., Wang J.Y., Moritz T., Grebe M., Benfey P.N., Sandberg G., Ljung K. (2009): An auxin gradient and maximum in the *Arabidopsis* root apex shown by high-resolution cell-specific analysis of IAA distribution and synthesis. Plant Cell 21: 1659-1668

Padgett H.S., Beachy R.N. (1993): Analysis of a tabacco mosaic virus strain capable of overcoming N gene-mediated resistance. The Plant Cell 5: 577-586

Poinar G.O.J. (1979): Nematodes for biological control of insects. CRC Press INC.

Poinar G.O.J., Thomas G.M., Hess R. (1977): Characteristics of the specific bacterium associated with *Heterorhabditis bacteriophora* heterorhabditidae rhabditida. Nematologica 23*:* 97–102

Ranocha, P.H. (2010): *Walls are thin 1* (*WAT1*), an *Arabidopsis* homolog of *Medicago truncatula NODULIN21*, is a tonoplast-localized protein required for secondary wall formation in fibers. Plant Journal 63: 469–483

Scheres B., Sijmons P.C., Van den Berg C., McKhann H., De Vrieze G., Willemsen V. and Wolkenfelt H. (1997): Root anatomy and development, the basis for nematode parasitism. Cellular and Molecular Aspects of Plant-Nematode Interactions 25-37

Siddique S., Endres S., Atkins J.M., Szakasits D., Wieczorek K., Hofmann J., Blaukopf C., Urwin P.E., Tenhaken R., Grundler F.M.W., Kreil D.P., Bohlmann H. (2009): Myo-inositol oxygenase genes are involved in the development of syncytia induced by *Heterodera schachtii* in *Arabidopsis* roots. New Phytologist 184: 457-472

Sikora A., Bridge J., (2005): Plant parasitic nematodes, S. 15ff.

Sijmons P.C. (1993): Plant-nematode interaction. Plant Molecular Biology 23: 917-931

Simon S., Petrášek P. (2011): Why plants need more than one type of auxin. Plant Science 180(3): 454–460

Simonetti E., Veronico P., Melillo M.T., Delibes A., Andres M.F., Lopez-Brana I. (2009): Analysis of Class 3 Peroxidase Genes Expressed in Roots of Resistant and Susceptible Wheat Lines infected by *Heterodera avenae*. Molecular Plant-Microbe Interaction 22 (9): 1081-1092

Smant G., Stokkermans J.P.W.G., Yan Y. (1998): Endogenous cellulose in animals: Isolation of beta-1,4-endoglucanase genes from two species of plant-parasitic cyst nematodes. PNAS 95: 4906-4911

Sobczak M., Golinowski W. (2011): Cyst nematodes and syncytia. Genomics and Molecular Genetics of Plant-Nematode Interactions 61-82

Swarup R., Parry G., Graham N., Allen T., Bennett M.J**.** (2002): Auxin cross-talk: integration of signalling pathways to control plant development. Plant Molelecular Biology 49**:** 411–426

Szakasits D., Heinen P., Wieczorek K., Hofmann J., Wagner F., Kreil D.P., Sykacek P., Grundler F.M.W., Bohlmann H. (2009): The transcriptome of syncycia induced by the cyst nematode *Heterodera schachtii* in *Arabidopsis* roots. The plant Journal 57: 71-784

The C. elegans Sequencing Consortium (1998): Genome sequence of the nematode *C. elegans*: A platform for investigating biology. Science 282: 2011-2046

Torres M.A., Jones J.D.G., Dangl J.L. (2006): Reactive oxygen species signaling in response to pathogens. Plant Physiology 141(2): 373-378

Torres M.A., Dangl J.L., Jones J.D. (2002): *Arabidopsis* gp91phox homologues AtrbohD and AtrbohF are required for accumulation of reactive oxygen intermediates in the plant defense response. Proc Natl Acad Sci USA 99: 517–522

Torres M.A., Onouchi H., Hamada S., Machida, Ch., Hammond-Kosack K., Jones J.D.G. (1998): Six *Arabidopsis thaliana* homologues of the human respiratory burst oxidase (gp91phox). The plant journal 14(3): 365-370

Torres M.A., Jones J.D.G., Dangl J.L. (2005): Pathogen-induced, NADPH oxidase-derived reactive oxygen intermediates suppress spread of cell death in *Arabidopsis thaliana*. Nature Genetics 37: 10

Torres M.A., Dangl J.L. (2005a): Functions of the respiratory burst oxidase in biotic interactions, abiotic stress and development. Plant Biology 8: 397-403

Trudgill D.L. (1976): Effect of Environment on Sex Determination in *Heterodera Rostochiensis.* Nematologica 13(2): 263

Ugarte C., Zaborski E., Wander M.M. (2013): Nematodes indicators as integrative measures of soil condition in organic cropping systems. Soil Biology and Biochemistry 64: 103-113

Vanholme B., De Meutter J., Tytgat T., Van Montagu M., Coomans A., Gheysen G., (2004): Secretions of plant-parasitic nematodes: a molecular update. Gene 332: 13-27

Vos P., Simons G., Jesse T., Wijbrandt J., Heinen L., Hogers R., Frijters A., Groenendijk J., Diergaarde P., Reijans M., Fierens-Onstenk J., de Both M., PelemanJ., Liharska T., Hontelez J., Zabeau M. (1998): The tomato *Mi-1* gene confers resistance to both root-knot nematodes and potato aphids. Nature Biotechnology 16: 1365-1369

Waetzig, Georg H., Grundler, F.M.W., Sobczak M., (1999): Localization of hydrogen peroxide during the defence response of *Arabidopsis thaliana* against the plant-parasitic nematode *Heterodera glycines*. Nematology 1(7-8): 681-686

Wang D., Pajerowska-Mukhtar K., Hendrickson Culler A., Dong X. (2007): Salicylic acid inhibits pathogen growth in plants through repression of the auxin signaling pathway. Current Biology 17: 1784-1790

Williamson V.M., Gleason C.A., (2003): Plant-nematode interactions; Current Opinion in Plant Biology 6(5): 327-333

Wieczorek K., Golecki B., Gerdes L., Heinen P., Szakasits D., Durachko D. M., Grundler, F.M.W. (2006): Expansins are involved in the formation of nematode-induced syncytia in roots of *Arabidopsis thaliana*. The Plant Journal 48(1): 98-112

Wieczorek K., Hofmann J., Blöchl A., Szakasits D., Bohlmann H., Grundler, F.M.W. (2008): Arabidopsis endo-1,4-β-glucanases are involved in the formation of root syncytia induced by *Heterodera schachtii*. The Plant Journal 53: 336–351.

Wieczorek K., El Ashry A., Quentin M., Grundler F.M.W., Favery B., Seifert G., Bohlmann H. (2014): A distinct role of pectate lyases in the formation of feeding structures induced by cyst and root-knot nematodes. MPMI 27: 901-912

Wojtaszek P. (1997): Oxidative burst: an early plant response to pathogen infection; Biochemical Journal 322: 681-692

Wyss U., Grundler F.M.W. (1992): Feeding-behaviour of sedentary plant parasitic nematodes. Netherlands Journal of Plant Pathology 98: 165-173

Wyss U., Zunke U. (1986): Observations on the behaviour of second stage juveniles of *Heterodera schachtii* inside host roots. Revue Nematology 9(2): 153-165

Zacheo G., Bleve-Zacheo T., Lamberti F. (1982): Role of peroxidase and superoxide dismutase activity in resistant and susceptible tomato cultivars infested by *Meloidogyne incognita*. Nematologia mediterranea 10: 75-80

Zacheo G., Bleve-Zacheo T. (1988): Involvement of superoxide dismutases and superoxide radicals in the susceptibility and resistance of tomato plants to *Meloidogyne incognita* attack. Physiological and molecular plant pathology 32(2): 313-322

Zhao Y., Christensen S. K., Fankhauser C., Cashman J. R., Cohen J. D., Weigel D., Chory J. (2001): A role for flavin monooxygenase-like enzymes in auxin biosynthesis. Science 291(5502): 306-309

Chapter 2

Parasitic Worms stimulate host NADPH oxidases to produce reactive oxygen species that limit cell death and promotes infection

Shahid Siddique, Christiane Matera, Zoran S. Radakovic, M. Shamim Hasan, Philipp Gutbrod, Elzbieta Rozanska, Miroslaw Sobczak, Miguel Angel Torres and Florian M. W. Grundler

Science Signaling (2014)

Vol. 7, Issue 320, pp. ra33
DOI: 10.1126/scisignal.2004777

Science Signaling
AAAS

` Parasitic Worms Stimulate Host NADPH Oxidases to Produce Reactive Oxygen Species That Limit Plant Cell Death and Promote Infection

Shahid Siddique, Christiane Matera, Zoran S. Radakovic, M. Shamim Hasan, Philipp Gutbrod, Elzbieta Rozanska, Miroslaw Sobczak, Miguel Angel Torres and Florian M. W. Grundler (8 April 2014)
Science Signaling **7** (320), ra33. [DOI: 10.1126/scisignal.2004777]

HOST-PATHOGEN INTERACTIONS

Parasitic Worms Stimulate Host NADPH Oxidases to Produce Reactive Oxygen Species That Limit Plant Cell Death and Promote Infection

Shahid Siddique,[1]* Christiane Matera,[1]* Zoran S. Radakovic,[1] M. Shamim Hasan,[1,2] Philipp Gutbrod,[1] Elzbieta Rozanska,[3] Miroslaw Sobczak,[3] Miguel Angel Torres,[4] Florian M. W. Grundler[1]†

Plants and animals produce reactive oxygen species (ROS) in response to infection. In plants, ROS not only activate defense responses and promote cell death to limit the spread of pathogens but also restrict the amount of cell death in response to pathogen recognition. Plants also use hormones, such as salicylic acid, to mediate immune responses to infection. However, there are long-lasting biotrophic plant-pathogen interactions, such as the interaction between parasitic nematodes and plant roots during which defense responses are suppressed and root cells are reorganized to specific nurse cell systems. In plants, ROS are primarily generated by plasma membrane–localized NADPH (reduced form of nicotinamide adenine dinucleotide phosphate) oxidases, and loss of NADPH oxidase activity compromises immune responses and cell death. We found that infection of *Arabidopsis thaliana* by the parasitic nematode *Heterodera schachtii* activated the NADPH oxidases RbohD and RbohF to produce ROS, which was necessary to restrict infected plant cell death and promote nurse cell formation. RbohD- and RbohF-deficient plants exhibited larger regions of cell death in response to nematode infection, and nurse cell formation was greatly reduced. Genetic disruption of *SID2*, which is required for salicylic acid accumulation and immune activation in nematode-infected plants, led to the increased size of nematodes in RbohD- and RbohF-deficient plants, but did not decrease plant cell death. Thus, by stimulating NADPH oxidase–generated ROS, parasitic nematodes fine-tune the pattern of plant cell death during the destructive root invasion and may antagonize salicylic acid–induced defense responses during biotrophic life stages.

INTRODUCTION

NADPH (reduced form of nicotinamide adenine dinucleotide phosphate) oxidase is a heteromultimeric enzyme complex involved in ROS production and immune response in a wide variety of organisms (*1*). The NADPH oxidase heavy chain subunit gp91^{phox} (also known as CYBB and NOX2) promotes the transfer of electrons to diatomic oxygen to generate superoxide anion (O_2^-) (*2*). The generation of superoxide starts a cascade of reactions that result in production of several highly reactive oxygen–derived small molecules collectively called reactive oxygen species (ROS).

Respiratory burst oxidase homologs (Rbohs), the plant homologs of *GP91PHOX*, are encoded by 10 genes in *Arabidopsis thaliana* (*RbohA* to *RbohJ*) (*3*–*5*). Rbohs generate ROS in response to bacterial and fungal pathogens (*3*, *6*), and genetic disruption of specific *Rbohs* alters plant responses to pathogens (*7*–*9*). In *A. thaliana*, loss of *RbohF* enhances cell death and increases resistance to a weakly virulent strain of the oomycete *Hyaloperonospora parasitica* (*3*). In contrast, in *Nicotiana benthamiana*, silencing of *RbohA* and *RbohB* reduces cell death and impairs plant resistance to infection by the oomycete *Phytophthora infestans* (*8*). These results point to a pathosystem-specific, sophisticated role of *Rbohs* in plant responses in infection.

Salicylic acid (SA) is a signaling molecule involved in plant defense against infection and interacts with ROS signaling. The concentration of SA increases in cells surrounding the infection site during the hypersensitive resistance response, a mechanism characterized by rapid death of the plant cells surrounding the infection site (*10*–*12*). ROS and SA form a feed-forward loop leading to induction of defense gene expression and cell death (*13*, *14*). In *A. thaliana*, loss of the gene encoding the zinc finger protein LSD1 (lesion stimulating disease 1), which inhibits SA-dependent cell death, results in runaway cell death phenotype (*15*). Plants with loss-of-function mutations in *LSD1* and *RbohD* or *LSD1* and *RbohF* have enhanced SA-induced cell death compared to those with *lsd1* mutations alone, suggesting that Rboh-derived ROS antagonize SA-dependent death signals to limit the spread of cell death during successful recognition of pathogens (*16*). Although there is evidence for a role of Rboh-derived ROS in resistance and cell death in different plant pathosystems, little is known about whether and how ROS might mediate biotrophic relationships.

Heterodera schachtii is a cyst nematode that establishes a biotrophic relationship with the roots of sugar beets and brassicaceaous plants, including *A. thaliana*. Second-stage juvenile (J2) nematodes invade plants primarily in the elongation zone above the root tips (*17*). After invasion, nematodes pierce individual root cells with their stylet, enter them, and travel through multiple cells to the vascular cylinder, leaving a path of collapsed, necrotic cells inside the root. In the vascular cylinder, nematodes use gentle stylet probing to identify cells that resist collapse and can serve as an initial syncytial cell (ISC) (*17*, *18*). Nematodes secrete factors through the stylet into the ISC that trigger partial dissolution of the cell wall and fusion of the ISC with neighboring root cells to form a multinucleate, hypertrophied, metabolically active nurse cell syncytium of more than 200 cells (*17*). Nematodes become sedentary and then form feeding tubes that connect the lumen of the stylet with the cytoplasm of the nurse cell. Feeding nematodes mature after three molts (J3, J4, and adult) over 2 weeks (*17*). Whereas females maintain interaction with the host plant, males cease

[1]Institute of Crop Science and Resource Conservation, Department of Molecular Phytomedicine, University of Bonn, 53115 Bonn, Germany. [2]Department of Plant Pathology, Faculty of Agriculture, Hajee Mohammad Danesh Science and Technology University, Dinajpur 5200, Bangladesh. [3]Department of Botany, Warsaw University of Life Sciences (SGGW), 02-787 Warsaw, Poland. [4]Centro de Biotecnología y Genomica de Plantas (UPM-INIA), ETSI Agrónomos, Universidad Politecnica de Madrid, Pozuelo de Alarcón, 28223 Madrid, Spain.
*These authors contributed equally to this work.
†Corresponding author. E-mail: grundler@uni-bonn.de

feeding after J3 (*19*). Accordingly, syncytia associated with female nematodes are larger than those associated with males (*20*). Moreover, under adverse conditions, such as nurse cell degeneration in resistant plant genotypes, more male than female nematodes develop. It is unknown whether this phenomenon results from epigenetic influences on sex determination or differences in the mortality of females and males (*21*, *22*). Here, we characterized the role of Rboh-dependent ROS in establishing a biotrophic relationship between *A. thaliana* and *H. schachtii*.

RESULTS

RbohD and RbohF promote nematode parasitism

RbohD or RbohF loss of function increases the susceptibility of host plants to infection by fungi or bacteria (*3*, *6*, *8*). We asked whether *A. thaliana* Rboh-family NADPH oxidases were involved in *H. schachtii* infection. We grew plants in agar medium under sterile conditions, and when the roots had spread through the agar, we inoculated cultures with 60 to 70 nematodes. We found that plants with loss-of-function mutations in *rbohD* or *rbohD* and *rbohF* (*rbohD/F*), but not *rbohA*, *rbohB*, *rbohC*, *rbohE*, *rbohF*, *rbohG*, or *rbohH*, showed reduced numbers of female nematodes present within roots 14 days after inoculation (dai) compared to wild-type (Col-0) plants (Fig. 1A and fig. S1A). In addition, the size of female nematodes and syncytia was significantly smaller in the *rbohD* or *rbohD/F* plants 14 dai (Fig. 1, B and C, and fig. S1, B and C). We also asked whether overexpression of *RbohD* in plants could affect nematode infection by assaying *35S::RbohD* transgenic plants (*16*), which expressed four times more *RbohD* in syncytium containing root segments than Col-0 plants (table S1). The total number of invaded nematodes and the average size of nematodes and syncytia were unchanged in *35S::RbohD* compared to Col-0 plants 14 dai (Fig. 1, A to C). Although the expansion of the syncytium reached its maximum size at about 14 dai, female nematodes continued to grow up to 4 weeks after inoculation. At 25 dai, we found that female nematodes were larger in *35S::RbohD* and smaller in *rbohD* or *rbohD/F* compared to Col-0 plants (Fig. 1D). Thus, RbohD is necessary but not sufficient to promote nematode invasion and growth and may be partially functionally redundant with RbohF in these processes.

To confirm the specificity of these observations, we used two complementary approaches. First, we used transgenic lines overexpressing *RbohD* in *rbohD* plants (*35S::RbohD/rbohD*). Unlike *rbohD* plants, *35S::RbohD/rbohD* plants did not show significant differences in the number of invaded nematodes or in the size of female nematodes or syncytia compared to Col-0 plants (fig. S2, A to D), suggesting that *35S::RbohD* complemented the *rbohD* mutation. Second, we treated plants with the compound diphenyliodonium (DPI), which inhibits Rboh activity (*23*, *24*). Col-0 plants treated with DPI had fewer invaded nematodes 14 dai compared to untreated control plants (Fig. 1E), and both female nematodes and syncytia were smaller (table S2).

DPI is an inhibitor of multiple flavoenzymes and could be toxic to nematodes. However, we found that rearing *Caenorhabditis elegans* larvae on nematode growth medium supplemented with DPI did not affect the number of eggs laid after 3 days (fig. S3A), suggesting that DPI does not affect nematode development and sexual maturation. Moreover, we found that incubating J2 *H. schachtii* in DPI for 5 days (approximately the time required for J2 nematodes to molt into J3 in plants) before inoculation decreased their ability to infect Col-0 plants (fig. S3B), but this effect was smaller than that seen when plants were treated with DPI (Fig. 1E). In addition, the size of female nematodes and syncytia was unchanged in DPI pretreated compared to control *H. schachtii* nematodes

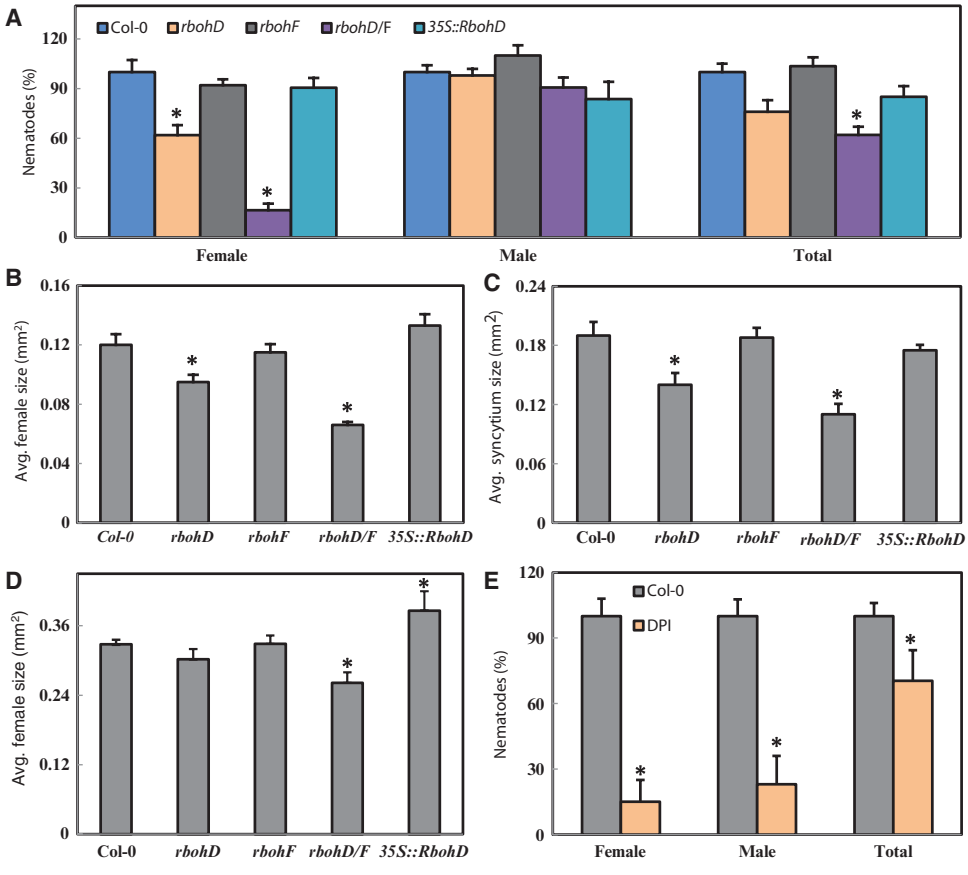

Fig. 1. Nematode infection assays in *Rboh* mutant, *RbohD* overexpressing, and DPI-treated plants. (**A**) Nematodes present in plant roots at 14 dai. Data points represent percent of nematodes where the number of nematodes per square centimeter of root area in Col-0 plants was set to 100%. (**B**) Average size of female nematodes 14 dai. (**C**) Average size of plant syncytia 14 dai. (**D**) Average size of female nematodes 25 dai. (**E**) Nematodes in DPI-treated plants 14 dai. Data points represent percent of nematodes where the number of nematodes per plant in Col-0 plants was set to 100%. For (A) to (E), data points represent three independent experiments (means ± SEM). Data were analyzed using single-factor analysis of variance (ANOVA) ($P < 0.05$). Asterisks indicate $P < 0.05$ compared to Col-0. Dunnett's tests were used for post hoc analyses.

(table S3). Thus, both genetic and pharmacological experiments suggest that Rboh activity is required in plants for successful nematode infection and growth.

Because *rbohD* and *rbohD/F* plants had reduced infection by nematodes, we characterized this process in more detail. We addressed whether reduced infection was due to decreased initial attraction of nematodes to roots by quantifying the number of successful invasions at an earlier time point. At 2 dai, there was no difference in nematode invasions between Col-0 and *rbohD* or *rbohD/F* plants (Fig. 2A). We also asked whether nematode migration or development within the plant was impeded by Rboh deficiency. Through repeated observations of the same invasion sites, we found that more nematodes left their initial invasion site in *rbohD/F* compared to Col-0 plants (Fig. 2B). In addition, more invaded nematodes were dead at 7 dai or failed to undergo sexual differentiation by 10 dai in *rbohD/F* compared to Col-0 plants (Fig. 2B). We assessed whether there could be defects in ISC establishment by monitoring for the cessation of stylet movements in nematodes that invaded roots 4 hours after inoculation (hai) and found that the average time to ISC establishment was increased in *rbohD/F* compared with Col-0 plants (Fig. 2C). Finally, we measured the growth of nematodes and syncytia after ISC establishment. We selected nematodes that successfully established an ISC at 2 dai to eliminate variability due to unsynchronized invasion and monitored their growth over 10 days. Both the nematodes (Fig. 2D) and syncytia (fig. S4) were significantly smaller by 3 dai and grew slower in *rbohD/F* compared to Col-0 plants. Thus, either RbohD or RbohF or both are required for nematode growth as well as ISC establishment and syncytium development, but not initial nematode invasion.

RbohD and RbohF are required for ROS production at early stages of nematode infection

Nematode infection triggers ROS production in plants (*25*). To identify whether RbohD and RbohF were required for this process in *H. schachtii*–infected roots, we visualized ROS with 3,3′-diaminobenzidine (DAB) (*26*) 1 dai. In the majority of Col-0 plants, DAB staining was increased at the site of nematode invasions (Fig. 3, A and B). However, the percent of invasion sites with increased DAB staining was reduced in *rbohD* or *rbohF* plants (Fig. 3, A, C, and D) and DPI-treated Col-0 plants (fig. S5) and eliminated in *rbohD/F* plants (Fig. 3, A and E). Overexpression of RbohD did not affect DAB staining in invaded roots (Fig. 3, A and F). Thus, RbohD and RbohF are required for ROS production during the initial stages of nematode infection.

To confirm the specificity of DAB-visualized ROS production, we labeled plants with 5-(and-6)-chloromethyl-2′,7′-dichlorodihydrofluorescein diacetate (CM-H_2DCFDA), which fluoresces when activated by ROS in living cells (*27*). We used confocal microscopy to monitor fluorescence in invaded roots of plants labeled with CM-H_2DCFDA 1 dai. We found that the extent of CM-H_2DCFDA fluorescence was increased in invaded roots of Col-0 (Fig. 3, G and H), but not *rbohD/F*, plants (Fig. 3I). Thus, during the early stages of nematode infection in plants, *RbohD* and *RbohF* produce ROS, which may support a biotrophic relationship.

RbohD and RbohF prevent cell death during syncytium formation

The delayed ISC selection by nematodes in *rbohD* and *rbohD/F* plants suggested that there could be anatomical changes in the roots that obstruct nematode migration. Using light and transmission electron microscopy, we examined cross sections of roots taken at the border of elongation and the root-hair zones associated with primary growth and at the lateral root formation zone associated with secondary thickening. The anatomy and growth of uninfected roots in both the primary (Fig. 4A) and secondary growth phases (fig. S6) were similar among Col-0 and *Rboh* mutant and overexpressing plants (*28*).

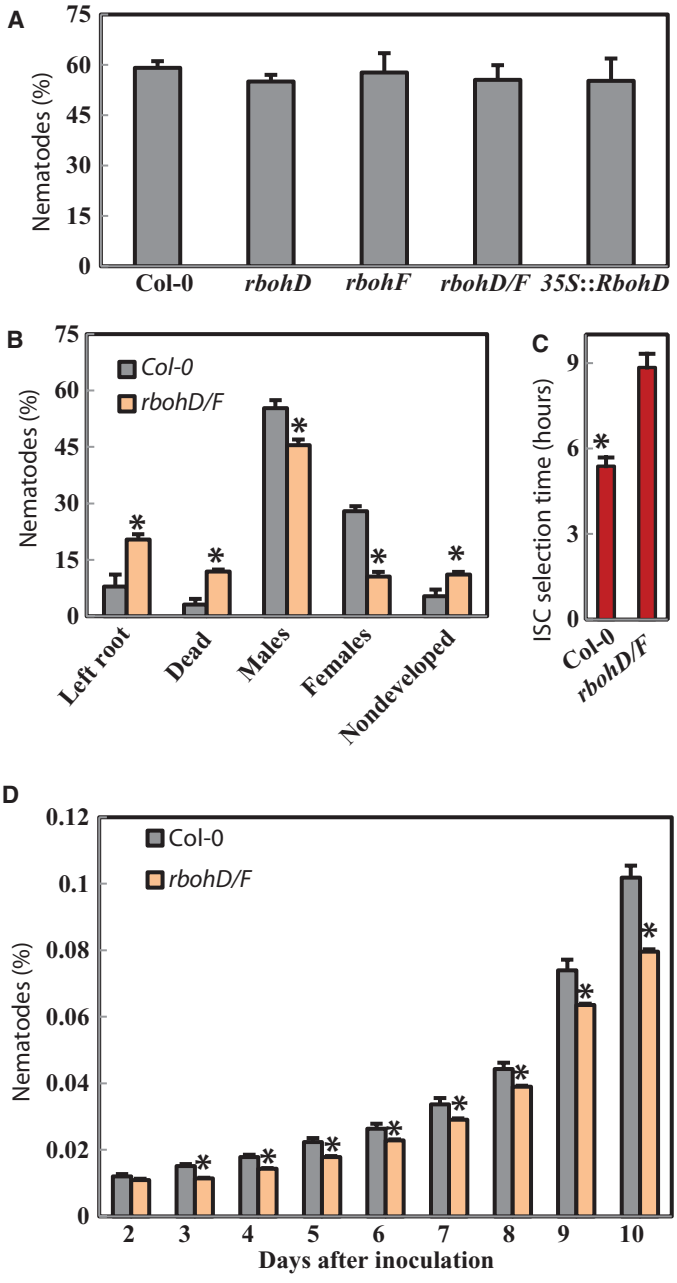

Fig. 2. Nematode infection assays in *Rboh* mutant plants. (A) Nematode invasion at 2 dai. Data represent percent of nematodes where the number of inoculated nematodes was set to 100%. (B) Observation of nematode behavior and development for 10 dai. Data represent percent of nematodes where the number of invaded nematodes was set to 100%. Left root, 3 dai. Dead, 7 dai. Nondeveloped, 10 dai. (C) ISC selection time. (D) Average size of female nematodes over 10 dai. For (A) to (C), data points represent three independent experiments (means ± SEM). Asterisks indicate $P < 0.05$ compared to Col-0 (*t* test).

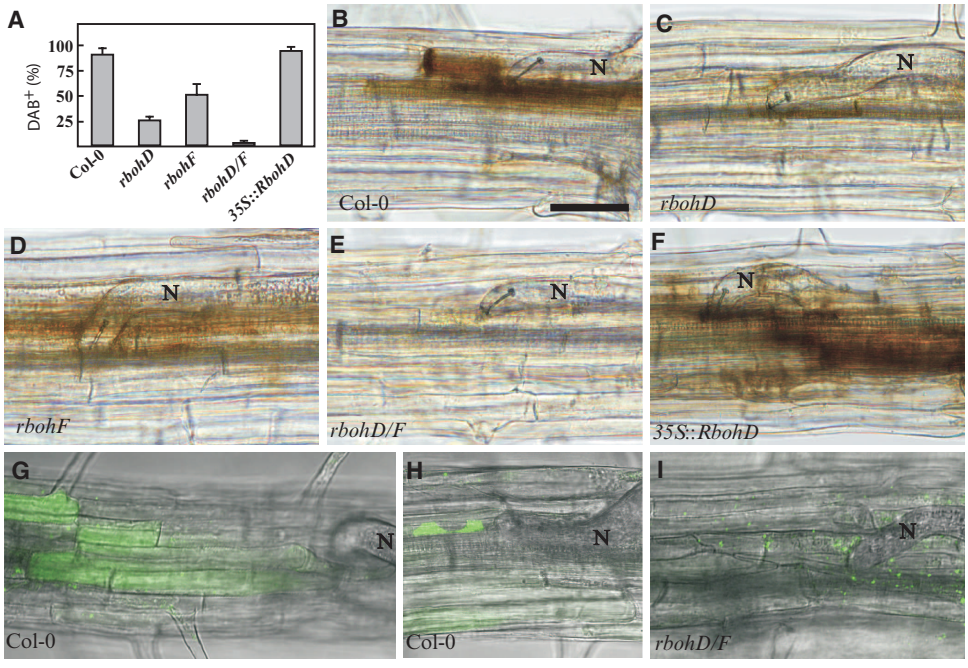

Fig. 3. Visualization of ROS in infected roots. (A) Quantification of DAB staining of ROS shown in (B) to (F). Data represent three independent experiments (means ± SEM). (B to F) DAB staining of ROS 1 dai on infected roots of plants with the indicated genotype. (G to I) CM-H_2DCFDA staining of ROS in living plant roots during migration (G and I) and ISC establishment (H). Scale bar, 50 μm. N, nematode.

To investigate structural changes in response to nematode infection, we analyzed cross sections of roots at 2, 5, and 14 dai. In Col-0, *rbohF*, and *35S::RbohD* plants, we found little evidence of necrosis (Fig. 4, A and B, and fig. S6). In contrast, in *rbohD* and *rbohD/F* plants, we found necrosis as early as 2 dai (Fig. 4A). Ultrastructural analysis suggested that these cells were outside the range of the nematode stylet and had osmiophilic deteriorated protoplasts and thickened cell walls (Fig. 4B). Moreover, depositions of callose-like material were present near cell walls neighboring necrotic cells (Fig. 4B). We found syncytia composed of several hypertrophied cells in Col-0, *rbohF*, and *35S::RbohD* plants 2 dai, whereas *rbohD* or *rbohD/F* plants contained no syncytia or only the ISC (Fig. 4, A and B). At 5 dai (Fig. 4, A and B, and fig. S7) and 14 dai (fig. S6), syncytia in *rbohF* or *35S::RbohD* roots resembled those in Col-0. In contrast, the few syncytia found in *rbohD* or *rbohD/F* roots at these times were smaller and composed of fewer and less hypertrophied cells (Fig. 4, A and B, and figs. S6 and S7). These syncytia had more osmiophilic cytoplasm with plastids containing starch grains (Fig. 4B and fig. S7), and the syncytial cell walls were thin with few openings (Fig. 4B and fig. S7). In *rbohD* or *rbohD/F* roots at 5 and 14 dai, some syncytia showed signs of cellular degradation such as an osmiophilic and flocculent or translucent cytoplasm (fig. S7), whereas other syncytia showed no features of degradation but were smaller in size and composed of fewer hypertrophied cells (fig. S7). These observations suggest that ISC selection is hampered in *rbohD* or *rbohD/F* plants and that necrosis of syncytia can occur at multiple times during its formation.

To confirm that *rbohD* or *rbohD/F* show enhanced syncytial necrosis, we quantified cell death using fluorescein diacetate (FDA) (*29*). We found a significant decrease in FDA fluorescence intensity in *rbohD/F* compared to Col-0 plants at 6 hai and 2 dai (Fig. 5), both during the early migratory stages and when nematodes are establishing the ISC, respectively. Col-0 plants treated with DPI also showed a significant decrease in FDA fluorescence compared to control-treated plants (fig. S8). Thus, cell death is enhanced in the absence of Rboh after nematode infection, implying that ROS produced by RbohD or RbohF or both during nematode migration and ISC selection prevents the activation of the plant defense responses, leading to cell death and enabling nematodes to establish syncytial nurse cells.

ROS limit cell death independent of SA

NADPH oxidases antagonize SA-dependent death-inducing signals during the hypersensitive resistance response in *A. thaliana* (*16*). We used real-time polymerase chain reaction (PCR) to assess changes in the expression of genes that are increased by SA or jasmonic acid signaling, or antioxidant accumulation. By analyzing root sections containing female nematode-associated syncytia 10 dai, we found that the expression of the SA-responsive genes *PR1*, *PR2*, and *PR5* increased in *rbohD/F* plants and that expression of *PR2* and *PR5* decreased in *35S::RbohD* compared to Col-0 plants (Fig. 6). Uninfected roots of *rbohD/F* and *35S::RbohD* plants did not show detectable changes in the expression of *PR* genes compared to control (fig. S9). In contrast, the expression of genes that respond to jasmonic acid signaling and antioxidant accumulation were not consistently changed in *rbohD/F* and *35S::RbohD* plants (Fig. 6 and fig. S9). Thus, the reduced growth of nematodes in *rbohD/F* plants could be due to the activation of local SA-mediated defense responses at infection sites.

To assess whether enhanced cell death in infected *rbohD/F* plants was due to failure in activation of SA-dependent cell death signals, we focused on SID2, a protein in the isochorismate synthase pathway (*30*). Plants with *SID2* loss of function have basal SA but do not increase SA in response to infection (*30*). Thus, we predicted that mutation of *SID2* could increase nematode infection as well as nematode and syncytia size in *rbohD/F* plants. We found that *sid2* plants had more invaded nematodes relative to Col-0 plants at 14 dai (Fig. 7A), indicating that SID2-dependent SA is required to limit nematode infection. However, the size of female nematodes (Fig. 7B) and syncytia (Fig. 7C) did not differ between *sid2* and Col-0 plants, suggesting that SID2 does not interfere with syncytium development or nematode growth. In *rbohD/F sid2* triple-mutant plants (*rbohD/F/sid2*), both the number of invaded nematodes (Fig. 7A) and the size of syncytia (Fig. 7C) were comparable to those of *rbohD/F* plants. Moreover, the size of female nematodes was comparable in *rbohD/F/sid2*, *sid2*, and Col-0 plants (Fig. 7B). Thus, the defect in nematode growth in *rbohD/F* plants is likely independent of SID2-dependent SA, and the retarded growth of female nematodes in *rbohD/F* plants could depend on SA-mediated defense responses.

We assessed whether SID2-dependent SA was required for enhanced cell death in *rbohD/F* plants responding to nematode infection. If SID2 was required for nematode resistance in *rbohD/F* plants, then we would expect to see that *rbohD/F/sid2* plants had reduced cell death compared to *rbohD/F* plants. *rbohD/F/sid2* plants had a significant decrease in

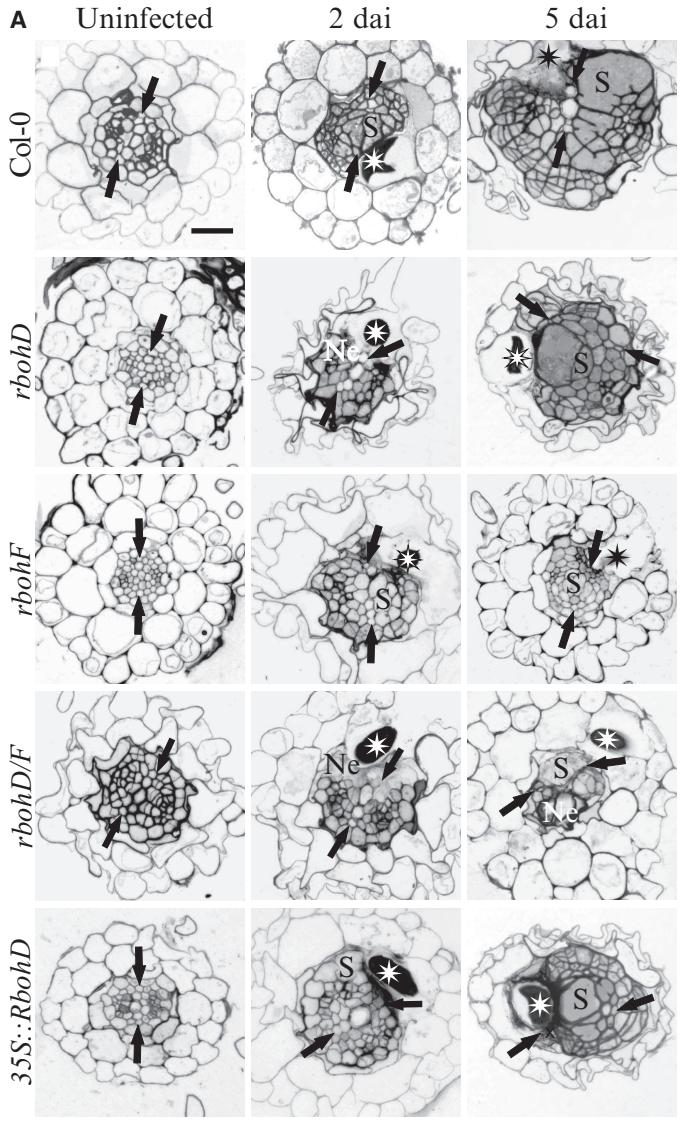

Fig. 4. Microscopic analysis of root anatomy and the development of nematode-induced syncytia in *Rboh* mutant and overexpressing plants. (**A**) Light microscopy micrographs of sections taken at root-hair zone of uninfected plants (left column) and at the nematode head region of infected roots 2 dai (middle column) or 5 dai (right column). Asterisks mark the nematode. Arrows indicate the position of primary xylem bundles. (**B**) Transmission electron microscopy micrographs of sections taken at nematode head region from 2 dai (left column) and 5 dai (right column) roots. Asterisks mark the nematode or the position of the nematode if the section was taken above its head or the head was located outside the field of view. Arrows point to cell wall stubs in syncytia. Triangles mark thickened cell walls. Arrowheads indicate callose depositions, and double arrowheads point to stylet insertion places. Ne, necrosis; S, syncytium; St, stylet; X, xylem vessel. Scale bars, 20 μm (A) and 5 μm (B).

the intensity of the FDA fluorescence at 6 hai compared to Col-0, but not *rbohD/F*, plants (Fig. 7D). These data support the model that the incompatibility of *rbohD/F* plants with the initial establishment of ISC is independent of *SID2*-dependent SA.

We found that loss of RbohD and RbohF increased the expression of SA-dependent genes in nematode-infected plants. To test whether SA was downstream of RbohD and RbohF, we assessed the expression of SA-dependent genes in *rbohD/F/sid2* plants. The expression of *PR1*, *PR2*, and *PR5* was at or below the limit of detection in infected root segments of *rbohD/F/sid2* plants, despite normal amounts of 18*S* (table S4). Thus, we were not able to calculate a fold difference relative to Col-0 plants. Nevertheless, there was no qualitative evidence of a large increase in expression of *PR1*, *PR2*, and *PR5* in *rbohD/F/sid2* compared to Col-0 plants, suggesting that SA-dependent gene expression is inhibited downstream of RbohD and RbohF during nematode infection.

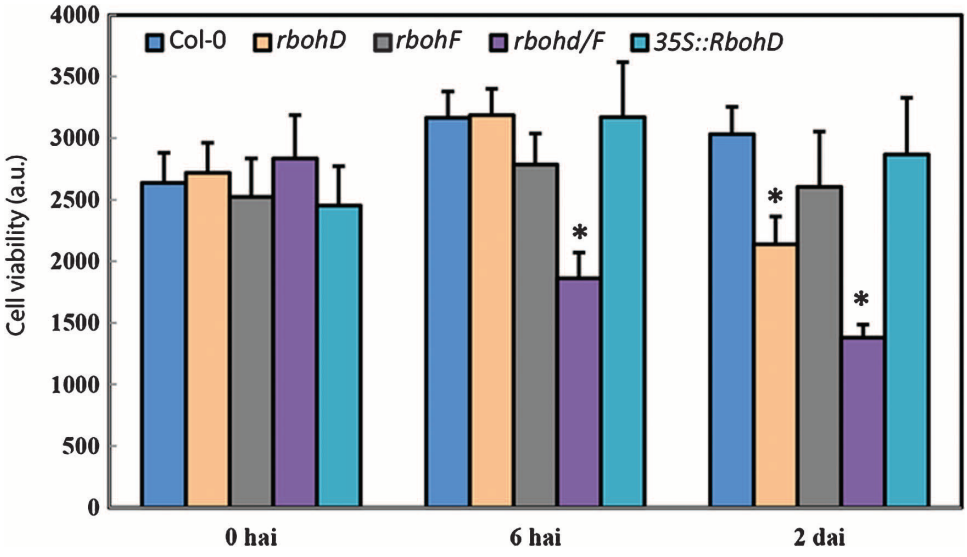

Fig. 5. Cell viability in infected or uninfected root sections of *Rboh* mutant and overexpressing plants. Cell viability depicted as the fluorescence intensity in arbitrary units (a.u.) of FDA staining in plants at the indicated times after inoculation. Data represent eight independent experiments with six root segments per genotype per experiment (means ± SEM). Data were analyzed using ANOVA ($P < 0.05$). Asterisks indicate $P < 0.05$ compared to Col-0. Dunnett's tests were used for post hoc analyses.

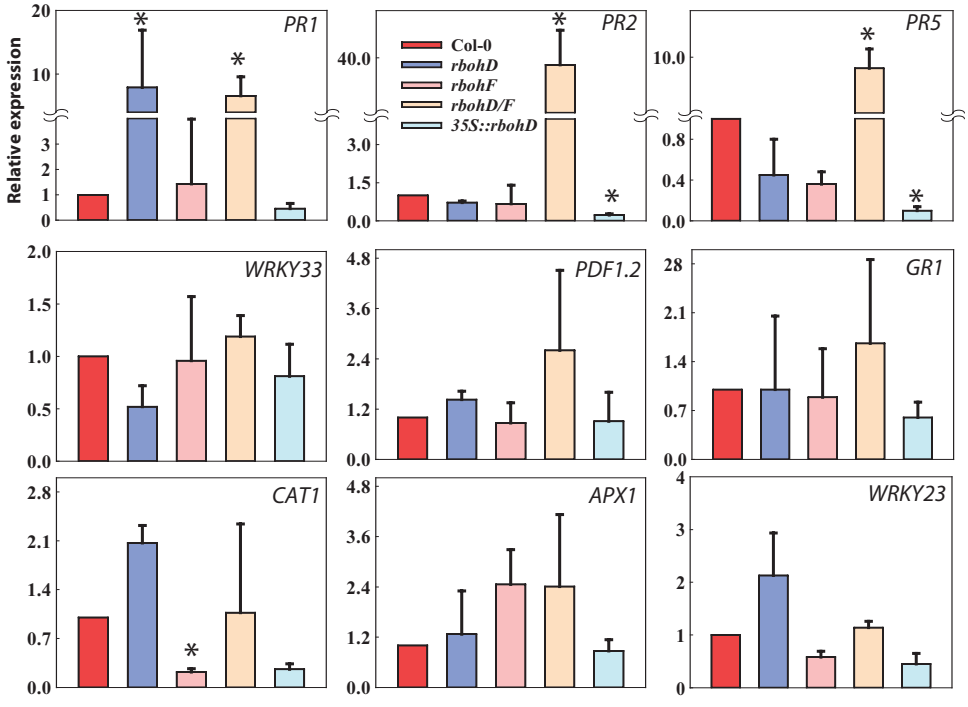

Fig. 6. Gene expression analysis on root segments with developing syncytia 10 dai. Data represent relative expression of the indicated genes with the value in Col-0 plants set to one. Data represent three independent experiments (mean + range). Asterisks indicate $P < 0.05$ compared to Col-0 (*t* test).

DISCUSSION

Rapid production of ROS (oxidative bursts) in the apoplast by NADPH oxidases is an early defense response after the successful recognition of pathogens by the plant immune system (*3*, *6*–*8*). Our analysis revealed that RbohD and RbohF are the main sources of host ROS produced during cyst nematode infections in *A. thaliana*. We predicted that host defense signals downstream of ROS would be inhibited by nematode-derived pathogenicity factors. However, we identified a previously uncharacterized function for RbohD- and RhobF-dependent ROS in facilitating nematode infection and feeding site development.

We propose that the infection of *A. thaliana* by *H. schachtii* proceeds in two phases: In the first phase, nematode invasion of roots and subsequent migration causes cellular damage that triggers cell death. NADPH oxidase–produced ROS disrupt the relay of death-inducing signals between the directly damaged and surrounding cells, thereby preventing the spread of cell death and supporting nematode infection. ROS also contribute to the process of ISC establishment. Thus, the increased cell death seen in *rbohD/F* plants (Figs. 4 and 5) could result from a failure of nematodes to establish syncytia. However, we found that cell death was increased in *rbohD/F* at the site of nematode invasion as early as 6 hai, when the nematodes were still in the migration phase (Fig. 5), suggesting that the failure of ISC establishment is not sufficient to explain all of the increased cell death in these plants. Moreover, because we found that mutation of *SID2* did not enhance nematode infection (Fig. 7A) or decrease early cell death in *rbohD/F* plants (Fig. 7D), we infer that this initial wave of increased cell death is independent of pathogen-induced SA signaling.

In the second phase of nematode infection, the establishment of the ISC and subsequent syncytium expansion is a prerequisite for biotrophic parasitism of the nematode. ROS signaling at infection site inactivates SA-mediated defense responses and enables the growth of nematodes. Consistent with this model, we found that female nematodes that were able to establish syncytia were significantly smaller in *rbohD/F* compared to Col-0 plants (Fig. 7B), but those in *rbohD/F/sid2* plants were not (Fig. 7B). It is possible that the decreased nematode size results indirectly from increased plant cell death in *rbohD/F* plants,

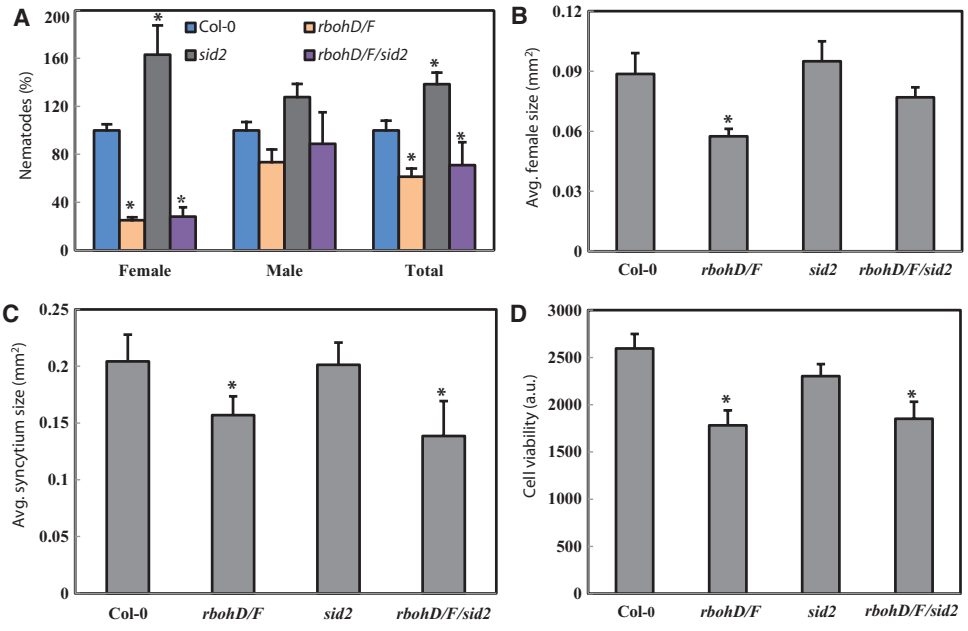

Fig. 7. Nematode infection assay and cell viability in *rbohD/F/sid2* plants. (A) Nematodes present in plant roots 14 dai. Data points represent percent of nematodes where the number of nematodes per plant in Col-0 was set to 100%. (B) Average size of female nematodes 14 dai. (C) Average size of plant syncytia 14 dai. (D) Cell viability depicted as the fluorescence intensity (in arbitrary units) of FDA staining in plants 6 hai. Data represent 10 independent experiments (means ± SEM). Data were analyzed using ANOVA ($P < 0.05$). Asterisks indicate $P < 0.05$ compared to Col-0. Dunnett's tests were used for post hoc analyses.

which would reduce the number of cells available to be included in the syncytia.

Our model is compatible in part with previous findings showing that pathogen-induced ROS suppress the spread of SA-mediated cell death signals in plants after infection (*16*, *31*). It was suggested that RbohD suppresses the spread of cell death by controlling the levels of antioxidants in cells at and around the infection site (*16*). In contrast, we found that the expression of antioxidant genes, *glutathione reductase 1*, *catalase 1*, and *ascorbate peroxidase 1*, did not change in *rbohD/F* roots with established syncytia. Thus, the role of Rbohs in the protection from SA-mediated cell death may not involve these genes.

This model raises the question of whether nematodes release factors that actively stimulate the formation of ROS. *H. schachtii* was found to secrete the effector protein 10A06 into host cells, which interacts with host spermidine synthase 2, leading to increased polyamine oxidase activity in syncytia (*32*). Increased polyamine oxidase may increase the production of ROS that serve as signaling molecules at low concentration for the development or function of syncytia (*32*).

Syncytium formation in host roots is accompanied by widespread transcriptional and metabolic changes in both the infected and systemic plant tissues (*33*, *34*), and ROS could alter these changes. We found that RbohD and RbohF have the capacity to influence SA-dependent gene expression in infected roots. However, Rboh activity may play a broader role in syncytium development and function. Moreover, the fact that RbohD mediates systemic signaling in response to diverse stimuli (*23*) suggests that ROS could be involved in systemic signaling between nurse cells and the host plant.

Suppression of death-inducing signals by ROS in compatible biotrophic interactions is previously uncharacterized. Our results provide further understanding of the molecular mechanism that enables pathogens with destructive invasive behavior to switch to a biotrophic life-style, leading to the establishment of a long-term feeding relationship with the host plant, suggesting a process in the coevolution of a nematode and host plant during which the parasite gains the ability to use NADPH oxidase–mediated cell death regulation to its own benefit.

MATERIALS AND METHODS

Plant material and growth conditions

A. thaliana plants were grown in petri dishes containing agar medium supplemented with modified Knop's nutrient solutions under conditions described previously (*35*). The *rboh* mutants and *35S::RbohD* strains have been described (*3*, *16*). The *Sid2* mutant strain was the allele *sid2-2/eds16-1* (*30*). *rbohD/F/sid2* plants were generated by crossing and confirmed by PCR. The primers are listed in table S5.

Nematode infection assays

Nematodes were inoculated onto the surface of agar medium in petri dishes. For each experiment, 30 plants were used for each genotype. The number of male and female nematodes per plant was counted at 14 dai. Alternatively, the number of nematodes per square centimeter of root area was calculated for *rbohdD*, *rbohF*, *rbohD/F*, or *35S::RbohD* plants for the data shown in Fig. 1A to rule out the influence of root area on nematode infection. For the root area calculation, the plants were photographed with a DM2000 dissection microscope (Leica Microsystems) at the time of infection, and the area was calculated using Leica Application Suite (LAS) software (Leica Microsystems). The average size of syncytia and associated nematodes was measured in longitudinal optical sections as described previously (*21*). Briefly, 50 infection sites in roots containing syncytia and nematodes were photographed with a Leica DM2000 dissection microscope at 14 dai. The syncytia or females were outlined, and the area was calculated using LAS software (Leica Microsystems).

DPI experiments

For experiments with DPI, Col-0 plants were grown as described above. After 5 days, seedlings were transferred to petri dishes containing agar medium supplemented with DPI (1 μM) and used for nematode infection assays. In experiments designed to test the direct effect of DPI on *H. schachtii* invasion, freshly hatched J2 nematodes were incubated with DPI (1 μM) for 5 days at room temperature. Then, the nematodes were collected and resuspended in 0.7% (w/v) GelRite (Duchefa) containing DPI (1 μM) to ensure prolonged contact with DPI. For the *C. elegans* development experiments, nematodes were reared in nematode growth medium (*36*) supplemented with DPI at the indicated concentrations. Synchronized L1 larvae were obtained by sodium hypochloride treatment (*36*). Nematodes were fed *Escherichia coli* OP50. Egg lays were counted after 3 days from three replicates.

Nematode behavioral assays

For nematode invasion assays (Fig. 2A), the number of nematodes invading the roots at 2 dai was counted. To assess nematode migration, death, and sexual development (Fig. 2B), nematodes invading the roots 1 or 2 dai were selected (with permanent marker on the petri dishes), and their behavior was followed during the next 10 days by taking photographs every 24 hours. For each experiment, 20 nematodes were examined for each plant genotype. For ISC selection experiments (Fig. 2C), nematodes that were invading the root at 4 hai were marked with permanent marker on the petri dishes, and their stylet movements were observed hourly for 16 hours. ISC selection was defined as the time when a nematode stopped stylet movements. For each experiment, 20 to 30 nematodes were observed for each plant genotype. For the long-term growth experiments (Fig. 2D), nematodes that established ISC at 1 dai were marked with permanent marker on the petri dishes and imaged daily. For each experiment, 30 to 40 nematodes were examined for each plant genotype.

ROS detection

To visualize H_2O_2, a type of ROS, roots were stained with DAB using a modification of the protocol described in (*28*). At 1 dai, infected roots were incubated in DAB solution (1 mg/ml in water) at room temperature for 3 to 5 hours in a high-humidity box. The samples were then fixed in a solution of ethanol/lactic acid/glycerol (3:1:1). Root segments without lateral root primordia, mechanical stress, and root tips were selected for imaging with a Leica DM4000 microscope (Leica Microsystems) equipped with an Olympus C-5050 digital camera. The average number of stained spots was calculated for 50 nematodes per plant genotype. For CM-H_2DCFDA (C6827, Molecular Probes) staining, plants were grown on coverslips. At 1 dai, the agar was carefully removed from around root segments containing nematodes. Root segments were incubated with CM-H_2DCFDA (10 μM) in phosphate-buffered saline for 90 min at 4°C (*3*). After incubation, the samples were washed with KCl (0.1 mM) and $CaCl_2$ (0.1 mM) to remove excess CM-H_2DCFDA. The samples were kept at room temperature for 1 hour and then imaged with a Zeiss CLSM 710.

Cell viability labeling

Root segments were cut (0.5 cm) and transferred to half-strength Murashige and Skoog basal medium (MS medium, Sigma-Aldrich) containing FDA (5 μg/ml) (*29*). FDA stocks (2 mg/ml in acetone) were stored at −20°C. Root segments without lateral roots or root tips were used for staining. After 10 min of incubation, root segments were washed five times with MS medium without FDA. The fluorescence emission intensities were measured at 535 nm after excitation at 485 nm by using a microplate reader (Infinite 200 Pro, Tecan) (*29*). For each experiment, six root segments were used per plant genotype.

Microscopic analysis

Root segments were dissected, fixed, dehydrated, and embedded in epoxy resin as described previously (*21*). Light and transmission electron microscopy analyses were conducted on sections obtained from the same samples. Root segments were serially sectioned on an RM2165 microtome (Leica Microsystems) into 2-μm sections. Sections were collected on glass slides, stained with an aqueous solution of crystal violet dye (1%, Sigma-Aldrich), and imaged on an AX70 Provis (Olympus) light microscope equipped with an Olympus DP50 digital camera (Olympus). At selected places, ultrathin sections (90 nm) were taken for transmission electron microscopy with a UCT ultramicrotome (Leica). Ultrathin sections were stained with a saturated ethanol solution of uranyl acetate (Sigma-Aldrich) followed by lead citrate (Sigma-Aldrich) and imaged on an FEI 268D Morgagni transmission electron microscope (FEI Company) equipped with an SIS Morada digital camera (Olympus SIS). Digital images were adjusted for similar contrast and brightness, cropped, and resized using Adobe Photoshop software.

Real-time PCR

Root segments (up to 200) containing syncytia associated with female nematodes were dissected at 10 dai. Total RNA was extracted using a NucleoSpin RNA kit (Macherey-Nagel) according to the manufacturer's instructions, including deoxyribonuclease digestion. Reverse transcription was performed with the High-Capacity cDNA Reverse Transcription Kit (Invitrogen) according to the manufacturer's instructions. Quantitative PCR was performed with the Stepone Plus Real-Time PCR System (Applied Biosystems). Each sample contained 10 μl of Fast SYBR Green qPCR Master Mix with uracil-DNA, glycosylase, and 6-carboxy-x-rhodamine (Invitrogen), 2 mM $MgCl_2$, 0.5 μl each of forward and reverse primers (10 μM), 2 μl of complementary DNA (cDNA), and water in a 20-μl total reaction volume. The primers are listed in table S5. Samples were analyzed in three technical replicates. 18*S* was used as an internal control. Relative expression was calculated by the $\Delta\Delta C_t$ method (*37*), where the expression of each gene was normalized to 18*S* and then to Col-0 to calculate fold change. The range shown in Fig. 6 was calculated from three experimental replicates (*37*).

SUPPLEMENTARY MATERIALS

www.sciencesignaling.org/cgi/content/full/7/320/ra33/DC1

Fig. S1. Nematode infection assays in *Rboh* mutant plants.
Fig. S2. Nematode infection assays in *35S::RbohD/rbohD* plants.
Fig. S3. Development and invasion of nematodes treated with DPI.
Fig. S4. Plant syncytium size in *rbohD/F* plants.
Fig. S5. ROS visualization in roots of DPI-treated Col-0 plants.
Fig. S6. Light microscopy of uninfected *Rboh* mutant plants in secondary growth and infected *Rboh* mutant plants 14 dai.
Fig. S7. Transmission electron microscopy of *Rboh* mutant plants 5 and 14 dai.
Fig. S8. Cell viability in nematode-infected and uninfected plants treated with DPI.
Fig. S9. Analysis of gene expression in uninfected roots.
Table S1. Expression of *RbohD* and *RbohF* in syncytia of *35S::RbohD* plants.
Table S2. Nematode and syncytium size in DPI-treated Col-0 plants 14 dai.
Table S3. Nematode and syncytium size in Col-0 plants 14 dai with nematodes preincubated with DPI.
Table S4. Expression of PR genes in Col-0 and *rbohD/F/sid2* uninfected roots.
Table S5. Primers sequences used in this study.

REFERENCES AND NOTES

1. B. H. Segal, M. J. Grimm, A. N. H. Khan, W. Han, T. S. Blackwell, Regulation of innate immunity by NADPH oxidase. *Free Radic. Biol. Med.* **53**, 72–80 (2012).
2. J. D. Lambeth, NOX enzymes and the biology of reactive oxygen. *Nat. Rev. Immunol.* **4**, 181–189 (2004).
3. M. A. Torres, J. L. Dangl, J. D. G. Jones, *Arabidopsis* gp91^{phox} homologues *AtrbohD* and *AtrbohF* are required for accumulation of reactive oxygen intermediates in the plant defense response. *Proc. Natl. Acad. Sci. U.S.A.* **99**, 517–522 (2002).
4. Q. J. Groom, M. A. Torres, A. P. Fordham-Skelton, K. E. Hammond-Kosack, N. J. Robinson, J. D. G. Jones, *rbohA*, a rice homologue of the mammalian *gp91phox* respiratory burst oxidase gene. *Plant J.* **10**, 515–522 (1996).
5. M. A. Torres, H. Onouchi, S. Hamada, C. Machida, K. E. Hammond-Kosack, J. D. G. Jones, Six *Arabidopsis thaliana* homologues of the human respiratory burst oxidase (*gp91^{phox}*). *Plant J.* **14**, 365–370 (1998).
6. N. Doke, Involvement of superoxide anion generation in the hypersensitive response of potato-tuber tissues to infection with an incompatible race of *Phytophthora infestans* and to the hyphal wall components. *Physiol. Plant Pathol.* **23**, 345–357 (1983).
7. C. Lamb, R. A. Dixon, The oxidative burst in plant disease resistance. *Annu. Rev. Plant Physiol. Plant Mol. Biol.* **48**, 251–275 (1997).
8. H. Yoshioka, N. Numata, K. Nakajima, S. Katou, K. Kawakita, O. Rowland, J. D. G. Jones, N. Doke, *Nicotiana benthamiana* gp91^{phox} homologs *NbrbohA* and *NbrbohB* participate in H_2O_2 accumulation and resistance to *Phytophthora infestans*. *Plant Cell* **15**, 706–718 (2003).

9. D. Marino, C. Dunand, A. Puppo, N. Pauly, A burst of plant NADPH oxidases. *Trends Plant Sci.* **17**, 9–15 (2012).
10. W. E. Durrant, X. Dong, Systemic acquired resistance. *Annu. Rev. Phytopathol.* **42**, 185–209 (2004).
11. D. A. Dempsey, J. Shah, D. F. Klessig, Salicylic acid and disease resistance in plants. *Crit. Rev. Plant Sci.* **18**, 547–575 (1999).
12. J. Durner, J. Shah, D. F. Klessig, Salicylic acid and disease resistance in plants. *Trends Plant Sci.* **2**, 266–274 (1997).
13. J. Draper, Salicylate, superoxide synthesis and cell suicide in plant defence. *Trends Plant Sci.* **2**, 162–165 (1997).
14. K. Overmyer, M. Brosché, J. Kangasjärvi, Reactive oxygen species and hormonal control of cell death. *Trends Plant Sci.* **8**, 335–342 (2003).
15. R. A. Dietrich, M. H. Richberg, R. Schmidt, C. Dean, J. L. Dangl, A novel zinc finger protein is encoded by the Arabidopsis *LSD1* gene and functions as a negative regulator of plant cell death. *Cell* **88**, 685–694 (1997).
16. M. A. Torres, J. D. G. Jones, J. L. Dangl, Pathogen-induced, NADPH oxidase–derived reactive oxygen intermediates suppress spread of cell death in *Arabidopsis thaliana*. *Nat. Genet.* **37**, 1130–1134 (2005).
17. U. Wyss, F. M. W. Grundler, Feeding behavior of sedentary plant parasitic nematodes. *Netherlands J. Plant Pathol.* **98**, 165–173 (1992).
18. M. Sobczak, W. A. Golinowski, F. M. W. Grundler, Ultrastructure of feeding plugs and feeding tubes formed by *Heterodera schachtii*. *Nematology* **1**, 363–374 (1999).
19. M. Sobczak, W. Golinowski, F. M. W. Grundler, Changes in the structure of *Arabidopsis thaliana* roots induced during development of males of the plant parasitic nematode *Heterodera schachtii*. *Eur. J. Plant Pathol.* **103**, 113–124 (1997).
20. J. Muller, K. Rehbock, U. Wyss, Growth of *Heterodera schachtii* with remarks on amounts of food consumed. *Revue Nematol.* **4**, 227–234 (1981).
21. S. Siddique, S. Endres, J. M. Atkins, D. Szakasits, K. Wieczorek, J. Hofmann, C. Blaukopf, P. E. Urwin, R. Tenhaken, F. M. W. Grundler, D. P. Kreil, H. Bohlmann, Myo-inositol oxygenase genes are involved in the development of syncytia induced by *Heterodera schachtii* in Arabidopsis roots. *New Phytol.* **184**, 457–472 (2009).
22. D. L. Trudgill, Effect of environment on sex determination in *Heterodera rostochiensis*. *Nematologica* **13**, 263–272 (1967).
23. G. Miller, K. Schlauch, R. Tam, D. Cortes, M. A. Torres, V. Shulaev, J. L. Dangl, R. Mittler, The plant NADPH oxidase RBOHD mediates rapid systemic signaling in response to diverse stimuli. *Sci. Signal.* **2**, ra45 (2009).
24. C. K. Auh, T. M. Murphy, Plasma membrane redox enzyme is involved in the synthesis of O_2^- and H_2O_2 by *Phytophthora* elicitor-stimulated rose cells. *Plant Physiol.* **107**, 1241–1247 (1995).
25. G. H. Waetzig, M. Sobczak, F. M. W. Grundler, Localization of hydrogen peroxide during the defence response of *Arabidopsis thaliana* against the plant-parasitic nematode *Heterodera glycines*. *Nematology* **1**, 681–686 (1999).
26. H. Thordal-Christensen, Z. G. Zhang, Y. D. Wei, D. B. Collinge, Subcellular localization of H_2O_2 in plants. H_2O_2 accumulation in papillae and hypersensitive response during the barley–powdery mildew interaction. *Plant J.* **11**, 1187–1194 (1997).
27. K. A. Kristiansen, P. E. Jensen, I. M. Møller, A. Schulz, Monitoring reactive oxygen species formation and localisation in living cells by use of the fluorescent probe CM-H_2DCFDA and confocal laser microscopy. *Physiol. Plant* **136**, 369–383 (2009).
28. L. Dolan, K. Janmaat, V. Willemsen, P. Linstead, S. Poethig, K. Roberts, B. Scheres, Cellular organisation of the *Arabidopsis thaliana* root. *Development* **119**, 71–84 (1993).
29. X. Y. Qiang, B. Zechmann, M. U. Reitz, K. H. Kogel, P. Schäfer, The mutualistic fungus *Piriformospora indica* colonizes *Arabidopsis* roots by inducing an endoplasmic reticulum stress–triggered caspase-dependent cell death. *Plant Cell* **24**, 794–809 (2012).
30. M. C. Wildermuth, J. Dewdney, G. Wu, F. M. Ausubel, Isochorismate synthase is required to synthesize salicylic acid for plant defence. *Nature* **414**, 562–565 (2001).
31. M. Pogány, U. von Rad, S. Grün, A. Dongó, A. Pintye, P. Simoneau, G. Bahnweg, L. Kiss, B. Barna, J. Durner, Dual roles of reactive oxygen species and NADPH oxidase RBOHD in an Arabidopsis-*Alternaria* pathosystem. *Plant Physiol.* **151**, 1459–1475 (2009).
32. T. Hewezi, P. J. Howe, T. R. Maier, R. S. Hussey, M. G. Mitchum, E. L. Davis, T. J. Baum, Arabidopsis spermidine synthase is targeted by an effector protein of the cyst nematode *Heterodera schachtii*. *Plant Physiol.* **152**, 968–984 (2010).
33. D. Szakasits, P. Heinen, K. Wieczorek, J. Hofmann, F. Wagner, D. P. Kreil, P. Sykacek, F. M. W. Grundler, H. Bohlmann, The transcriptome of syncytia induced by the cyst nematode *Heterodera schachtii* in Arabidopsis roots. *Plant J.* **57**, 771–784 (2009).
34. J. Hofmann, A. El Ashry, S. Anwar, A. Erban, J. Kopka, F. Grundler, Metabolic profiling reveals local and systemic responses of host plants to nematode parasitism. *Plant J.* **62**, 1058–1071 (2010).
35. P. C. Sijmons, F. M. W. Grundler, N. von Mende, P. R. Burrows, U. Wyss, *Arabidopsis thaliana* as a new model host for plant-parasitic nematodes. *Plant J.* **1**, 245–254 (1991).
36. T. Stiernagle, Maintenance of *C. elegans*, in *C. elegans: A Practical Approach*, I. Hope, Ed. (Oxford University Press, Oxford, 2006).
37. K. J. Livak, T. D. Schmittgen, Analysis of relative gene expression data using real-time quantitative PCR and the $2^{-\Delta\Delta CT}$ method. *Methods* **25**, 402–408 (2001).

Acknowledgments: We acknowledge the technical support of G. Sichtermann, U. Schlee, S. Neumann, T. Gerhardt, J. Holbein, and B. Klinzer. We are thankful to D. Szakasits for her critical revision of the manuscript. We appreciate the valuable comments of J. Dangl on the manuscript. We acknowledge M. Hoch for giving us access to the confocal microscope and the microplate reader. **Funding:** M.A.T. was supported by grant (2007)D/562971 from the International Reintegration Program from the European Union. E.R. and M.S. were supported by grant 116/N-COST/2008/0 from The Polish Ministry of Science and Higher Education. **Author contributions:** S.S. and F.M.W.G. designed the research and wrote the paper. S.S. and C.M. conducted the majority of experiments. M.S.H. and P.G. conducted gene expression experiments. Z.S.R. carried out infection assays with triple mutants. E.R. and M.S. carried out the microscopic analyses. M.A.T. identified mutant combinations. All authors commented on the manuscript. **Competing interests:** The authors declare that they have no competing financial interests. **Data and materials availability:** Materials used in this study are available on request.

Submitted 1 October 2013
Accepted 21 March 2014
Final Publication 8 April 2014
10.1126/scisignal.2004777
Citation: S. Siddique, C. Matera, Z. S. Radakovic, M. S. Hasan, P. Gutbrod, E. Rozanska, M. Sobczak, M. A. Torres, F. M. W. Grundler, Parasitic worms stimulate host NADPH oxidases to produce reactive oxygen species that limit plant cell death and promote infection. *Sci. Signal.* **7**, ra33 (2014).

Chapter 3

Insights into Rboh-mediated susceptibility of *Arabidopsis thaliana* to the cyst nematode *Heterodera schachtii*

Christiane Matera, Shahid Siddique, Oliver Chitambo, Axel Mithöfer, Florian M.W. Grundler

Abstract

Plants produce reactive oxygen species (ROS) in response to pathogen infections. The major source of these ROS in plants is a plasma membrane-bound nicotinamide adenine dinucleotide phosphate (NADPH) oxidase, which is known as respiratory burst oxidase homologue (Rboh). Cyst nematodes are obligate biotrophs that establish syncytial feeding sites in roots of the host plants. We previously showed that mutation in Arabidopsis Rboh homologues RbohD and RbohF (*rbohD/F*) has a strong negative effect on susceptibility to nematodes. Here, we characterize the mechanism behind the role of Rboh-mediated ROS in nematode infection process. We performed a comparative transcriptome analysis between Col-0 and *rbohD/F* during early stages of infection. Transcript abundance of 3157 genes showed increase and 2922 genes showed a decrease in *rbohD/F* mutant as compared to Col-0. The gene that showed the strongest decrease in transcript abundance in *rbohD/F* upon nematode infection encodes for a plant-specific vacuolar auxin transporter Walls Are Thin1 (WAT1). The regulation of *WAT1* expression by ROS in an infection specific manner was confirmed by performance of quantitative RT-PCR and GUS assays. Genetic disruption of WAT1 has a strong effect on susceptibility of these plants to nematodes in a pattern similar to that of *rbohD/F*. Moreover, auxin content of infected root segments was decreased strongly in *wat1* and *rbohD/F* as compared with Col-0. Thus, parasitic worms stimulate NADPH oxidase to produce ROS, which activate the expression of WAT1 to modulate auxin homeostasis. This modulation of auxin homeostasis is the cornerstone for successful establishment and development of syncytium and nematodes.

Introduction

Nematodes belong to the phylum Nematoda. They possess a vermiform, multicellular unsegmented body. These organisms live under different environmental conditions ranging from high mountains to the sediments of the oceans (Blaxter et al., 1998). Plant-parasitic nematodes are obligate biotrophs that have a very specific feeding behavior. These nematodes establish a narrow relationship with their hosts because they feed on the host throughout their lifecycle. They have adverse effects on the yield of crop plants by damaging the crops either directly or as virus vectors. In Europe, one of the most important plant-parasitic nematodes is the cyst nematode *H. schachtii* (Müller 1999). These nematodes emerge from cysts as second stage juveniles (J2) and search for roots led by exudates, which are released from young roots during growth. J2s invade the host plant roots with the help of their stylet near the root elongation zone. After perforation of the rhizodermis, they migrate intracellularly through different tissue layers towards the vascular cylinder. Upon reaching the vascular cylinder, the nematodes probe single cells one-by-one to find a suitable initial syncytial cell (ISC), which will be the origin of a syncytial feeding site. The syncytium is the only source of the nutrients for the nematodes throughout their life (Jones, 1981). To establish the syncytium from the ISC, nematodes secret several effectors via their stylet into the cell. This results in a remarkable reorganization of the plant's transcriptomic and metabolomics machinery (Hofmann et al. 2010; Hofmann *et al*. 2008; Siddique et al*.,* 2009; Szakasits et al*.,* 2009). Although certain nematode proteins have been identified that might be involved in the syncytium functioning (Jaubert et al*.,* 2002; Vanholme et al*.,* 2004; Gardner et al., 2015), little is known of the mechanisms by which nematodes induce the formation of the syncytium.

Reactive oxygen species (ROS) are formed as by-products inside plant cells during normal oxygen metabolism and include superoxide (O_2^-), hydrogen peroxide (H_2O_2) and hydroxyl radicals (•OH). Because of the presence of unpaired valence shell electrons, ROS are highly reactive. Nevertheless, they play an important role as key regulators of biological processes, including growth, development and stress responses (Kovtun et al., 2000; Foreman et al., 2003; Miller et al. 2009) where they act as signalling molecules to activate signaling cascades or gene expression (Hancock et al., 2001.) ROS production during pathogen attack is one of the earliest

observed defense responses and in context of plant-nematode interaction, Waetzig et al. (1999) showed the production of ROS during the hypersensitive response (HR) reactions between *Heterodera glycines* and *Arabidopsis thaliana.* In another recent study, it has been shown that wheat apoplastic peroxidase genes has different expression patterns in resistant and susceptible varieties and might be responsible for the different responses of plants to the cyst nematode *Heterodera avenae* (Simonetti et al., 2009).

The major source of pathogenesis-related ROS in plants is a plasma membrane-bound nicotinamide adenine dinucleotide phosphate (NADPH) oxidase (Lamp, 1997), which is homologous to a plasma membrane bound enzyme in mammalian phagocytes that destroys microbes. This enzyme complex consists of a cytosolic 300-amino-acid N-terminal domain, which acts as activator, a six transmembrane-spanning domain, which is used for electron transport from inside to outside of the cell and a carboxy-terminal region, which transfers electrons to the transmembrane section (Apel, 2004; Torres, 1998). The structure of the NADPH oxidase in plants is well researched, and based on the homology to the mammalian oxidase, the encoding genes in plants are called *respiratory burst oxidase homologues* (RBOH). The *rice respiratory oxidase homolog* (OsrbohA gene) was the first plant NADPH oxidase identified, and ten genes of this family have been found in *A. thaliana* (AtRBOHA - AtRBOHJ) (Torres et al*.,* 1998). The mechanism that controls the expression of different RBOH genes is not well understood; however, their spatio-temporal distribution hint that different RBOHs have different roles and are capable of complementing each other functions. AtRBOHD and AtRBOHF are reported to be involved in most ROS produced in response to avirulent bacteria and oomycetes (Torres et al., 2002), whereas AtRBOHC is required for ROS production during root hair growth.

We have recently characterized the role of RBOH-mediated ROS in plant-nematode interaction (Siddique et al. 2014). We found that Arabidopsis loss-of-function mutants RbohD (*rbohD*) showed a decrease in susceptibility of plants to the cyst nematode *H. schachtii* and this effect was increased in double mutant for RbohD and RbohF (*rbohD/F*). A detailed analysis demonstrated that the absence of ROS led to a delay in ISC establishment independent of pathogenesis-resistance gene (PR genes) response by the plant. These findings gave new insights on how nematode

manipulates the host defense mechanisms to its own benefit. However, the underlying mechanistic details of RBOH-mediated susceptibility of plants to nematodes remained largely unknown. Here, we have extended this work by performing a comparative transcriptome analysis between Col-0 and *rbohD/F* upon nematode infection. Our data showed that more than 6000 genes were differently regulated. Whereas, upon infection, Col-0 showed a strong upregulation of genes encoding enzymes for tryptophan, indole glucosinates (IGS) and camalexin biosynthesis, the infection of *rbohD/F* resulted in decreased transcript abundance for chorismate metabolism and subsequent pathways leading to tryptophan, auxin and IGS. We therefore suggest that a specific mechanism channeling away the metabolites from indole to Salicylic acid is responsible for the nematode resistant phenotype of *rbohD/F*.

Results

Comparative transcriptome analysis of *rbohD/F* and Col-0

We have recently described that RbohD/F loss-of-function mutants (*rbohD/F*) show a strong decrease in susceptibility of plants to the nematodes (Siddique et al., 2014); however, the underlying mechanism is not well understood. As we demonstrated that nematodes have a delayed ISC establishment in *rbohD/F* mutants, we asked whether Rboh-mediated ROS were involved in this aspect of nematode infection. We addressed this by performing a transcriptome analysis between Col-0 and *rbohD/F* after *H. schachtii* infection. We grew the Col-0 and *rbohD/F* plants in Knop medium under sterile conditions, and inoculated them with nematodes as described in methods section. Small root segments surrounding the nematode head (0.1 cm) were cut at 10 hours post inoculation (hpi). This time-point reflect the initial stages of the nematode infection including the ISC establishment as concluded from an earlier study (Kammerhofer et al, 2015). Total RNA was extracted, labelled and amplified to hybridize with the GeneChip® Arabidopsis ATH1 Genome (Affymetrix UK Ltd). Our data analysis showed that out of 24,000 genes that can be detected by the ATH1

Table 1: Change in gene expression in *rbohD/F* compared to Col-0 measured by qRT-PCR for validation of Genechip data. Transcripts were measured from root segments containing infections sites 10hpi and compared with those from root segments as used for GeneChips.

	GeneChip data		**qRT-PCR**		
Gene	**M value (log_2)**	**Fold change**	**Ct value (log_2)**	**Fold change**	**Name**
At1g75500	-5.27	-38.83	23.74	-31.18	WAT1
At4g40090	-4.73	-26.63	22.72	-29.49	AGP3
At1g19920	-1.32	-2.51	21.08	-4.25	APS2
At4g39980	1.70	-3,52	19.82	-5.3	DHS1
At3g46530	3.89	14.85	28.01	13.62	RPP13
At5g44420	2.99	7.97	26.25	6.24	PDF1.2

Genome Array, 6079 were differently regulated (Fold change > 2 at FDR < 5%). Transcript abundance of 3157 genes showed increase and 2922 genes showed a decrease in *rbohD/F* mutant as compared to Col-0. Microarray results were verified via qRT-PCR for highly different regulated genes, which showed that overall our microarrays data was reliable and well supported by qRT-PCR (Tab.1).

To explore the regulation of biological process, molecular functions and their distributions across different cellular components; we performed a gene ontology enrichment analysis with significantly up- and down-regulated genes between Col-0 and *rbohD/F.* The categories that were particularly over-represented in differentially

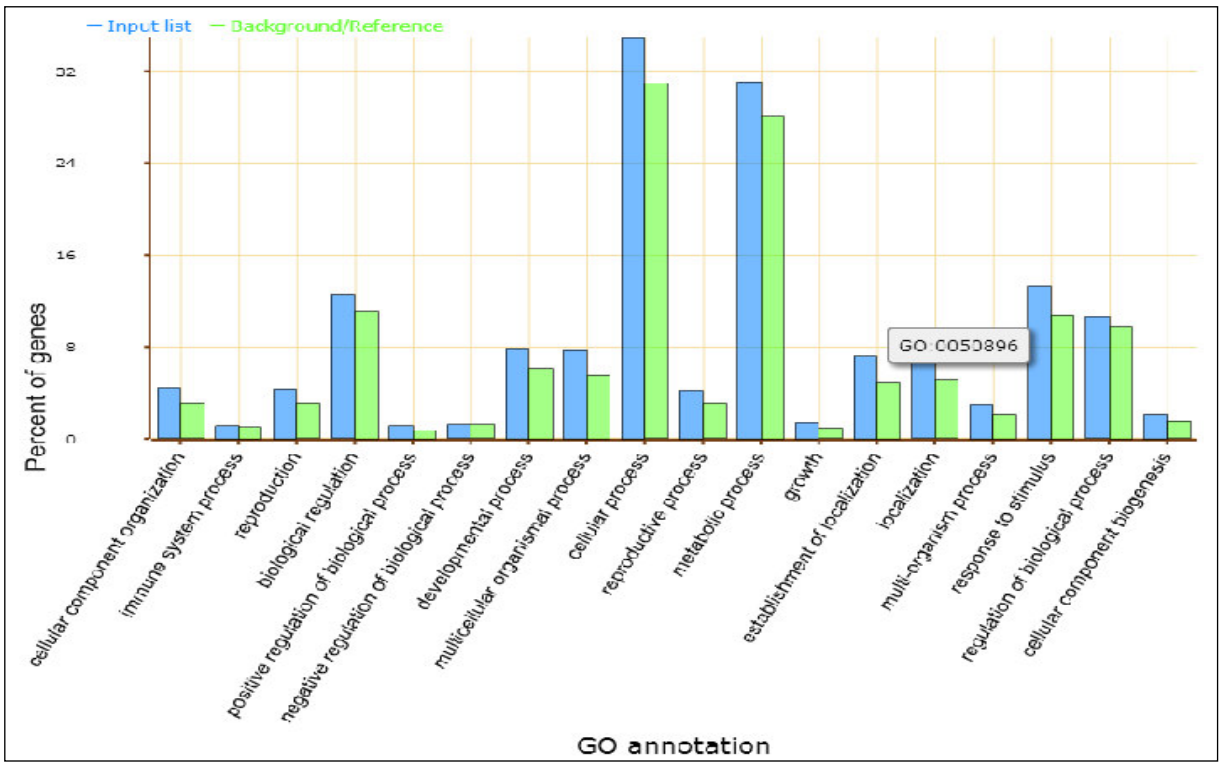

Figure 1: Categorization of differently regulated genes in *rbohD/F* compared to Col-0 detected at 10hpi by ATH1 Genome Array. Out of 24,000 genes, 6079 were differently regulated, whereby 3157 showed increased and 2922 decreased transcripts**.** To analyze the regulation of biological process and molecular functions, we conducted a gene ontology enrichment analysis. Among 18 different categories, seven were overrepresented including cellular component organization, biological regulation, developmental processes, multicellular processes, cellular processes, metabolic processes, response to stimulus and regulation of biological processes.

regulated genes include transport, metabolic process, response to stimulus and others (Fig.1).

Walls are thin 1 (*WAT1*) is strongly downregulated in *rbohD/F* upon nematode infection

Although more than 6000 genes showed differential regulation upon nematode infection in *rbohD/F* plants, the gene that shows the most severe downregulation (Fold change = -38.85) encodes a plant-specific vacuolar auxin efflux carrier (WAT1, Walls Are Thin1) and is a member of the plant drug metabolite exporter family (P-DME). WAT1 is involved in diverse plant-pathogen interactions and loss-of-function mutants for *WAT1* confer a broad spectrum resistance to vascular pathogens including the bacteria *Ralstonia solanacearum* and *Xanthomonas campestri*, and the fungi *Verticillium dahlia* and *Verticillium albo-atr*. Further, *wat1* shows a drastic reduction in secondary cell wall thickness of stem fibres. A detailed transcriptomic and metabolomics analysis with *wat1* mutants suggested that a specific mechanism channelling away the metabolites from indole to salicylic acid is responsible for plethora of phenotypes *wat1* exhibits (Denancè et al., 2013).

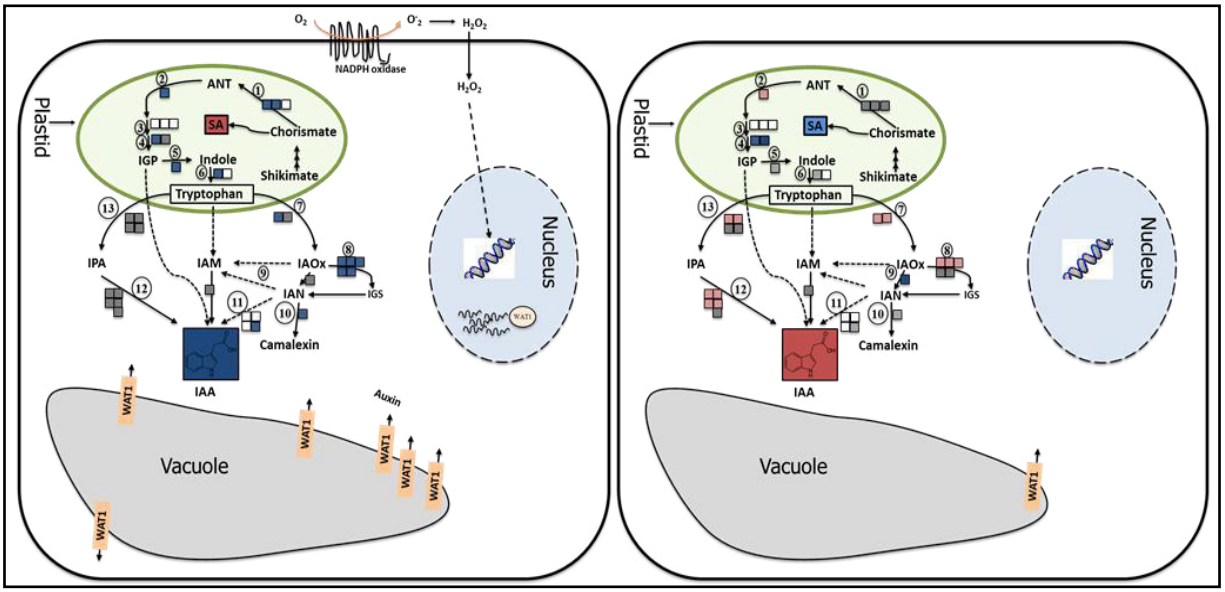

Figure 2: Chorismate pathway leading to tryptophan and IAA biosynthesis in Arabidopsis. (Left) Col-0 control vs Col-0 infected at 10hpi. (Right) Col-0 infected vs *rbohD/F* infected at 10hpi. Blue colour represents significant increase, red colour represent significant decrease; white colour represent genes whose probeset are not specific and grey colour represent no change. Values are specified in Appendix Tab.S2.

The fact that WAT1 is strongly downregulated upon nematode infection in *rbohD/F* suggested that it might be a link between ROS and auxin metabolism, and may cause the nematode resistant phenotype of *rbohD/F*. To assess the role of WAT1 in *rbohD/F*-mediated susceptibility of plants to nematodes, we had a detailed look at our

transcriptome data and found out that nematode infection triggers a strong upregulation of genes encoding enzymes for tryptophan, IGS and camalexin biosynthesis in Col-0 (Fig.2, Appendix Tab.S1). However, in comparison to Col-0, infection of *rbohD/F* plants resulted in a strong decrease of these transcripts (Fig.2, Appendix Tab.S1). Our results are similar to previous transcriptomic analysis for *wat1* mutants where a specific suppression of indole metabolism has been shown (Denancè et al., 2013).

Interestingly, transcripts for auxin transport and signaling genes were consistently and strongly downregulated (Tab.2, Appendix Tab.S2). These results hinted that there might be interplay between ROS and auxin during early stages of nematode infection. This is supported by previous studies showing that auxin-related lateral root development and syncytium formation have some features in common including cell cycle modification and cell wall remodeling.

Table 2: Change in gene expression in *rbohD/F* compared to Col-0 10 hours post infection (hpi). GeneChip data reveal a strong and consistent downregulation in transcripts for auxin transport (green), biosynthesis (grey) and signaling genes (blue).

Name	Gene	Fold change	P-Value	Function
PIN1	At1g73590	-3,77	0,05	Auxin efflux carrier
PIN2	At5g57090	-2,8	0,01	Auxin efflux carrier
PIN3	At1g70940	-5,5	0,01	Auxin efflux carrier
AUX1	At2g38120	-12,86	0,02	Auxin influx transporter
LAX2	At2g21050	-2,97	0,01	Auxin influx transporter
LAX3	At1g77690	-12,46	0,01	Auxin influx transporter
WAT1	At1g75500	-38,83	0,04	Auxin efflux carrier
DHS1	At4g39980	-3,52	0,02	Synthase for aromatic amino acid biosynthesis
SUR2	At4g31500	-1,92	0,05	Enzyme in biosynthetic pathway of glucosinolate
SUR1	At2g20610	-1,22	0,04	Synthase for glucosinolate biosynthesis
SOT16	At1g74100	-3,33	0,05	Enzyme for final step of glucosinolate core structure biosynthesis

PAT1	At5g17990	-2,5	0,02	Tryptophan biosynthesis
PAL1	At2g37040	-2,93	0,01	Enzyme for polyphenol compound biosynthesis
TIR1	At3g62980	-1,98	0,02	Auxin binding
IAA5	At1g15580	-2,24	0,01	Transcription factor
IAA8	At2g22670	-2,08	0,03	Transcription factor
IAA11	At4g28640	2,79	0,03	Transcription factor
IAA19	At3g15540	-1,48	0,08	Transcription factor
ARF2	At5g62000	-1,77	0,05	Transcription factor
ARF12	At1g34310	-13,28	0,01	Transcription factor

To address whether similar changes in transcript abundance occur between Col-0 and *rbohD/F* plants without nematode infection, we cut root segments from roots of uninfected plants and performed expression analysis for number of genes in chorismate pathway and also *WAT1* via qPCR. We found no significant change in transcript abundance between Col-0 and *rbohD/F* (Fig.3).

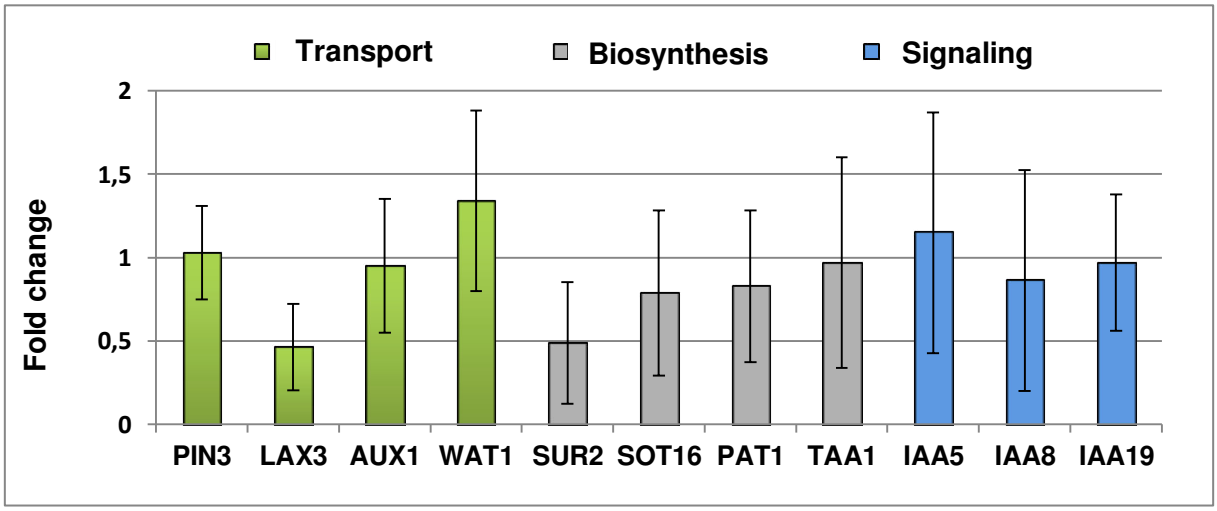

Figure 3: Comparison of expression levels for auxin related genes in *rbohD/F* and Col-0. Results of qRT-PCR; Expression level of auxin related genes in uninfected roots of *rbohD/F* compared to Col-0. No significant transcript abundance was detectable between Col-0 and *rbohD/F*. Samples were analyzed in three technical replicates and 18S was used as an internal control.

RbohD and WAT1 co-regulation

To further confirm whether RbohD and WAT1 commonly regulate indole metabolism, we performed a micro-array wide analysis to search 1000 highly co-regulated genes for WAT1 or RbohD with ATTED-II, a database of co-expressed and co-regulated genes in Arabidopsis (http://atted.jp/). A venn diagram of two data sets showed that 48 genes were shared in both data sets (Fig.4). Consistent with our hypothesis, the list of commonly regulated genes includes 17 genes involved in IAA or indole glucosinolate metabolism (Appendix Tab.S3).

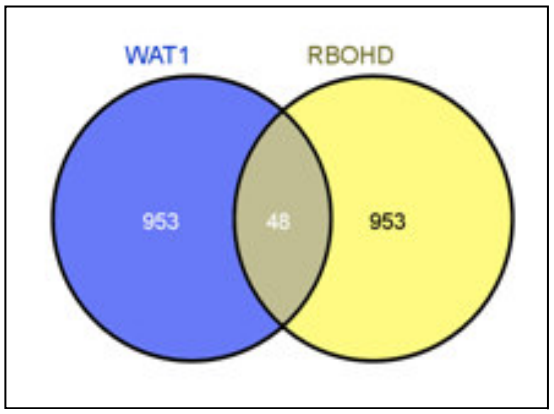

Figure 4: Venn diagram for co-expressed genes between RbohD and WAT1. Of the 48 genes that are co-regulated, 17 genes are involved in IAA or glucosinolate metabolism including SOT, SUR and CYP genes.

WAT1 is expressed during early stage of infection

Although WAT1 is strongly down-regulated in *rbohD/F* upon nematode infection, spatio-temporal expression of *WAT1* during infection process was not clear. Therefore, we visualized *WAT1* expression by infecting previously described *proWAT1:GUS* plants with *H. schachtii* and observed the GUS expression at 12hpi, 1dpi, 2dpi, 3dpi and 5dpi (Fig.5). We observed a strong GUS expression during early stages of infection, which overlaps with production of Rboh-mediated ROS (Fig.6 and Siddique et al., 2014).

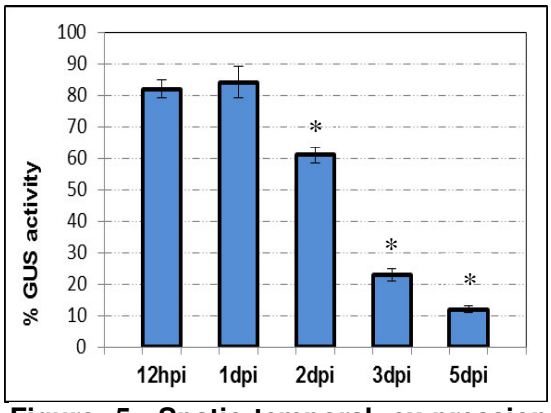

Figure 5: Spatio-temporal ex-pression of WAT1 after infection with *H. schachtii*. Quantification of GUS activity (*ProWAT1::GUS*) at nematode invasion site at 12hpi, 1dpi, 2dpi, 3dpi and 5dpi with *H. schachtii*. Each time point reflects the results of about 30 nematode invasion sites.

Figure 6: Expression of WAT1 upon infection with *H. schachtii* 1dpi. Staining was specific at invasion sites of nematodes (left) and control roots remain unstained (right). N = Nematode, IS = Infection site

However, there was a strong decrease in intensity and occurrence of GUS staining as the infection proceeds (Fig.5), which suggest that WAT1 is expressed during initial stages of infection and that it is important for establishment and development of nematode infection. To address whether expression of WAT1 is induced by ROS, we treated *proWAT1:GUS* with different concentration of IAA (1µM) or H_2O_2 (1, 5, 10, 50 mM) and detected GUS expression after 1 hour (Fig.7). We observed that GUS expression was strongly induced by both IAA and H_2O_2 treatment, which is consistent

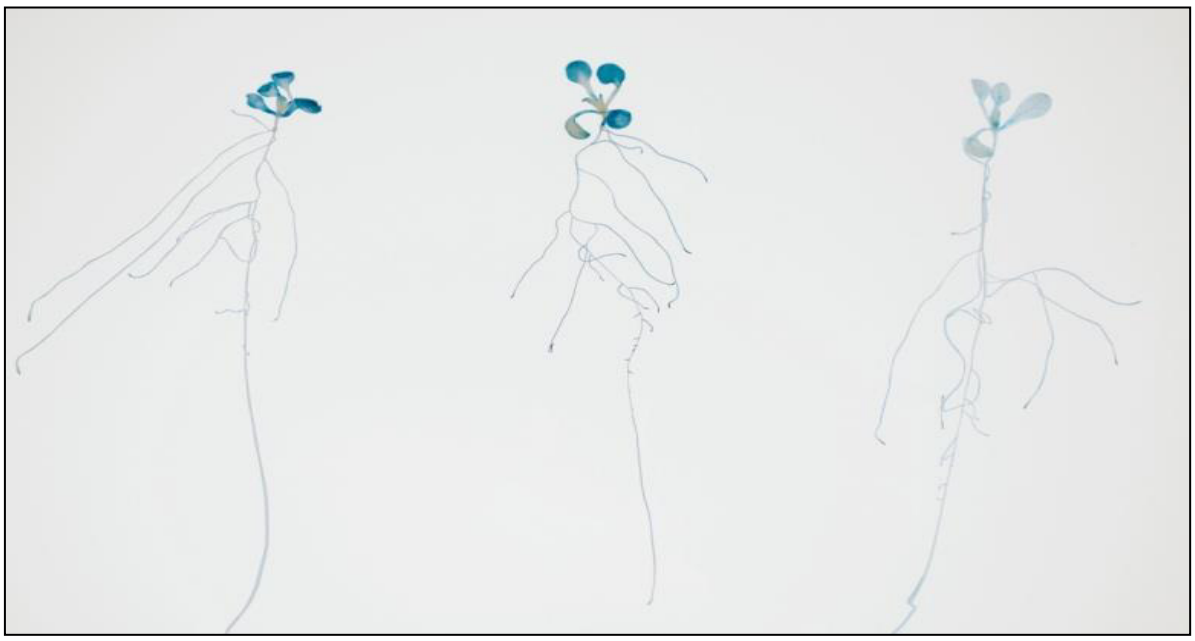

Figure 7: GUS expression in *proWAT1:GUS* after different treatments. IAA (left) and H_2O_2 (middle) induced the promoter. Changes in H_2O_2 concentration did not influenced the intensity of the staining. Plant with water treatment (right) remained unstained.

with our hypothesis that expression of WAT1 is induced by Rboh-mediated ROS.

Infection assay with *wat1* plants reveals reduced susceptibility to nematodes

Previous studies suggested that *wat1* mediates a wide-range resistance to vascular fungi and baterial pathogens including *Verticillium dahlia*, *Verticillium albo-atrum*, *Ralstonia solanacearum* and *Xanthomonas campestris* (Denancé *et al.*, 2013). To assess whether *WAT1* is also involved in the infection process of nematodes, we infected Col-0, *wat1, rbohD/F* and *35S:WAT1* plants with *H. schachtii*. We counted the number of males and females. In addition, the size of females and their associated syncytium were measured at 14dpi. The results showed a significant reduction in numbers of female per plant when compared to Col-0 plants (Fig.8A). Furthermore, the average size of female nematodes and associated-syncytia was also significantly smaller in *wat1* mutant (Fig.8B). In contrast to *wat1*, overexpression of WAT1 (*35S:WAT1*) did not result in any change in susceptibility of plants to nematodes. Thus, *WAT1* is required for the establishment and early development of nematodes, but overexpression of *WAT1* does not increase susceptibility.

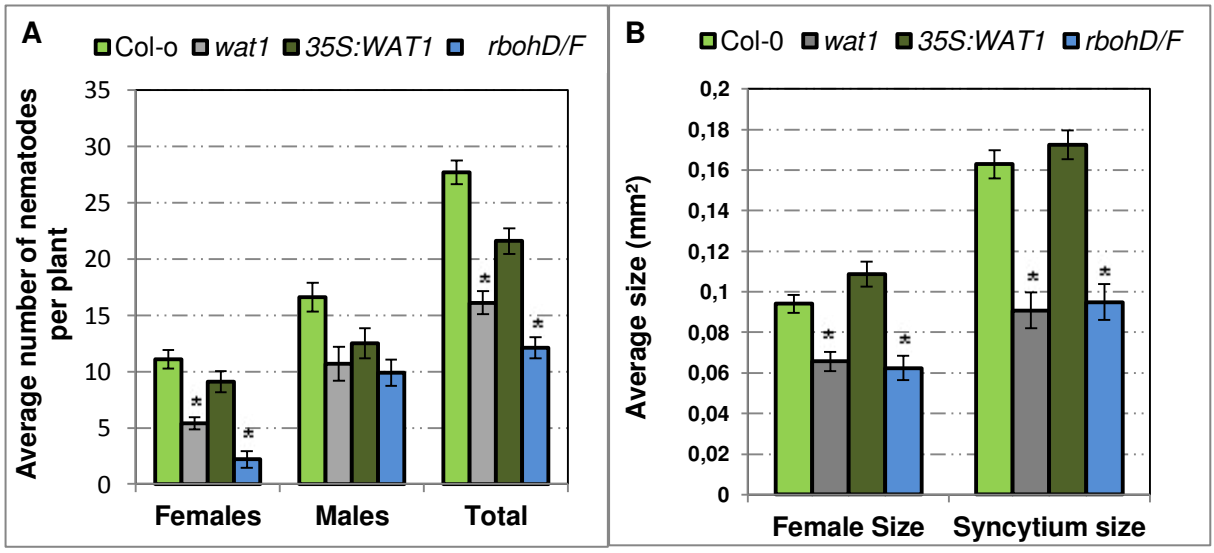

Auxin content decreased significantly in *rbohD/F* upon infection

Figure 8: Comparison of nematode development in *wat1, rbohD/F, 35S:WAT1* and Col-0. Nematode infection assay with *wat1, rbohD/F, 35S:WAT1* and Col-0. 10 days after germination, plants were inoculated with 60 nematodes per plant. (A) 12 dpi, number of males, females and total number was evaluated. Significant reduction of females and total number of nematodes in *rbohD/F* and *wat1* could be observed. (B) 14 dpi, size of females and associated syncytium have been measured. Female and syncytium size was significantly decreased in *wat1* and *rbohD/F*.

As transcript abundance for tryptophan metabolism was significantly decreased in roots of *rbohD/F* plants upon infection, we postulated that auxin contents would also be lower. Therefore, we sampled root segments containing infection sites at 3 dpi from Col-0, *wat1* and *rbohD/F*, and determined the level of free IAA (Fig.9). For comparison, uninfected roots and shoots were also cut and analyzed. Whereas, we did not see any significant difference in uninfected roots, shoots and infected shoots between Col-0 and *rbohD/F*, the auxin content was constitutively lower in *wat1* roots. In contrast to uninfected roots, the auxin content of infected root segments was severely reduced in *rbohD/F* and *wat1* as compared with Col-0.

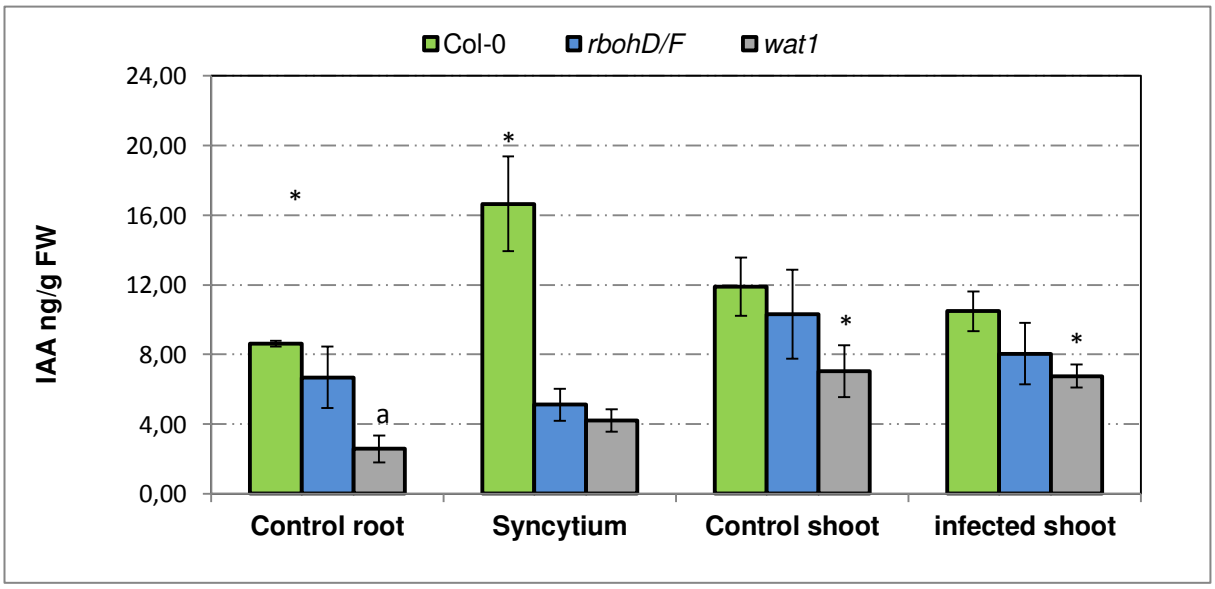

Figure 9: IAA content in roots and leaves of Col-0, *rbohD/F* and *wat1* plants without infection and at 3dpi. 10 days after germination, plants were inoculated with 100 nematodes per plant. Three days after inoculation, root segments containing syncytia without nematodes were cut and approximately 50mg per mutant plant have been collected. Control plants were cut 13 days after germination. Syncytia of Col-0 showed a significant increase of IAA level compared to control roots. This increase did not occure in syncytia of *rbohD/F* and *wat1*.

Discussion

The rapid production of reactive oxygen species (ROS) in the apoplast, the “oxidative burst”, by respiratory burst oxidase homologs (Rbohs) is one of the earliest defense responses in plants upon pathogen recognition. The role of Rboh-mediated ROS during plant-pathogen interactions is a matter of ongoing debate. Initially, ROS were thought to be associated with pathogen resistance or positive regulation of cell death. However, contrasting results were obtained in other studies where ROS acted as an important susceptibility factor for successful infections by pathogens. All these observations pointed to a pathosystem-specific role of ROS. Nevertheless, the mechanistic details for such a role remained elusive.

In a previous study, we characterized the role of Arabidopsis Rbohs in its interaction with cyst nematode *H. schachtii*. We found that RbohD and RbohF are required for production of oxidative burst in response to nematode attack. Unexpectedly, RbohD and RbohF loss-of-function double mutants (*rbohD/F*) showed a strong decrease in susceptibility to nematodes. Since salicylic acid (SA) has been demonstrated to antagonize ROS defense responses, we reasoned that the resistance phenotype of *rbohD/F* might be due to accumulation of SA. However, the triple mutant *rbohD/F/sid2* (salicylic acid induction deficient 2), which has been tested in previous study, did not show an enhanced susceptibility as compared to *rbohD/F.* This was surprising, therefore, we took an unbiased approach and performed a genome-wide transcriptome profiling of *rbohD/F* plants upon infection. This study was carried out by cutting root segments at 10 hours post inoculation (hpi), which reflects the initial stages of nematode infection including initial syncytial cell (ISC) establishment. The most striking feature of transcriptome analysis was a concomitant decrease in transcript abundance for indole and tryptophan metabolism. The gene that showed strongest decrease in transcript abundance was WAT1 (walls are thin 1). Since this observation pointed to a role of WAT1 in *rbohD/F* mediated resistance to nematodes, we have further characterized the functions of WAT1 in the development of syncytium and nematodes in this thesis. Denancé et al. (2013) challenged *wat1* plants with different fungal and bacterial pathogens and found out that *wat1* confers a broad spectrum resistance to vascular pathogens including *Ralstonia solanacearum* and *Xanthomonas campestris* pv. *campestris* and the fungi *Verticillium dahliae* and *Verticillium albo-atrum*. Furthermore, these authors restored full susceptibility to *R.*

solanacearum and *X.campestris pv. Campestris* through the introduction of *NahG*, the bacterial SA-degrading salicylate hydroxylase gene, into *wat1* mutants. In contrast, our studies with *rbohD/rbohF/NahG* triple mutant, did not restore the phenotype of Col-0 (Matera et al., 2014, unpublished data).

We propose that the production of Rboh-mediated ROS upon nematode infection results in the transcriptional activation of WAT1 at and around the infection site (Siddique et al., 2014; Tab.2; Fig.6). The activation of WAT1 expression is required for optimal channelization of the indole metabolites towards auxin and away from SA, thereby supporting the proper development of syncytium. Thus, the decreased susceptibility of *rbohD/F* to nematodes may result from a failure to activate the expression of WAT1 in response to nematode infection (Tab.2). We tested this by performing the infection assays with the loss-of-function mutant for WAT1, *wat1, and* WAT1 overexpression*, 35S:WAT1.* We found that *wat1* showed a strong decrease in average number of female nematodes as compared with Col-0 (Fig.8A). In addition, the average size of female- and associated syncytium also decreased significantly (Fig.8B). Nevertheless, we also found that the average number of females in *rbohD/F* was still significantly less as compared to *wat1.* Although, we cannot rule out the possibility that ROS is involved in pathways important for syncytium establishment other than activating WAT1, we speculate that redundancy in WAT1 function is responsible for the partial resistant phenotype of *wat1*.

To assess whether the transcriptional inactivation of WAT1 in *rbohD/F* leads to a failure in auxin accumulation at the infection site, we measured auxin content of Col-0, *rbohD/F* and *wat1* at 3pi (Fig.9). We observed a strong increase in auxin content in Col-0 at 3dpi. These findings are in agreement with those of previous studies showing strong activation of IAA signaling in response to nematode infection. Goverse et al. (2000) found that auxin-insensitive tomato mutants (*dgt*) demonstrated strongly decreased susceptibility to the potato cyst nematode *Globodera rostochiensis.* The authors asserted that penetration and migration in the *dgt* roots was normal, but the nematodes were not capable of developing into adult females. Moreover, the mutant tomato plants showed a range of phenotypes including a reduced number of cysts per plant (71%), a reduction in egg number per cyst, a decrease in cyst size, and a degradation of syncytial cytoplasm as compared to the control. These authors hypothesized that a local increase of auxin occurs upon

nematode infection, which is important for the morphogenesis of syncytium. In addition, Grunewald et al. (2009) visualized auxin accumulation at a cellular level during nematode infection using an auxin responsive reporter line (*DR5::GUS*). They found out that GUS staining persists in the developing syncytium until two days post inoculation and becomes less specific to the syncytium during the later stages of development. To accumulate auxin at infection site, nematodes must manipulate the cell in such a way that either its influx is increased or its efflux is inhibited. Therefore, the authors infected *PIN::GUS* transgenic plants and showed that especially *PIN3* and *PIN4* were specifically and highly expressed during syncytium development. Interestingly, *PIN1* and *PIN7* activity was missing in the developing syncytium and only detectable in the vasculature of infected and uninfected tissue. These findings suggest that nematodes manipulate not only the upregulation of *PIN* expression but also downregulation to facilitate their infection. Moreover, Grunewald et al. (2009) performed infection assays with *pin* mutations resulting in a 10%-25% reduction in the number of cysts, whereby *PIN3* and *PIN4* led only to smaller cysts, indicating their importance in later stages of infection. However, we did not find an increase in auxin content for *rbohD/F* at 3dpi and *wat1* showed a constitutive decrease in auxin content in the roots (Fig.9). This is in line with our hypothesis that RbohD/F mediated ROS activate the expression of WAT1 in an infection specific manner.

Our hypothesis also raised the interesting question of how a subcellular transporter such as WAT1 modulates the intracellular auxin metabolism. However, our hypothesis is supported by previous studies showing that two ER-localized transporters PIN 5 and PIN 8 mediate auxin flow at the ER-membrane and regulate auxin homeostasis at the cellular and subcellular level (Mravec et al., 2009). We speculate that WAT1-based modulation of auxin metabolism would be similar to that for PIN 5 and PIN 8.

Despite the importance of ROS during the plant-pathogen interaction, little is known about the components working downstream of ROS that mediate their sophisticated pathosystem-specific role. Our results provide a molecular framework for understanding the mechanistic details of the role of ROS as susceptibility factors. The regulation of auxin metabolism by ROS via WAT1 enables biotrophic pathogens such as nematodes to establish a long-term feeding relationship with their hosts. Our

data also provide insights into how a parasitic nematode hijacks the plant's defense pathways for its own benefit.

Materials and Methods

Plant material and growth conditions

A. thaliana plants were grown under sterile conditions in petri dishes containing agar medium supplemented with modified Knop's nutrient solutions with a 16h light and 8h dark cycle at 25°C. *Wat1-1, p35S::WAT1:GFP* and *ProWAT1:GUS* were provided by Ranocha et al. and isolated from a transfer DNA mutagenized population as described (Ranocha et al., 2010). *RbohD/F* was provided by Torres et al. (1998).

Nematode infection assay

To address the impact of loss-of-function mutants for nematode development, 120 sterile nematodes were inoculated onto the surface of agar medium in petri dishes containing two 12-days old plants. For each experiment, 30 plants were used for each genotype. The number of males and female nematodes per plant was counted at 14 dpi. The average size of syncytia and associated nematodes was measured in longitudinal optical sections. For that reason, 70 infection sites in roots containing syncytia and nematodes were photographed with a Leica DM2000 dissection microscope at 14 dpi. The syncytia and female nematodes were outlined, and the area was calculated using LAS software (Leica Microsystems)

GUS staining

(A) To observe the spatio-temporal expression of WAT1 during infection process, 12-days old Arabidopsis *proWat1*::GUS seedlings were inoculated with 60-65 nematodes per plant. At 8 hpi, 12 hpi, 1 dpi, 2 dpi and 5 dpi *proWat1*::GUS seedlings were incubated with staining solution. Uninfected *proWat1*::GUS seedlings were used as controls. *ProWat1*::GUS seedlings were then submerged in GUS solution at their respective time points after nematode infection.

(B) To address whether expression of WAT1 is induced by ROS, we treated 10-days old *proWAT1:GUS* seedlings with 1µM IAA and 1mM, 5mM, 10mM or 50mM H_2O_2 and detected GUS expression after 1 hour. Water-treated *proWAT1:GUS* seedlings were used as control.

The staining solution consisted of 1M Na2HPO4/NaH2PO4 pH 7.5, 2mM X-Gluc, 5mM EDTA pH 8 and 0.01% Triton X-100 and the seedlings were incubated at 37°C for 5 hours. After 5 hours the reaction was stopped by washing away the GUS solution with 70% ethanol. For imaging with a Leica DM4000 inverted microscope (Leica Microsystems) fitted with an Olympus C-5050 digital camera, the entire plant or root segments without lateral root primordial, mechanical stress, and root tips were used.

Comparative transcriptome analysis

To explore the molecular mechanisms underlying the reduced susceptibility of *rbohD/F* and ROS mediated suppression of cell death, transcriptome comparison between the Col-0 and *rbohD/F* was performed. Small root segments surrounding nematode head (0.1 cm) were cut at 10 hpi. Total RNA was extracted, labelled and amplified to hybridise with the GeneChip® Arabidopsis ATH1 Genome (Affymetrix UK Ltd).

Real-time PCR

To address whether similar changes in transcript abundance occur between Col-0 and *rbohD/F* plants without nematode infection, we cut root segments (up to 100mg) from roots of uninfected plants. Root segments without lateral root primordia, mechanical stress, and root tips were selected. Total RNA was extracted using a NucleoSpin RNA kit (Macherey-Nagel) according to the manufacturer's instructions, including deoxyribonuclease digestion. Reverse transcription was performed with the High-Capacity cDNA Reverse Transcription Kit (Invitrogen) according to the manufacturer's instructions. Quantitative PCR was performed with the Stepone Plus Real-Time PCR System (Applied Biosystems). Each sample contained 10 µl of Fast SYBR Green qPCR Master Mix with uracil-DNA, glycosylase, and 6-carboxy-x-rhodamine (Invitrogen), 2 mM MgCl2, 0.5 µl each of forward and reverse primers (10 µM), 2 µl of complementary DNA (cDNA), and water in a 20-µl total reaction volume. The primers are listed in table S5. Samples were analyzed in three technical replicates. 18S was used as an internal control. Relative expression was calculated

by the DDCt method, where the expression of each gene was normalized to 18S and then to Col-0 to calculate fold change.

Quantification of IAA in plant tissue

To quantify the IAA content in different plant tissues, 12-days old Arabidopsis plants were inoculated with 100 nematodes. For every experiment, 25 plants were used for each genotype. After 3 days, small root segments surrounding nematodes head were cut (up to 50mg) excluding lateral root primordial, root tips and parts with mechanical stress. Leaves of infected and uninfected plants were cut as well. Quantification of IAA level has been performed in the Max Plank Institute for Chemical Ecology using Iontrap mass spectrometry as described (Trapp et al., 2014).

References

Apel K., Hirt H. (2004): Reactive oxygen species: metabolism, oxidative stress, and signal transduction. Plant Biology 55: 373-99

Blaxter M.L, De Ley P., Garey J.R., Liu L.X., Scheldeman P., Vierstraete A., Vanfleteren J.R., Mackey L.Y., Dorris M., Frisse L.M., Vida J.T., Thomas W.K. (1998): A molecular evolutionary framework for the phylum Nematoda. Nature 392(6671): 75-5

Denancé N., Ranocha P., Oria N., Barlet X., Rivière M.-P., Yadeta K. A., Hoffmann L., Perreau F., Clément G., Maia-Grondard A., van den Berg G. C.M., Savelli B., Fournier S., Aubert Y., Pelletier S., Thomma B. P.H.J., Molina A., Jouanin L., Marco Y., Goffner D. (2013): Arabidopsis *wat1* (*walls are thin1*)-mediated resistance to the bacterial vascular pathogen, *Ralstonia solanacearum*, is accompanied by cross-egulation of salicylic acid and tryptophan metabolism. The Plant Journal 73(2): 225–239

Foreman J., Demidchik V., Bothwell J.H., Mylona P., Miedema H., Torres M.A., Linstead P., Costa S., Brownlee C., Jones J.D. (2003): Reactive oxygen species produced by NADPH oxidase regulate plant cell growth. Nature 422: 442-446

Gardner M., Verma A., Mitchum M. G. (2015): Emerging roles of cyst nematode effectors in exploiting plant cellular processes. Advances in Botanical Research 73: 259-291

Goverse A., Overmars H., Engelbertink J., Schots A., Bakker J., Helder, J. (2000): Both induction and morphogenesis of cyst nematode feeding cells are mediated by auxin. Molecular Plant-Microbe Interactions 13(10): 1121-1129

Grunewald W., Cannoot B., Friml J., Gheysen G. (2009): Parasitic nematodes modulate PIN-mediated auxin transport to facilitate infection. PLoS pathogens 5(1): e1000266

Hancock J.T., Desikan R., Neill S.J. (2001): Role of reactive oxygen species in cell signaling pathways. Biochemical and Biomedical Aspects of Oxidative Modification 29(2): 345-350

Hofmann J., El Ashry A., Anwar S., Erban A., Kopka J., Grundler F.M.W. (2010): Metabolic profiling reveals local and systemic responses of host plants to nematode parasitism. Plant Journal 62: 1058-1071

Hofmann J., Szakasits D., Blochl A., Sobczak M., Daxbock-Horvath S., Golinowski W., Bohlmann H., Grundler F.M.W. (2008): Starch serves as carbohydrate storage in nematode-induced syncytia. Plant Physiol 146(1): 228-235

Jaubert S., Ledger T.N., Laffaire J.B., Piotte C., Abad P., Rosso M.N. (2002): Direct identification of stylet secreted proteins from root-knot nematodes by a proteomic approach. Molecular and Biochemical Parasitology 121(2): 205-11

Jones M. G. K. (1981): Host cell responses to endoparasitic nematode attack: structure and function of giant cells and syncytia. Annals of Applied Biology 97(3): 353-372

Kovtun Y., Chiu W-L., Tena G. (2000): Functional analysis of oxidativ stress-activated mitogen-activated protein kinase cascade in plants. Proc Natl Ascad Sci USA 97 2940-2945

Lamp C., Dixon R.A. (1997): The oxidative burst in plant disease resistance. Plant Physiology 48: 251-75

Miller G., Schlauch K., Tam R., Cortes D., Torres M., Shulaev V., Dangle J.L., Mittler R. (2009): The plant NADPH oxidase RBOHD mediates rapid systematic signaling in response to diverse stimuli. Science Signaling 2

Mravec J., Skůpa P., Bailly A., Hoyerová K., Křeček P., Bielach A., Petrasek J., Zhang J., Gaykova V., Stierhof Y.D., Dobrev P.I., Schwarzerova K., Rolcik J., Seifertova D., Luschnig C., Benkova E., Zazilmalova E., Geisler M., Friml J. (2009): Subcellular homeostasis of phytohormone auxin is mediated by the ER-localized PIN5 transporter. Nature 459(7250): 1136-1140

Müller J. (1999): The economic importance of *Heterodera schachtii* in Europe. Helminthologia 36: 205–213

Ranocha P., Denancé N., Vanholme R., Freydier A., Martinez Y., Hoffmann L., Köhler L., Pouzet C., Renou J.P., Sundberg B., Boerjan W., Goffner, D. (2010): Walls are thin 1 (WAT1), an Arabidopsis homolog of Medicago truncatula NODULIN21, is a tonoplast-localized protein required for secondary wall formation in fibers. The Plant Journal 63(3): 469-483

Siddique S., Endres S., Atkins J.M., Szakasits D., Wieczorek K., Hofmann J., Blaukopf C., Urwin P.E., Tenhaken R., Grundler F.M.W., Kreil D.P., Bohlmann H. (2009): Myo-inositol oxygenase genes are involved in the development of syncytia induced by *Heterodera schachtii* in *Arabidopsis* roots. New Phytologist 184: 457-472

Siddique S., Matera C., Radakovic Z. S., Hasan M. S., Gutbrod P., Rozanska Sobczak M., Torres M.A., Grundler F.M.W. (2014): Parasitic worms stimulate host NADPH oxidases to produce reactive oxygen species that limit plant cell death and promote infection. Science Signaling 7(320): ra33-ra33

Simonetti E., Veronico P., Melillo M.T., Delibes A., Andres M.F., Lopez-Brana I. (2009): Analysis of Class 3 Peroxidase Genes Expressed in Roots of Resistant and Susceptible Wheat Lines infected by *Heterodera avenae*. Molecular Plant-Microbe Interactions 22(9): 1081-1092

Szakasits D., Heinen P., Wieczorek K., Hofmann J., Wagner F., Kreil D.P., Sykacek P., Grundler F.M.W., Bohlmann H. (2009): The transcriptome of syncycia induced by the cyst nematode *Heterodera schachtii* in *Arabidopsis* roots. The plant Journal 57: 71-784

Torres M.A., Onouchi H., Hamada S., Machida, Ch., Hammond-Kosack K., Jones J.D.G. (1998): Six *Arabidopsis thaliana* homologues of the human respiratory burst oxidase (gp91phox). The plant journal 14(3): 365-370

Torres M.A., Dangl J.L., Jones J.D. (2002): *Arabidopsis* gp91phox homologues AtrbohD and AtrbohF are required for accumulation of reactive oxygen intermediates in the plant defense response. Proc Natl Acad Sci USA 99: 517–522

Trapp M. A., De Souza G. D., Rodrigues-Filho E., Boland W., Mithöfer A. (2014): Validated method for phytohormone quantification in plants. Frontiers in plant science 5

Waetzig Georg H., Grundler F.M.W., Sobczak M. (1999): Localization of hydrogen peroxide during the defence response of *Arabidopsis thaliana* against the plant-parasitic nematode *Heterodera glycines*. Nematology 1(7-8): 681-686

Vanholme B., De Meutter J., Tytgat T., Van Montagu M., Coomans A., Gheysen G., (2004): Secretions of plant-parasitic nematodes: a molecular update. Gene 332: 13-27

Chapter 4

Discussion and Perspective

The production of reactive oxygen species (ROS) in apoplast, the oxidative burst, is one of the earliest defense responses during plant-pathogen interactions. The role of oxidative burst in limiting pathogen growth and development has been well documented in a variety of plant-pathosystems (Zacheo and Bleve-Zacheo 1988, Grundler et al. 1997, Alvarez et al. 1998, Melillo et al. 2006, Simonetti et al. 2009). A review of previously published work showed that ROS execute their anti-pathogenic role in a number of ways such as cross linking of cell wall, callose deposition and acting as signaling molecule to activate expression of defense-related genes (Levine et al. 1994, Kovtun et al., 2000, Mou et al., 2003, Mur et al., 2008). Pathogenesis-related ROS are produced by various sources in host plants but membrane-localized NADPH oxidase are shown to be the main source in majority of the studies performed so far.

Sedentary endoparasitic nematodes are obligate biotrophs that establish long-term feeding relationships with their hosts by inducing permanent feeding sites in roots. The development of nematode feeding sites is accompanied by structural, transcriptomic and metabolomics changes at the site of infection. However, the mechanisms underlying initiation, formation and maintenance of nematode feeding sites are not well understood and remained a challenge for coming research. An important aspect of feeding site development is the activation of host defense responses. How nematodes are able to cope and even manipulate the host defense responses is a matter of ongoing research. This thesis is an attempt to get mechanistic understanding of defense-related signaling networks that are associated with nematode infection. The work builds on previously published research of our working group which showed that reactive oxygen species (ROS) are produced during an incompatible interaction between soybean cyst nematode *Heterodera glycines* and host plant *Arabidopsis thaliana* (Grundler et al., 1997). A few years later, Waetzig et al. (1999) localized the generation of these pathogen-mediated ROS at the plasma membrane, suggesting that the membrane-bound NADPH oxidase has a key role during the incompatible interaction between *H.glycines* and *A.thaliana*. Considering the traditional role of ROS during plant-pathogen interaction, it is

expected that production of ROS in Arabidopsis-*H. glyines* pathosystem is associated with activation of defense responses in these plants.

During this thesis, we characterized the role of ROS in a compatible interaction between Arabidopsis and cyst nematode *Heterodera schachtii*. Therefore, we focused on the NADPH oxidases encoding Rboh (respiratory burst oxidase homolog) genes. To start with, we used *Arabidopsis* Rboh mutants (*rbohA-J*) to see whether these are involved in the generation of ROS during early stages of nematode infection on plant roots. Our analysis figured out that RbohD and RbohF are the main sources of host ROS produced upon infection with *H. schachtii*. These data are in agreement with earlier studies where a similar role of RbohD and RbohF was implicated (Torres et al., 2002). Further, NtRBOH was shown to have similar role in elicited tobacco cells (Simon-Plas et al, 2002). However, in contrast to other studies, our results showed that a loss-of-function double mutant for RbohD and RbohF (*rbohD/F*) was strongly impaired in various aspects of nematode infection process. A similar positive correlation between reduced pathogen susepcitiblity and ROS production has already been shown in few studies (Torres et al. 2002, Trujillo et al., 2006) but the role of ROS in a compatible biotrophic interaction is relatively unknown. We used a number of marker genes to perform a comparative gene expression analysis between syncytia growing on Col-0 or *rbohD/F* via qPCR. The data figured out that the marker genes for salicylic acid (SA) signaling were highly upregulated in *rbohD/F* as compared to Col-0. Since SA has been identified to act as a systemic and local signaling molecule that is accumulated in cells around infection sites of diverse pathogens (Malamy et al., 1990; Yalpani et al., 1991), we hypothesized that activation of SA-mediated defense responses at the nematode feeding site in *rbohD/F* may contribute to decreased susceptibility of these plants to nematodes. These findings are in agreement with previous work reporting that ROS antagonize SA. Torres et al. (2005) showed that RBOHD and RBOHF activity antagonized SA-induced pro-death signals in Arabidopsis by using *lsd1/rbohD* (**l**esion **s**imulating **d**isease 1) and *lsd1/rbohF* double mutants. They demonstrated that the characteristic “spreading cell death” phenotype of *lsd1* mutant was even increased in the absence of RBOHD and RBOHF. Additionally, double mutants showed an enhanced pathogen-mediated cell death. This view is additionally supported by our experiments showing that infection of *rbohD/F* led to an increased cell death during the early migration and establishment phase of the nematode (Siddique et al., 2014).

Therefore, we performed infection assays with *rbohD/F/sid2* (**S**A **i**nduction-**d**eficient) triple mutants. Surprisingly, *rbohD/F/sid2* did not show an enhanced susceptibility as compared to *rbohD/F*. This raises the question, which pathways other than SA are influenced by ROS that positively regulate nematode infection.

To answer the question, we performed a genome-wide transcriptome profiling of *rbohD/F* plants upon infection. This study was carried out by cutting root segments at 10 hours post inoculation (hpi), which reflects the initial stages of nematode infection including the establishment of initial syncytial cell (ISC). The most striking feature of the transcriptome analysis was a concomitant decrease in transcript abundance for genes encoding enzymes involved in indole and tryptophan metabolism. The gene that showed the strongest decrease in transcript abundance was WAT1 (**w**alls **a**re **t**hin 1), a vacuolar auxin transport facilitator which is necessary for optimal cellular auxin homoeostasis (Ranocha et al. 2013). This observation pointed to a role of *WAT1* in *rbohD/F* mediated decreased susceptibility to nematodes. This was tested by performing infection assays with *wat1*, which led to a similar decrease in susceptibility as seen in *rbohD/F*. These results are in agreement with previous studies, where *wat1* is shown to confer a broad spectrum resistance to vascular pathogens including the fungi *Verticillium dahlia* and *Verticillium albo-atrum*, and the bacteria *Ralstonia solanacearum* and *Xanthomonas campestri* (Denancé et al., 2013). Thus, decreased susceptibility of *rbohD/F* to nematodes could result from a failure to activate the expression of WAT1 in response to nematode infection, which is perhaps required for modulation of auxin homeostasis at the cellular and subcellular level.

We were able to measure the auxin content in root segments containing three days old syncytia and confirmed a lower amount of free indole-3-acetic acid (IAA) in *rbohD/F* and *wat1* compared to Col-0. The importance of auxin during different plant-microorganism interactions has been described. Thimann et al. (1936) figured out that nodules of rhizobia contain a high level of auxin and recent studies in *Medicago trancatula* have shown that development of nodules are regulated by flavonoids, which act as auxin transport inhibitors (Wasson et al., 2006). In addition, Hutangura et al. (1999) suggested that *Meloidogyne javanica* manipulates the auxin distribution in white clover roots by modulating the flavonoid pathway, supposing that auxin acts as a trigger for root gall formation. More recent studies confirmed that auxin is also

involved in plant-cyst nematode interaction (Goverse et al., 2000; Karczmarek et al., 2004; Grunewald et al., 2008). Nevertheless the absence of auxin also influences other pathways, e.g. auxin-inducible ethylene production, which could also contribute to the reduced susceptibility of *rbohD/F* plants. Goverse et al. (2000) showed that the auxin-induced ethylene-insensitive mutant *axr2* (**a**u**x**in **r**esistant 2) inhibits successful nematode parasitism. Further, Wubben et al. (2001) demonstrated that Arabidopsis mutants that overproduce ethylene are much more susceptible to *H.schachtii* then ethylene insensitive mutants. The same is true for plants which are treated with 1-aminocyclopropane-1-carboxylic acid (ACC), an ethylene precursor. The same authors reported that nematodes are capable of down-regulating RDH1 (**r**oot **h**air **d**efective 1) gene expression, leading to enhanced sensitivity of root tissue to ethylene and auxin (Wubben et al., 2004). Pogány et al. (2009) observed that *rbohD* mutants infected with *Alternaria brassicicola* accumulate not only SA but also ethylene suggesting that RbohD-mediated ROS may inhibit both SA and ethylene.

During this thesis we did not address the contribution of ethylene to the Rboh-mediated decreased susceptibility of plants to nematodes; therefore, it remains to be seen whether the reduced amount of auxin at the infection site in *rbohD/F* has an effect on ethylene signaling.

It is difficult at this point to assess the relative contribution of the decrease in auxin transport and the reduction in auxin biosynthesis in lower auxin content at the infection zone. To answer this question, we would need to perform genetic and biochemical complementation to restore the Col-0 phenotype for *rbohD/F* during infection. This could be achieved by crossing *rbohD/F* with *35S:WAT1* plants. Alternatively*, rbohD/F* plants can be grown in a medium containing auxin or tryptophan for the performance of nematode infection assays. Apart from this, future studies should address how a vacuolar transporter such as WAT1 can modulate intracellular auxin homeostasis. We hypothesize that this subcellular transporter modulates the intracellular auxin metabolism as it has been shown in previous studies where two ER-localized transporters PIN 5 and PIN 8 mediate auxin flow at the ER-membrane and regulate auxin homeostasis at the cellular and subcellular level (Mravec et al., 2009).

Nevertheless, our results point to the importance of WAT1 expression for the development of nematodes as well as to its major role during the early stages of

nematode infection. Therefore, it should be investigated whether the reduction in the number of females and the decreased size of females and associated syncytium in *wat1* can be linked to a similar delay in establishment of the ISC as observed in *rbohD/F*. The same applies for the regulation of WAT1. Although we showed that ROS can activate WAT1 expression, it remains still unclear whether ROS trigger this activation directly or the activation requires additional regulatory components. To answer these questions, further experiments will be necessary. The results could provide additional details for the role of WAT1 as a link between two major signaling networks in plants.

The aim of this thesis was to understand the role of plant NADPH oxidase mediated ROS production during the infection of plant-parasitic nematodes. Surprisingly, we discovered that *H.schachtii* uses the defense mechanisms of *A.thaliana* to its own benefit, what has not been observed so far. Further, we tried to analyze the mechanical details behind the rbohD/F-mediated reduced susceptibility, leading to the suggestion that nematodes manipulate specific pathways in plants for their establishment and development. Our results increase knowledge of biological processes during the complex nematode-plant interaction on a molecular level. For that reason, our data can be used as a foundation for applied science to develop novel measures and treatments for nematode management. This could be helpful to switch away from the use of toxic nematicides, which are strictly restricted, to more target-specific application to control nematode-induced crop damage.

References

Alvarez M.E., Pennell R., Meijer P-J., Ishikawa A., Dixon R.A., Lamb C. (1998): Reactive oxygen intermediates mediate a systemic signal network in the establishment of plant immunity. Cell 92: 773-784

Denancé N., Ranocha P., Oria N., Barlet X., Rivière M.-P., Yadeta K. A., Hoffmann L., Perreau F., Clément G., Maia-Grondard A., van den Berg G. C.M., Savelli B., Fournier S., Aubert Y., Pelletier S., Thomma B. P.H.J., Molina A., Jouanin L., Marco Y., Goffner D. (2013): Arabidopsis *wat1* (*walls are thin1*)-mediated resistance to the bacterial vascular pathogen, *Ralstonia solanacearum*, is accompanied by cross-egulation of salicylic acid and tryptophan metabolism. The Plant Journal 73: 225–239

Goverse A., Overmars H., Engelbertink J., Schots A., Bakker J., Helder, J. (2000): Both induction and morphogenesis of cyst nematode feeding cells are mediated by auxin. Molecular Plant-Microbe Interactions 13(10): 1121-1129

Grundler F.M.W., Sobczak M., Lange S. (1997): Defence responses of *Arabidopsis thaliana* during invasion and feeding site induction by the plant-parasitic nematode *Heterodera glycines*. Physiological and Molecular Pathology 50: 419-429

Grunewald W., Karimi M., Wieczorek K., Van de Cappelle E., Wischnitzki E., Grundler F.M.W., Inzé D., Beeckman T., Gheysen G. (2008): A role for AtWRKY23 in feeding site establishment of plant-parasitic nematodes. Plant physiology 148(1): 358-368

Hutangura P., Mathesius U., Jones M.G.K., Rolfe B.G. (1999): Auxin induction is a trigger for root gall formation by root.knot nematodes in white clover and is asscociated with the activation of the flavonoid pathway. Australian Journal of Plant Physiology 26(3): 221-231

Karczmarek A., Overmars H., Helder J., Goverse A. (2004): Feeding cell development by cyst and root-knot nematodes involves a similar early, local and transient activation of a specific auxin-inducible promoter element. Molecular Plant Pathology 5(4): 343-346

Kovtun Y., Chiu W-L., Tena G. (2000): Functional analysis of oxidativ stress-activated mitogen-activated protein kinase cascade in plants. Proc Natl Ascad Sci USA 97: 2940-2945

Levine A., Tenhaken R., Dixon R., Lamb C.J. (1994): H_2O_2 from the oxidative burst orchestrates the plant hypersensitive disease resistance response. Cell 79: 583–593

Malamy J., Carr J.P., Klessig D.F., Raskin I. (1990): Salicylic acid: A likely endogenous signal in the resistance response of tobacco to tobacco mosaic virus. Science 25: 1002–1006

Melillo M. T., Leonetti P., Bongiovanni M., Castagnone-Sereno P., Bleve-Zacheo T. (2006): Modulation of reactive oxygen species activities and H2O2 accumulation during compatible and incompatible tomato–root-knot nematode interactions. New Phytologist, 170(3): 501-512

Mou Z., Fan W., Dong X. (2003): Inducers of plant systemic acquired resistance regulate NPR1 function through redox changes. Cell 113: 935–944

Mur L.A.J., Kenton P., Lloyd A.J., Ougham H., Prats E. (2008): The hypersensitive response; the centenary is upon us but how much do we know? J Exp Bot 59: 501–520

Pogány M., von Rad U., Grün S., Dongó A., Pintye A., Simoneau P., Bahnweg G., Kiss L., Barna B., Durner J. (2009): Dual Roles of Reactive Oxygen Species and NADPH Oxidase RBOHD in Arabidopsis-*Altanaria* Pathosystem. Plant Physiology 151(3): 1459-1475

Ranocha P., Dima O., Nagy R., Felten J., Corratgé C., Novák O., Morreel K., Lacombe B., Martinez Y., Pfrunder S., Jin X., Ranou J.P. Thibaud J.B., Ljung K, Fischer U., Martinoia E., Boerjan W., Goeffner D. (2013): Arabidopsis WAT1 is a vascuolar auxin transport facilitator required for auxin homoeostasis. Nature Communications 4: 2625

Thimann K. V. (1936): On the Physiology of the Formation of Nodules on Legume Roots. Proceedings of the National Academy of Sciences of the United States of America 22(8): 511–514

Torres M.A., Dangl J.L., Jones J.D.G. (2002): *Arabidopsis* gp91phox homologues AtrbohD and AtrbohF are required for accumulation of reactive oxygen intermediates in the plant defense response. Proc Natl Acad Sci USA 99: 517–522

Torres M.A., Jones J.D.G., Dangl J.L. (2005): Pathogen-induced, NADPH oxidase-derived reactive oxygen intermediates suppress spread of cell death in *Arabidopsis thaliana*. Nature Genetics 37: 10

Trujillo M., Ichimura K., Casais C., Shirasu K. (2008): Negative regulation of PAMP-triggered immunity by an E3 ubiquitin ligase triplet in Arabidopsis. Current Biology 18(18):1396-1401

Siddique S., Matera C., Radakovic Z. S., Hasan M. S., Gutbrod P., Rozanska E., Sobczak M., Torres M.A., Grundler F.M.W. (2014): Parasitic worms stimulate host NADPH oxidases to produce reactive oxygen species that limit plant cell death and promote infection. Science Signaling 7(320): ra33-ra33

Simonetti E., Veronico P., Melillo M.T., Delibes A., Andres M.F., Lopez-Brana I. (2009): Analysis of Class 3 Peroxidase Genes Expressed in Roots of Resistant and Susceptible Wheat Lines infected by *Heterodera avenae*. Mol Plant Microbe In 22 (9): 1081-1092

Simon-Plas F., Elmayan T., Blein J.P. (2002): The plasma membrane oxidase NtrbohD is responsible for AOS production in elicited tabacco cells. The Plant Journal 31(2): 137-147

Waetzig Georg H., Grundler F.M.W., Sobczak M. (1999): Localization of hydrogen peroxide during the defence response of *Arabidopsis thaliana* against the plant-parasitic nematode *Heterodera glycines*. Nematology 1(7-8): 681-686

Wasson A.P., Pellerone F.I., Mathesius U. (2006): Silencing the Flavonoid Pathway in *Medicago truncatula* Inhibits Root Nodule Formation and Prevents Auxin Transport Regulation by Rhizobia. The Plant Cell 7: 1617-1629

Wubben M.J.E., Su H., Rodermel S.R., Baum T.J. (2001): Susceptibility to the Sugar Beet Cyst Nematode Is modulated by Ethylene Signal Transduction in *Arabidopsis thaliana*. Molecular Plant-Microbe Interactions 14(10): 1206-1212

Wubben M. J., Rodermel S. R., Baum T. J. (2004): Mutation of a UDP-glucose- 4- epimerase alters nematode susceptibility and ethylene responses in Arabidopsis roots. The Plant Journal 40(5): 712-724

Yalpani N., Silverman P., Wilson T.M.A., Kleier D.A., Raskin I. (1991): Salicylic acid is a systemic signal and an inducer of pathogenesis-related proteins in virus-infected tobacco. Plant Cell 3: 809–818

Zacheo G., Bleve-Zacheo T., Lamberti F. (1982): Role of peroxidase and superoxide dismutase activity in resistant and susceptible tomato cultivars infested by *Meloidogyne incognita*. Nematologia mediterranea 10: 75-80

Zacheo G., Bleve-Zacheo T. (1988): Involvement of superoxide dismutases and superoxide radicals in the susceptibility and resistance of tomato plants to *Meloidogyne incognita* attack. Physiological and molecular plant pathology 32(2): 313-322

Appendix

Supplementary Material Chapter 2

Supplementary Material Chapter 3

Science Signaling
AAAS

www.sciencesignaling.org/cgi/content/full/7/320/ra33/DC1

Supplementary Materials for

Parasitic Worms Stimulate Host NADPH Oxidases to Produce Reactive Oxygen Species That Limit Plant Cell Death and Promote Infection

Shahid Siddique, Christiane Matera, Zoran S. Radakovic, M. Shamim Hasan, Philipp Gutbrod, Elzbieta Rozanska, Miroslaw Sobczak, Miguel Angel Torres, Florian M. W. Grundler*

*Corresponding author. E-mail: grundler@uni-bonn.de

Published 8 April 2014, *Sci. Signal.* **7**, ra33 (2014)
DOI: 10.1126/scisignal.2004777

The PDF file includes:

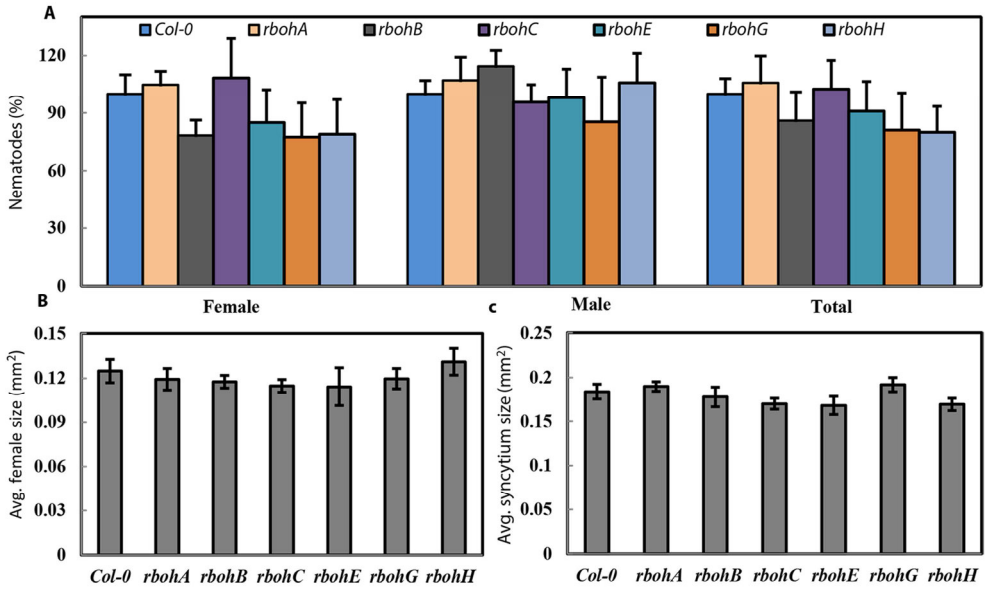

Fig. S1: Nematode infection assays in *Rboh* mutant plants. (A) Nematodes at 14 dai. Data points represent percent of nematodes where the number of nematodes per plant in Col-0 was set to 100%. (B) Average size of female nematodes 14 dai. (C) Average size of plant syncytia 14 dai. Data points represent three independent expreiments (mean ± s.e.m).

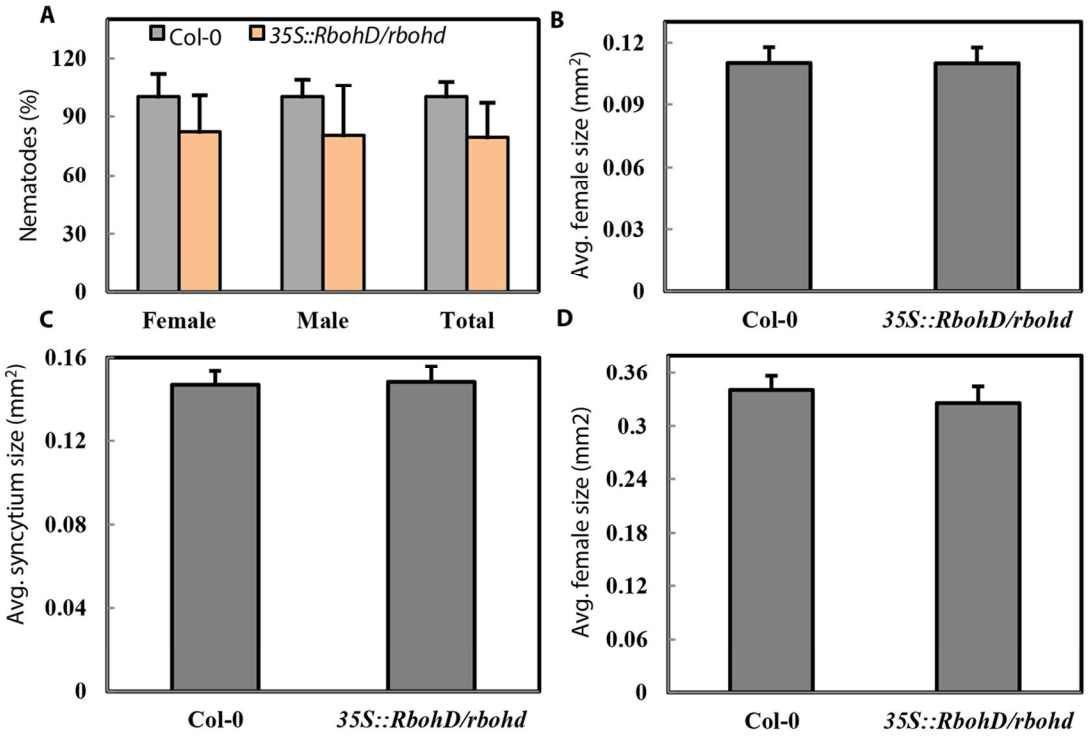

Fig. S2. Nematode infection assays in *35S::RbohD/rbohD* plants. (A) Nematodes 14 dai. Data points represent percent of nematodes where the number of nematodes per plant in Col-0 was set to 100%. (B) Average size of female nematodes 14 dai. (C) Average size of plant syncytia 14 dai. (D) Average female size 25 dai. Data points represent three independent experiments (mean ± s.e.m).

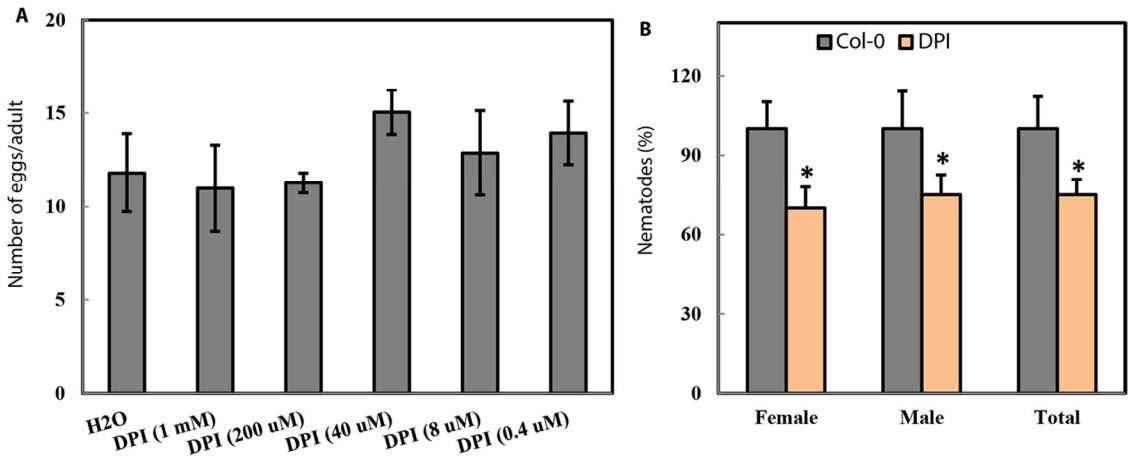

Fig. S3. Development and invasion of nematodes treated with DPI. (A) Number of eggs per adult in *C. elegans* after three days of development. (B) Nematodes 14 dai. Data points represent percent of nematodes where the number of nematodes per plant in Col-0 was set to 100%. Data represent three independent expreiments (mean ± s.e.m). Asterisks indicate $p<0.05$ compared to Col-0. *t*-test.

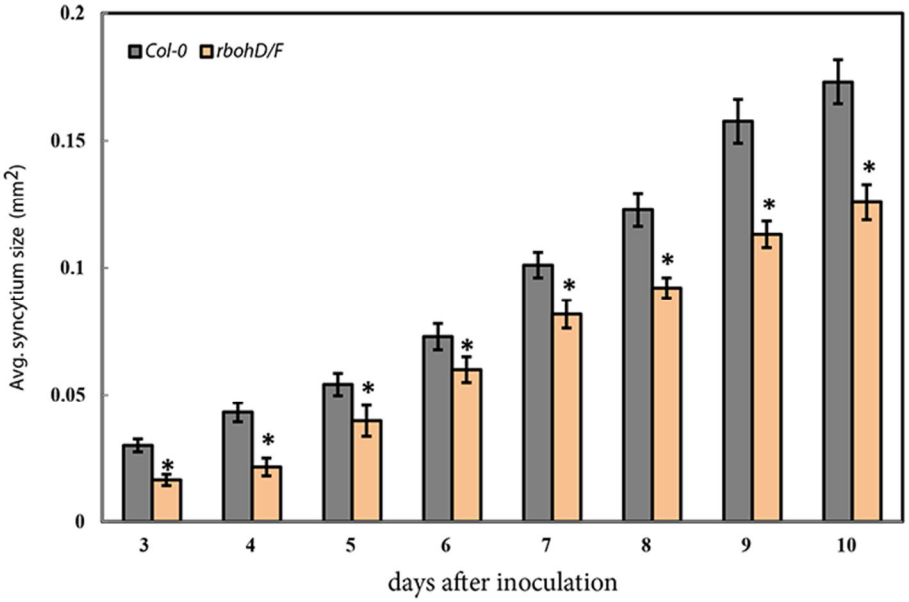

Fig. S4. Plant syncytium size in *rbohD/F* plants. Average size of plant syncytia over ten dai. Data represent three independent experiments (mean ± s.e.m). Asterisks indicate $p<0.05$ compared to Col-0. *t*-test.

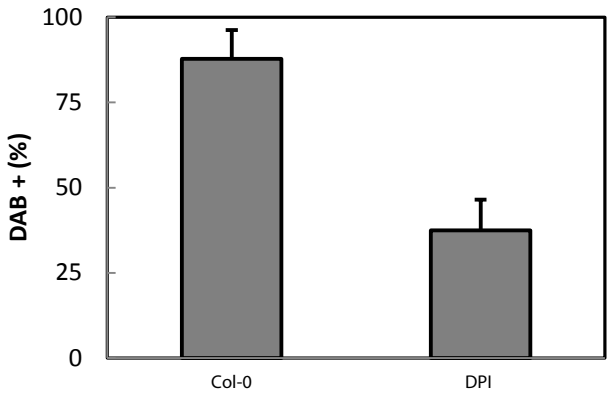

Fig. S5. ROS visualization in roots of DPI-treated Col-0 plants. Quantification of the DAB staining of ROS in roots of Col-0 plants. Data represent two independent experiments (mean ± S.D).

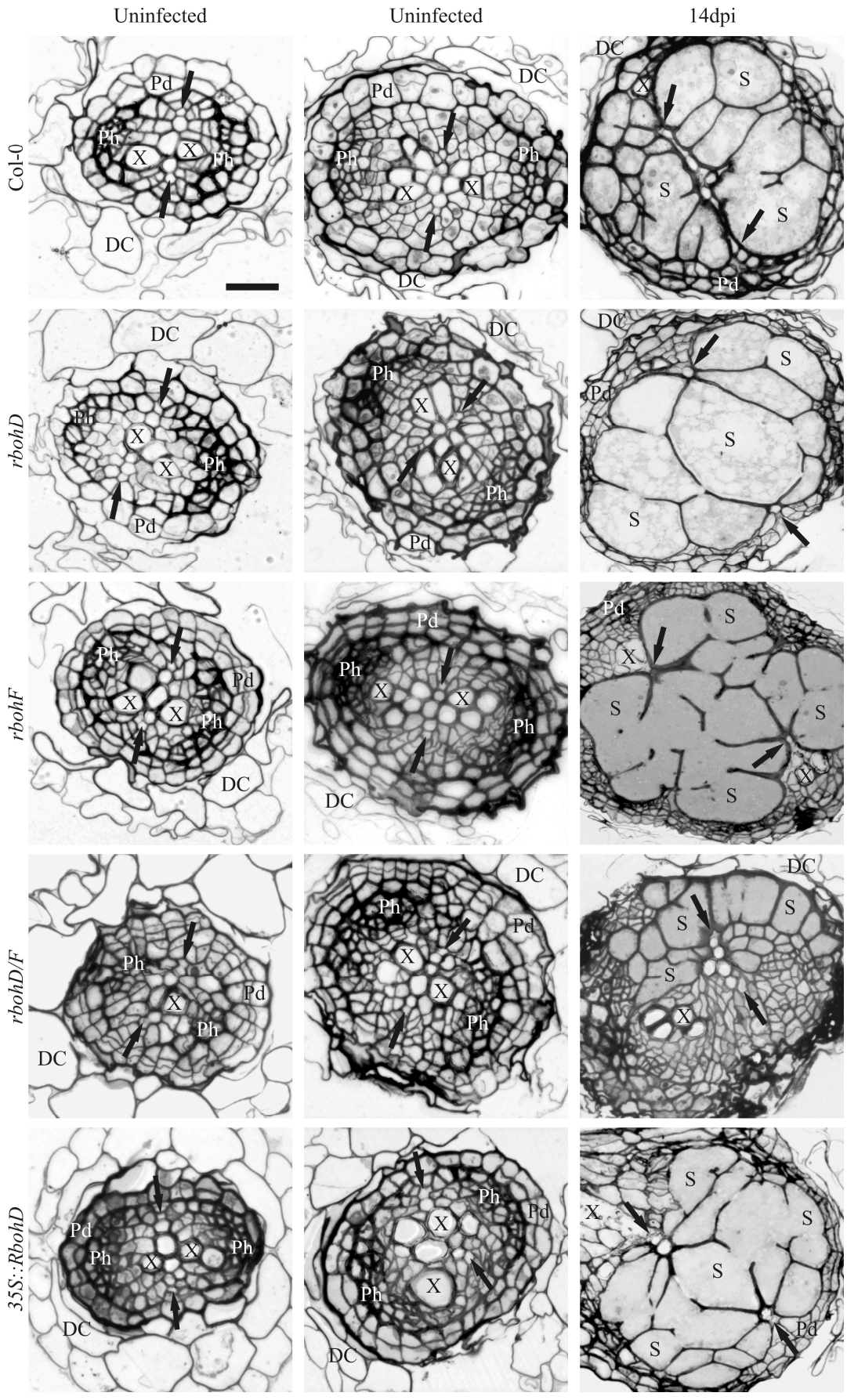
Uninfected
Uninfected
14dpi
Col-0
rbohD
rbohF
rbohD/F
35S::RbohD
Pd
Ph
X
DC
S

Fig. S6. Light microscopy of uninfected *Rboh* mutant plants in secondary growth and infected *Rboh* mutant plants 14 dai. Light microscopy micrographs of cross sections taken from samples of uninfected roots in early (left column) or advanced (middle column) stages of the secondary growth. Section of roots containing syncytia 14 dai (right column) taken at the broadest parts of syncytia located away from the nematode heads. Arrows indicate the position and direction of primary xylem bundles. Abbreviations: DC = degraded cortical parenchyma. Pd=peridermis. Ph=phloem. S=syncytium. X=secondary xylem vessel. Scale bar = 20 μm.

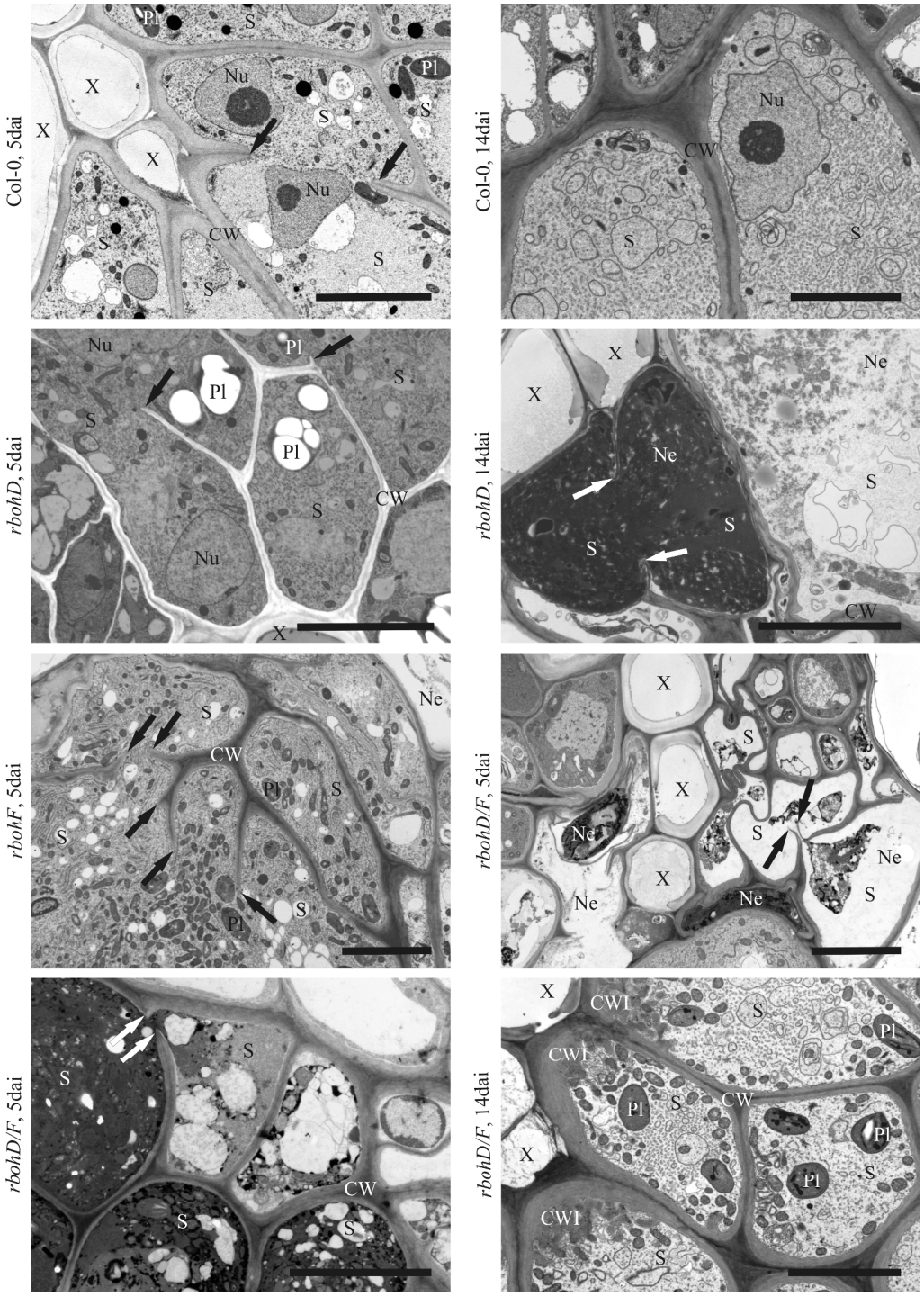

Fig. S7. Transmission electron microscopy of *Rboh* mutant plants 5 and 14 dai. Arrows point to cell wall stubs in syncytia. Abbreviations: CW = cell wall. CWI = cell wall ingrowths. Ne = necrosis. Nu = nucleus. Pl = plastid. S = syncytium. X = xylem vessel. Scale bars = 5 µm.

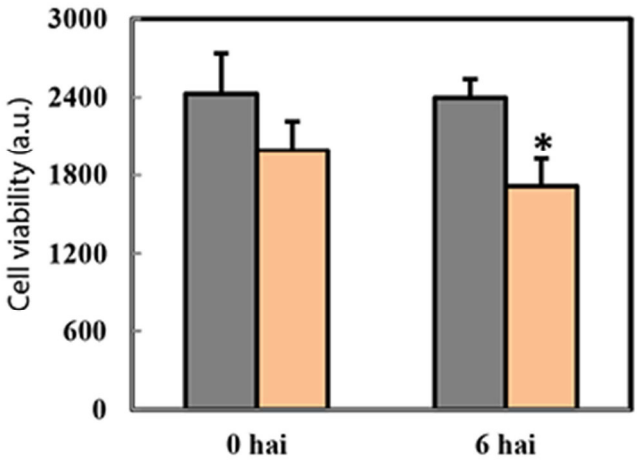

Fig. S8. Cell viability in nematode-infected and uninfected plants treated with DPI. Cell viability determined by fluorescence intensity in arbitrary units (a.u.) of FDA staining. Data represent four independent experiments (mean ± s.e.m). Asterisks indicate $p<0.05$ compared to control treated plants. *t*-test.

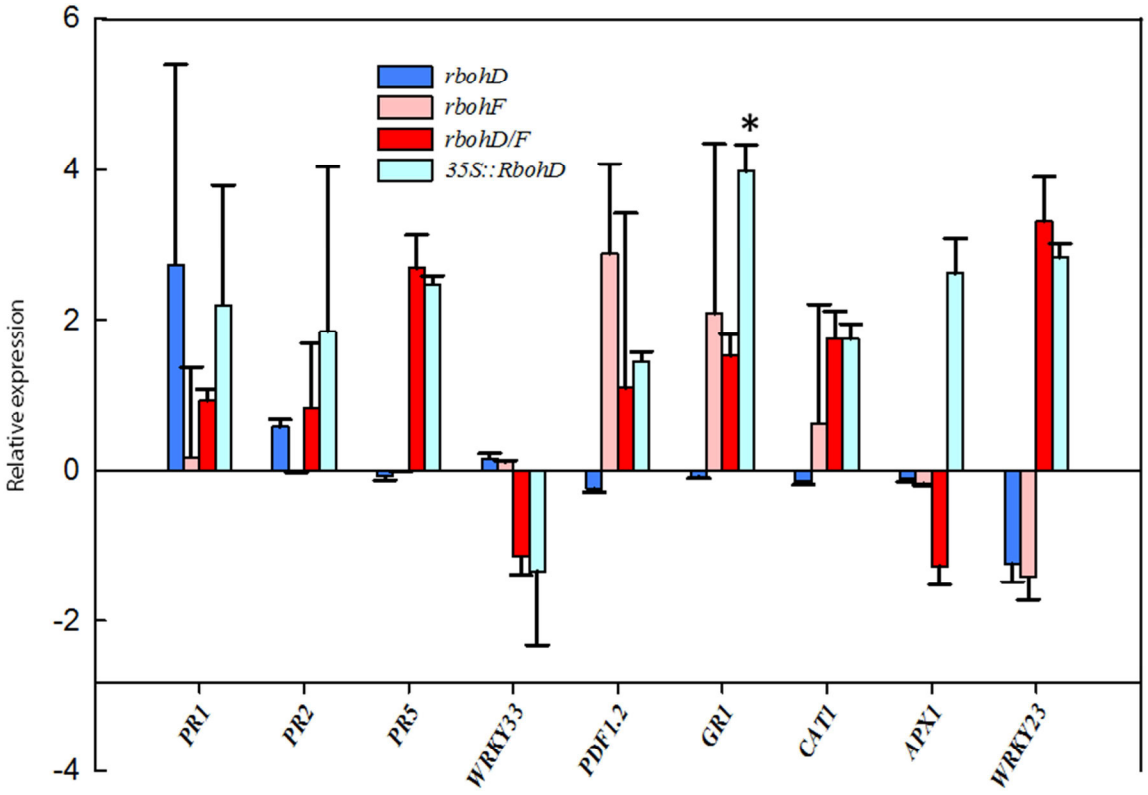

Fig. S9. Analysis of gene expression in uninfected roots. Data show relative expression where expression in Col-0 was set to 0. Each difference of 1 represents a 100% change in expression. Data represent three independent experiments. Asterisk indicates $p<0.05$ compared to Col-0. *t*-test.

Gene	Relative expression
RbohD	4.63 (3.98-6.14)
RbohF	0.50 (0.29-0.75)

Table S1. Expression of *RbohD* and *RbohF* in syncytia of *35S::RbohD* plants. RNA expression of the indicated RNA relative to Col-0.*18S* RNA was used as internal control. Data represent three independent experiments (mean, min, and max).

Treatment	Avg. female size (mm^2)	Avg. syncytium size (mm^2)
Without DPI	0.125±0.0075	0.145±0.014
With DPI	0.09±0.008*	0.106±0-013*

Table S2. Nematode and syncytium size in DPI-treated Col-0 plants 14 dai. Data points represent three independent experiments (mean ± s.e.m). Asterisks indicate $p<0.05$ compared to Col-O without DPI. *t*-test.

Treatment	Avg. female size (mm^2)	Avg. syncytium size (mm^2)
H_2O	0.118±0.006	0.155±0.024
DPI	0.113±0.009	0.135±0.012

Table S3. Nematode and syncytium size in Col-0 plants 14 dai with nematodes preincubated with DPI.
Data points represent mean of three independent experiments (mean ± s.e.m).

Genotype	**Ct *18S***	**Ct *PR1***	**Ct *PR2***	**Ct *PR5***
Col-0	18.75	35.96	36.628	33.501
rbohD/F/sid2	17.886	n.d	40.695	36.996

Table S4. Expression of PR genes in Col-0 and *rbohD/F/sid2* uninfected roots.

n.d = not detected. Representative of three independent experiments.

	Forward	Reverse
18S	GGTGGTAACGGGTGACGGAGAAT	CGCCGACCGAAGGGACAAGCCGA
PR1	AAGGAGCATCATATGCAGGA	ATTTAAATAGATTCTCGTAATCTCAGC
PR2	CTTGAACGTCTCGCCTCCAGTC	TCCAGAAACCGCGTTCTCGATG
PR5	CAATTGCCCTACCACCGTCTGG	CTTAGACCGCCACAGTCTCCG
PDF1.2	GCTAAGTTTGCTTCCATCATCACC	GTGTGCTGGGAAGACATAGTTGC
WRKY33	TTACGCCACAAACAGAGCAC	CCAAAAGGCCCGGTATTAGT
APX1	ATGACGAAGAACTACCCAAC	GCTTGCTCAGCGTCAAACCT
GR1	GGCGAGGAAGATGCTTGTTG	GCACCGATGACAAACAAATCA
CAT1	CAGACTCCTGTTATCGTTCG	CGGTTTCAATGCATGGACCA
WRKY23	AGTCTCGGTAATGGTGATTG	TGTTGCTGCTGTTGGTGATGG
RbohD	CTGGACACGTAAGCTCAGGA	GCCGAGACCTACGAGGAGTA
RBohF	TCACAAATCAACGACGAGAGTT	CCCATCTTCATTCTTGTCCA
Primers for mutant identifications		
D211	GTCGCCAAAGGAGGCGCCGA	
D92b	GGATACTGATCATAGGCGTGGCTCCA	
F 171	CTTCCGATATCCTTCAACCAACTC	
F212	CGAAGAAGATCTGGAGACGAGA	
dSpm1	CTTATTTCAGTAAGAGTGTGGGGTTTTGG	
dSpm11	GGTGCAGCAAAACCCACACTTTTACTTC	
eds16 Fw	ATGCTTCATTTCTTGGATAATAG	
eds16 Rev	GGGAGAAAGAGATCAAATAAGC	

Table S5. Primers sequences used in this study.

universitätbonn INRES

Supplementary Materials

Insights into Rboh-mediated susceptibility of *Arabidopsis thaliana* to the cyst nematode *Heterodera schachtii*

Christiane Matera, Shahid Siddique, Oliver Chitambo, Axel Mithöfer, Florian M.W. Grundler

The PDF file includes:

Tab.S1. **Genexpression values of genes encoding enzymes for tryptophan, indole glucosinolates and camalexin.** Comparison between infected *rbohD*/F plants and Col-0 revealed that nematode infection triggers a strong upregulation for these genes. In contrast, nematodes are not capable to increase the genexpression in *rbohD/F.* Moreover, the transcripts are even decreased. Blue color indicates significant upregulation, red color significant downregulation.

		Col-0 uninfected vs Col-0 infected		**Col-0 infected vs *rbohD*/F infected**			
Gene	**Locus**	**No. in Fig.**	**Fold change**	**p-value**	**Fold change**	**p-value**	**Function**
ASA1/WEI2	At5g05730	1	6,46	0,00002	-1,04	0,82	Anthranilate synthase alpha subunit 1
ASA2	At2g29690		1,22	0,03	1,51	0,03	Anthranilate synthase 2
ASB1/TRP4/ WEI7	At1g25220		0	0	0	0	Anthranilate synthase beta subunit 1
PAT1/TRP1	At5g17990	2	5,3	0,00001	-2,45	0,006	Phosphoribosylanthranilate transferase 1
PAI1/TRP6	At1g07780	3	0	0	0	0	Phosphoribosylanthranilate isomerase 1
PAI2	At5g05590		0	0	0	0	Phosphoribosylanthranilate isomerase 2
PAI3	At1g29410		0	0	0	0	Phosphoribosylanthranilate isomerase 3
IGPS	At2g04400	4	5,15	0,00006	2,12	0,0004	Indole-3-glycerol phosphate synthase
IGPS	At5g48220		-1,25	0,02	2,64	0,001	Indole-3-glycerol phosphate synthase
TSA1/TRP3	At3g54640	5	4,74	0,00008	-1	0,06	Tryptophan synthase alpha chain
TSB1/TRP2	At5G54810	6	0	0	0	0	Tryptophan synthase beta subunit 1
TSB2	At4g27070		4,03	0,0002	-1,21	0,14	Tryptophan synthasebeta subunit 2
CYP79B2	At4g39950	7	3,31	0,0001	-1,89	0,01	Converts Trp to indo-3-acetaldoxime (IAOx), a precursor to IAA and indole glucosinolates
CYP79B3	At2g22330		1,6	0,04	-1,92	0,006	Converts Trp to indo-3-acetaldoxime (IAOx), a precursor to IAA and indole glucosinolates
SUR2/ CYP83B1	At4g31500	8	1,96	0,005	-1,92	0,049	required for phytochrome signal transduction in red light
SUR1	At2g20610		1,57	0,002	-1,22	0,04	involved in converting S-alkylthiohydroximate to thiohydroximate in

							glucosinolate biosynthesis
SOT16	At1g74100	8	2,55	0,001	-3,33	0,05	involved in the final step of glucosinolate core structure biosynthesis.
UGT74B1	At1G24100		1,88	0,001	1,56	0,08	involved in glucosinolate biosynthesis
CYP81F2	At5g57220		16,66	0,01	-2,28	0,01	involved in glucosinolate metabolism
CYP71A13	At2G30770	9	1,67	0,11	11,00	0,00	
CYP71B15	At3G26830	10	16,81	0,0007	-1,71	0,03	Catalyzes the final step to calamixin
YUCCA1	At4g32540	12	1,1	0,14	-2,1	0,02	Flavin Monooxygenase-Like Enzyme
YUCCA2	At4g13260		-1	0,22	-1,34	0,07	Catalyzes conversion of IPA (indole-3-pyruvic acid) to IAA (indole-3-acetic acid) in auxin biosynthesis pathway.
YUCCA4	At5g11320		1,08	0,47	-1,58	0,02	involved in auxin biosynthesis and plant development.
YUCCA5	At5g43890		1,31	0,055	-2,11	0,002	Encodes a YUCCA-like putative flavin monooxygenase
YUCCA6	At5g25620		-1,26	0,04	-2,77	0,006	Flavin Monooxygenase-Like Enzyme
TAA1	At1g70560	13	1,07	0,74	-2,18	0,03	Tryptophan aminotransferase response
TAR1	At1g23320		1,07	0,03	-1	0,65	Encodes a protein with similarity to the TAA1 trytophan aminotransferase involved in IAA biosynthesis
TAR2	At4g24670		-1,98	0,03	1,39	0,14	Encodes a protein with similarity to the TAA1 trytophan aminotransferase involved in IAA biosynthesis

Tab.S2 Downregulation in transcripts for auxin transport, biosynthesis and signaling genes.

Name	Locus	Fold change	Function
PIN1	At1g73590	-3,77	Encodes an auxin efflux carrier involved in shoot and root development.
PIN2	At5g57090	-2,8	PIN2/EIR1 ETHYLENE INSENSITIVE ROOT 1; auxin efflux transmembrane transporter/ auxin:hydrogen symporter/ transporter
PIN3	At1g70940	-5,55	A regulator of auxin efflux and involved in differential growth. PIN3 is expressed in gravity-sensing tissues, with PIN3 protein accumulating predominantly at the lateral cell surface
PIN4	At2g01420	-2,57	PIN4 PIN-FORMED 4; auxin:hydrogen symporter/ transporter
PIN5	At5g16530	-2,07	PIN5 PIN-FORMED 5; auxin:hydrogen symporter/ transporter
PIN6	At1g77110	-2,27	PIN6 PIN-FORMED 6; auxin:hydrogen symporter/ transporter
AUX1	At2g38120	-12,86	AUX1 AUXIN RESISTANT 1; amino acid transmembrane transporter/ auxin binding / auxin influx transmembrane transporter/ transporter
LAX1	At5g01240	-1,24	Encodes LAX1 (LIKE AUXIN RESISTANT), a member of the AUX1 LAX family of auxin influx carriers. Required for the establishment of embryonic root cell organization.
LAX2	At2g21050	-2,97	Encodes LAX2 (LIKE AUXIN RESISTANT), a member of the AUX1 LAX family of auxin influx carriers. Required for the establishment of embryonic root cell organization.
LAX3	At1g77690	-12,46	LAX3 LIKE AUX1 3; amino acid transmembrane transporter/ auxin influx transmembrane transporter/ transporter
WAT1	At1g75500	-38,83	Homolog of Medicago truncatula NODULIN21 (MtN21). The gene encodes a plant-specific, predicted integral membrane protein and is a member of the Plant-Drug/Metabolite Exporter (P-DME) family
AFB2	At3g26810	-1,21	AUXIN SIGNALING F-BOX 2; auxin binding / ubiquitin-protein ligase
AFB3	At1g12820	-1,85	AUXIN SIGNALING F-BOX 3; auxin binding / ubiquitin-protein ligase
GRH1	At4g03190	1,27	GRR1-LIKE PROTEIN 1; auxin binding / protein binding / ubiquitin-protein ligase
ATAUX 2-11	At5g43700	1,35	AUXIN INDUCIBLE 2-11; DNA binding / transcription factor
IAA5	At1g15580	-2,24	INDOLE-3-ACETIC ACID INDUCIBLE 5; transcription factor
IAA6	At1g52830	-1,50	INDOLE-3-ACETIC ACID 6; transcription factor
IAA7	At3g23050	-1,46	INDOLE-3-ACETIC ACID 7; transcription factor
IAA8	At2g22670	-2,08	Transcription factor

IAA9	At5g65670	1,03	INDOLE-3-ACETIC ACID INDUCIBLE 9; transcription factor
IAA10	At1g04100	2,84	Transcription factor
IAA11	At4g28640	2,79	INDOLE-3-ACETIC ACID INDUCIBLE 11; transcription factor
IAA12	At1g04550	1,77	AUXIN-INDUCED PROTEIN 12; transcription factor/ transcription repressor
IAA13	At2g33310	1,52	Transcription factor
IAA19	At3g15540	-1,48	INDOLE-3-ACETIC ACID INDUCIBLE 19; transcription factor
IAA27	At4g29080	-2,0	PAP2 PHYTOCHROME-ASSOCIATED PROTEIN 2; transcription factor
IAA28	At5g25890	-1,20	INDOLE-3-ACETIC ACID INDUCIBLE 28; transcription factor
IAA29	At4g32280	1,22	INDOLE-3-ACETIC ACID INDUCIBLE 29; transcription factor
IAA30	At3g62100	1,14	INDOLE-3-ACETIC ACID INDUCIBLE 30; transcription factor
IAA31	At3g17600	1,13	INDOLE-3-ACETIC ACID INDUCIBLE 31; transcription factor
IAA33	At5g57420	1,50	INDOLE-3-ACETIC ACID INDUCIBLE 33; transcription factor
IAA34	At1g15050	1,46	INDOLE-3-ACETIC ACID INDUCIBLE 34; transcription factor
ARF2	At5g62000	-1,77	AUXIN RESPONSE FACTOR 2; protein binding / transcription factor
ARF3	At2g24765	-1,03	ADP-RIBOSYLATION FACTOR 3; protein binding
ARF4	At5g60450	1,14	AUXIN RESPONSE FACTOR 4; transcription factor
ARF5/ MP	At1g19850	2,12	MONOPTEROS; transcription factor
ARF6	At1g30330	-2,44	AUXIN RESPONSE FACTOR 6; transcription factor
ARF8	At5g37020	-2,23	AUXIN RESPONSE FACTOR 8; transcription factor
ARF9	At4g23980	-1,34	AUXIN RESPONSE FACTOR 9; transcription factor
ARF10	At2g28350	-2,05	AUXIN RESPONSE FACTOR 10; miRNA binding / transcription factor
ARF11	At2g46530	1,29	AUXIN RESPONSE FACTOR 11; transcription factor
ARF12	At1g34310	-13,28	Transcription factor
ARF16	At4g30080	-1,49	AUXIN RESPONSE FACTOR 16; miRNA binding / transcription factor
ARF17	At1g77850	-1,18	AUXIN RESPONSE FACTOR 17; transcription factor
ARF18	At3g61830	1,87	AUXIN RESPONSE FACTOR 18; transcription factor
ARF19	At1g19220	1,41	AUXIN RESPONSE FACTOR 19; DNA binding / transcription factor
TIR1	At3g62980	-1,98	Auxin binding

NPH4	At5g20730	2,29	NON-PHOTOTROPHIC HYPOCOTYL; DNA binding / transcription activator/ transcription factor/ transcription regulator
DHS1	At4g39980	-3,52	Encodes a 2-deoxy-D-arabino-heptulosonate 7-phosphate (DAHP) synthase, which catalyzes the first committed step in aromatic amino acid biosynthesis
ASA1	At1g19920	-2,5	Encodes a chloroplast form of ATP sulfurylase.
ATR1/ Myb34	At5g60890	-1,1	Myb-like transcription factor that modulates expression of ASA1, a key point of control in the tryptophan pathway; mutant has deregulated expression of ASA1 in dominant allele
SUR2	At4g31500	-1,92	Encodes an oxime-metabolizing enzyme in the biosynthetic pathway of glucosinolates. Is required for phytochrome signal transduction in red light. Mutation confers auxin overproduction.
SUR1	At2g20610	-1,22	Confers auxin overproduction. Mutants have an over-proliferation of lateral roots. Encodes a C-S lyase involved in converting S-alkylthiohydroximate to thiohydroximate in glucosinolate biosynthesis
SOT16	At1g74100	-3,33	Encodes a desulfoglucosinolate sulfotransferase, involved in the final step of glucosinolate core structure biosynthesis.
PAT1	At5g17990	-2,5	TRP1 tryptophan biosynthesis 1; anthranilate phosphoribosyltransferase
PAL1	At2g37040	-2,93	Phenylalanine ammonia lyase PAL1

Tab.S3 Co-regulated genes for WAT1 and RbohD. Our analysis revealed that out of 1000 highly co-expressed and co-regulated genes for WAT1 and RbohD, 48 were shared in both data sets. Among these, 17 genes are involved in IAA or indole glucosinolate metabolism and listed in this table.

Gene	Locus	Fold change		Fold change	Adj. P-value	Description
SOT16	At1g74100	2,55	0,001	-3,77	0,02	desulfoglucosinolate sulfotransferase
CYP83B1/ SUR2	At4g31500	1,96	0,005	-1,91	0,01	cytochrome P450 monooxygenase
4CL1	At1g51680	2,32	0,000 9	-4,29	0,000 2	4-coumarate--coenzyme A ligase
UGT74B1	At1g24100	1,88	0,001	1,56	0,046	Encodes UDP-glycosyltransferase/ thiohydroximate
SUR1	At2g20610	1,57	0,002	-1,22	0,013	S-alkylthiohydroximate lyase
CYP711A1	At2g26170	-1,08	0,44	1,07	0,64	electron carrier/ heme binding / iron ion binding / monooxygenase/ oxygen binding
	At5g03610	1,89	0,002	1,37	0,1	GDSL-like Lipase/Acylhydrolase protein; hydrolase activity, acting on ester bonds
SOT17	At1g18590	2,68	0,000 3	-2,5	0,002	desulfoglucosinolate sulfotransferase/ sulfotransferase
PARVUS	At1g19300	-1,37	0,02	-2,5	0,002	polygalacturonate 4-alpha-galacturonosyltransferase / transferase, transferring glycosyl groups / transferase, transferring hexosyl groups
GTR2	At5g62680	1,71	0,005	-3,12	0,002	peptide transporter
CCOAOMT	At4g34050	1,41	0,006	-1,74	0,000 7	caffeoyl-CoA O-methyltransferase - like protein
CCR1	At1g15950	1,13	0,24	-1,69	0,051	cinnamoyl-CoA reductase
ATCPK5	At4g35310	-1,4	0,46	-1,08	0,37	calmodulin-domain protein kinase CDPK isoform 5 (CPK5)

Table S4. Primer pairs used for quantitative RT-PCR of uninfected root segments of *rbohD/F* and Col-0

Gene	Forward primer	Reverse primer
WAT1	ACGGTAAGAGCGAAGAGAGG	CGACTTGATGGAGTTGCGAG
AGP3	TATCACGTTTCTCCCTCCGG	TGGGTTCGTTGGCTGGAATA
APS2	TCTCGATCTTTCCGTCACCG	CTGCAGGATCACGACCTACA
RPP13	TGAGAGTGAGACAACTTCGG	CAAGTGCAGTCTTTCCAAGG
DHS1	ACGCCAATGAGCTTGAGTCT	TTACCAACAGCAGCATCAGC
PDF1.2a	AGTTGTGCGAGAAGCCAAGT	GTTGCATGATCCATGTTTGG
18S	GGTGGTAACGGGTGACGGAGAAAT	TCGGCTTTGTCCCTTCGGTCGG

Acknowledgment

I would like to express my gratitude to Prof. Grundler, who gave me the possibility to complete my dissertation in his laboratory, and especially to Dr. Shahid Siddique, who supported me with all his knowledge and experience. I'm also very thankful to Oliver Chitambo, Marion Hütten, Julia Holbein and Zoran Radakovic and as well to all other colleagues at the Institute of Moleculare Phytomedicine. Their assistance regarding theoretical and practical issues and also their friendship helped me a lot to complete my degree.

Last but not least, I want to thank my mother and sister, as well as my friends, outside of the university, for their patience and support.